

**Testing, advancing, and applying an isotope mass balance model to investigate
nitrogen uptake and assimilation in poplar and willow**

by

Yi Hu

B.S.F. Sichuan Agricultural University, 2013

M.Sc. Sichuan Agricultural University, 2015

A THESIS SUBMITTED IN PARTIAL FULFILLMENT OF
THE REQUIREMENTS FOR THE DEGREE OF

DOCTOR OF PHILOSOPHY

in

**The Faculty of Graduate and Postdoctoral Studies
(Forestry)**

THE UNIVERSITY OF BRITISH COLUMBIA

(Vancouver)

May 2022

©Yi Hu, 2022

Abstract

Poplars and willows are widely distributed in temperate ecosystems and are important woody crops, but their growth depends on adequate (and often replete) supplies of water and nitrogen. Nitrogen isotope discrimination ($\Delta^{15}\text{N}$) have utility as an indicator of nitrogen-use in plants, and an isotope mass balance (IMB) model has been proposed to estimate the fluxes across root plasma membranes (E/I), the proportion of inorganic nitrogen assimilated in roots (P_{root}) and translocation of inorganic nitrogen to shoots (T_i/T_t) under steady-state conditions. Good correspondence between model-estimated E/I and compartmental analysis of tracer efflux has been demonstrated. In this thesis, the IMB model was further validated and then, after adjusting the $\Delta^{15}\text{N}$ value of nitrate reductase (Δ_{enzyme}), used to explore intraspecific variation in nitrogen-use in black cottonwood (*Populus trichocarpa* Torr. & Gray) and heart-leaved willow (*Salix eriocephala* Michx.).

To test the IMB model, I measured concentrations and $\delta^{15}\text{N}$ of inorganic and organic nitrogen in xylem sap extracted from stems of black cottonwood provisioned hydroponically with nitrate. Direct determinations of T_i/T_t and P_{root} compared very favorably with IMB model-derived estimates. The difference in $\delta^{15}\text{N}$ between organic-N and NO_3^- -N fractions in xylem sap (24.9‰) suggests a Δ_{enzyme} of 25.1‰, which is higher than previously assumed by the IMB model, but close to recent estimates that average $\sim 22\%$. There was significant variation in nitrogen-use related traits in both poplar and willow. In heart-leaved willow, variation in $\delta^{15}\text{N}$, $\delta^{13}\text{C}$ and C/N ratios indicated differences in nitrogen uptake and assimilation, WUE, and NUE. Clinal variation in $\delta^{15}\text{N}$ was found in field and hydroponic experiments, possibly related to water availability. The absence of a trade-off between E/I , WUE, and NUE in willow suggests that additive variation in these traits can be captured without compromise. Variation in growth, R:S ratio, $\Delta^{15}\text{N}$, and C/N ratio was also found in black cottonwood, but biogeoclimatic correlations were not strong. The GWAS study using root and leaf $\Delta^{15}\text{N}$ and other traits did not find

significant genes related to nitrate transport or assimilation. There was one for root $\Delta^{15}\text{N}$ and several for R:S ratio, which was in turn correlated with whole-plant $\Delta^{15}\text{N}$ and E/I .

Lay Summary

Water and nitrogen frequently limit plant growth, and differences in water- or nitrogen-use efficiency are necessary for plants to adapt to environmental change over time and space. Adaptive trade-offs, however, may compromise one while optimizing the other. Isotope-based methods for estimating water-use efficiency are well established but the same is not true for nitrogen. I tested and adjusted a nitrogen isotope-based model that provides a new way to assess plant nitrogen-use traits. I applied the model to identify genetic variation in nitrogen uptake and assimilation in poplar and willow. In willow, I found that efficiencies of nitrogen uptake, water-use and nitrogen-use were not inter-correlated, suggesting that selection for these traits can occur without trade-off. Candidate genes for the nitrogen isotopic composition of roots and for root-to-shoot ratio were identified in poplar. Variation in the efficiency of nitrogen uptake may be linked to differences in root-to-shoot ratio in both species.

Preface

The research chapters of this thesis were (or will be) submitted as a series of manuscripts for peer-reviewed journals for publication purposes. For my role, I designed the hydroponic experiments and collected and analyzed the data for Chapters 2 and 3. The provenance trial utilized in Chapter 3 was designed by Dr. Raju Soolanayakanahally. For Chapter 4, I designed the last experiment (batch #9), did all the sample preparation, and collected and analyzed the data. Dr. Jaroslav Klápště provided bioinformatics assistance. For all research chapters, I took the lead in writing the draft manuscripts, in addition to all tables and figures. My supervisor, Dr. Robert Guy, assisted with experimental design, data interpretation and editing throughout all chapters.

A version of Chapter 2 has been published as: “Hu Y, Guy RD. 2020. Isotopic composition and concentration of total nitrogen and nitrate in xylem sap under near steady-state hydroponics. *Plant, Cell & Environment* 43(9):2112-2123”.

A version of Chapter 3 has been published as: “Hu Y, Guy RD, Soolanayakanahally RY. 2022. Genotypic variation in C and N isotope discrimination suggests local adaptation of heart-leaved willow. *Tree Physiology* 42(1):32-43”.

A version of Chapter 4 will be submitted for peer-review publication as: “Genome-wide association study and identification of candidate genes for $\Delta^{15}\text{N}$ in black cottonwood (*Populus trichocarpa*)”.

Table of Contents

Abstract	iii
Lay Summary.....	v
Preface.....	vi
Table of Contents	vii
List of Tables	x
List of Figures	xii
List of Abbreviations.....	xvi
Acknowledgements	xviii
Dedication.....	xix
1. Introduction and research objectives	1
1.1 Nitrogen use and availability	1
1.2 Stable isotopes	2
1.3 Poplar and willow as model species	6
1.4 Impacts of N transport, remobilization, relocation and loss on $\delta^{15}\text{N}$	7
1.5 Model testing	9
1.6 Model application	13
1.7 Research objectives	16
2. Isotopic composition and content of total nitrogen and nitrate in xylem sap under near steady-state hydroponics.....	17
2.1 Summary	17
2.2 Introduction	17
2.3 Material and Methods	21
2.3.1 <i>Plant material and experiment design</i>	21
2.3.2 <i>Hydroponics system</i>	23
2.3.3 <i>Sampling and natural abundance isotope analysis</i>	24
2.3.4 <i>Calculations</i>	26
2.3.4 <i>Statistics</i>	28
2.4 Results.....	29
2.4.1 <i>Nitrogen concentration and $\delta^{15}\text{N}$ in xylem sap</i>	29

2.4.2	<i>Estimated organic nitrogen concentration and $\delta^{15}\text{N}$ in xylem sap</i>	30
2.4.3	<i>Diurnal pattern in nitrogen isotope discrimination in xylem sap</i>	34
2.4.4	<i>Plant tissue discrimination and IMB model prediction</i>	37
2.5	Discussion	41
2.5.1	<i>Whole-plant and organ level variation in $\delta^{15}\text{N}$</i>	41
2.5.2	<i>$\delta^{15}\text{N}$ of total soluble organic N, NO_3^- and organic N of root tissue</i>	42
2.5.3	<i>N content and ^{15}N-patterns of shoot xylem sap</i>	43
2.5.4	<i>Convergence of direct measurement and IMB model prediction</i>	47
2.6	Conclusion	47
3.	Genotypic variation in carbon and nitrogen isotope discrimination suggests local adaptation of heart-leaved willow (<i>Salix eriocephala</i> Michx.)	49
3.1	Summary	49
3.2	Introduction	50
3.3	Methods	53
3.3.1	<i>Common garden experiment</i>	54
3.3.2	<i>Hydroponic experiment</i>	55
3.3.3	<i>Carbon and Nitrogen Isotope analysis</i>	56
3.3.4	<i>Calculations</i>	57
3.3.5	<i>Statistics</i>	58
3.4	Results	58
3.4.1	<i>Common garden experiment</i>	58
3.4.2	<i>Hydroponics experiment</i>	63
3.4.3	<i>Genotypic differences</i>	68
3.5	Discussion	71
3.6	Conclusion	75
Chapter 4	Geographic variation in $\delta^{15}\text{N}$ of black cottonwood (<i>Populus trichocarpa</i>) and identification of candidate genes for isotope discrimination by genome-wide association	76
4.1	Summary	76
4.2	Introduction	77
4.3	Methods and materials	80
4.3.1	<i>Plant materials</i>	80

4.3.2 Hydroponic system	82
4.3.3 $\delta^{15}\text{N}$ phenotyping.....	82
4.3.4 Geo-climatic patterns in $\Delta^{15}\text{N}$	83
4.3.5 Heritability estimates and GWAS analysis	84
4.4 Results	86
4.4.1 Heritability of biomass and nitrogen related traits	86
4.4.2 Correlation matrix	93
4.4.3 Genome-wide association analysis.....	96
4.5 Discussion.....	99
4.5.1 Leaf discrimination is representative of whole-plant discrimination	99
4.5.2 Root-related traits show signals of local adaptation	101
4.5.3 SNP associations to isotope discrimination and R:S ratio	102
4.6 Conclusion.....	104
5. Conclusion	105
5.1 The N isotopic composition of xylem sap	106
5.2 Intraspecific variation in carbon and nitrogen isotopic composition of heart-leaved willow	108
5.3 Geographic variation in $\Delta^{15}\text{N}$ of black cottonwood and identification of candidate genes by genome-wide association	110
5.4 Limitations and future application of the IMB model	111
References	114
Appendix – Supplemental measurements	132

List of Tables

Table 2.1. Genotypes of black cottonwood (<i>Populus trichocarpa</i>) used in this study.	22
Table 2.2. Concentrations and $\delta^{15}\text{N}$ values of total N (<i>Nt</i>) and nitrate (<i>Ni</i>) in xylem sap collected from the shoots of three genotypes of <i>Populus trichocarpa</i> hydroponically grown with NO_3^- . Mean values ($\pm\text{SE}$) are for four biological replicates, each representing pooled sap collected from 10 plants over the low pressure range. $[\text{Ni}]/[\text{Nt}]_{\text{xylem}}$ is the percent fraction of NO_3^- in the total N. Different letters indicate significant differences at $P<0.05$	33
Table 2.3. Concentrations and $\delta^{15}\text{N}$ values of total N (<i>Nt</i>), nitrate (<i>Ni</i>) and organic nitrogen (<i>No</i>) in xylem sap collected from the shoots of five genotypes of <i>Populus trichocarpa</i> hydroponically grown with NO_3^- . Mean values ($\pm\text{SE}$) are for five biological replicates, each representing pooled sap expressed from 10 plants over the 0-1 MPa range. Different letters indicate significant differences at $P<0.05$	36
Table 2.4 Percentages of NO_3^- (<i>Ni</i>) in total nitrogen (<i>Nt</i>) in xylem sap as directly measured after collection ($[\text{Ni}]/[\text{Nt}]$) or estimated percentage of inorganic nitrogen (<i>Ti</i>) relative to total nitrogen (<i>Tt</i>) translocated to the leaves (Ti/Tt) from the isotope mass balance (IMB) model for <i>Populus trichocarpa</i> genotypes grown under 0.5 mM NO_3^- for 45 days. Model predictions of Ti/Tt are given for calculations where discrimination (Δ) by nitrate reductase is taken to be either 15.4‰ or 25.1‰. Data are means $\pm\text{SE}$ ($n=5-10$). Different individual ramets were used for sap collection and for model analysis.	39
Table 3.1. Overall means of measured plant traits, and associated population effects from the common garden experiment. Traits measured or estimated include nitrogen percentage (N, %), carbon isotopic composition ($\delta^{13}\text{C}$, ‰), nitrogen isotopic composition ($\delta^{15}\text{N}$, ‰), the carbon to nitrogen (C/N) ratio of leaves and stems.....	60

Table 3.2. Pearson correlations (r) between geographic, climatic and physiological variables for all 21 genotypes in the hydroponic experiment. Bolding indicates significance at $P < 0.05$; Bold* indicates significance at $P < 0.001$ 66

Table 3.3. Canonical structure between geoclimatic parameters and plant traits with the first two canonical variables, CLIM1 and CLIM2. 67

Table 3.4. Overall means and ranges of measured plant traits, and associated genotype effects, in the hydroponics experiment. Traits measured or estimated include biomass (g), root-shoot ratio, carbon isotopic composition ($\delta^{13}\text{C}$, ‰) at organ and whole-plant (WP) levels, nitrogen isotope discrimination ($\Delta^{15}\text{N}$, ‰) at organ and whole-plant levels, the ratio of inorganic to total nitrogen transported in the xylem (T_i/T_t), the proportion of plant nitrogen assimilated in roots (P_{root}), efflux/influx (E/I), and leaf and root assimilation activity (AC , $\mu\text{mol mg dw}^{-1}$). 69

Table 4.1. Overall genotypic means and ranges of whole-plant (WP) biomass, root-to-shoot (R:S) ratio, organ and whole-plant level nitrogen isotope discrimination ($\Delta^{15}\text{N}$), and carbon to nitrogen ratio (C/N), and related broad-sense heritability estimates (H^2) across *Populus trichocarpa* accessions. 88

Table 4.2. Population-wide relationships between nitrogen-related physiological variables and geo-climatic variables for *Populus trichocarpa* accessions. Bolding indicates significance at $P < 0.05$; Bold* indicates significance at $P < 0.01$ 94

Table 4.3. Canonical structure between geoclimatic parameters and plant traits with the first two canonical variables, CLIM1 and CLIM2. 95

Table 4.4. Genes and their *Arabidopsis thaliana* (AT) homologs identified by GWAS with SNP markers associated with root-to-shoot (R:S) ratio, or both root ^{15}N discrimination ($\Delta^{15}\text{N}$) and the leaf-root difference in discrimination ($\Delta^{15}\text{N}_{\text{root-leaf}}$) in *Populus trichocarpa*. Information under “potential significance” comes from the online platform DICOTS PLAZA V4.5 except where otherwise indicated. 97

List of Figures

- Figure 1.1. Diagram of plant nitrogen fluxes during the uptake of inorganic nitrogen from the substrate pool and assimilation into either root or leaf organic nitrogen as proposed in the isotope mass balance model. Arrows refer to unidirectional fluxes of nitrogen between leaf (green) and root (yellow) pools. T_o represents the organic nitrogen translocated to the leaves and T_i represents the inorganic nitrogen translocated to the leaves. Stem tissue is assumed to arise from a mixture of leaf and root organic pools. 12
- Figure 2.1. Concentrations of total N (a) and nitrate (b), and $\delta^{15}\text{N}$ of total N (c) and nitrate (d) in *Populus trichocarpa* xylem sap collected from lower and upper shoot sections at low pressure and higher pressure. Bars or symbols represent means of six samples ($\pm\text{SE}$; omitted from panel d because they are smaller than the symbol size). Effects of the main factors pressure or position, and their interaction, are indicated: *n.s.*, not significant; *, $P<0.05$; **, $P<0.01$; ***, $P<0.001$. Dotted lines in panels c and d represent the $\delta^{15}\text{N}$ of NO_3^- in the hydroponic medium (-1.69‰). 31
- Figure 2.2. Estimated concentration (a) and $\delta^{15}\text{N}$ (b) of organic N in xylem sap collected from lower and upper shoot sections at low pressure and higher pressure. Bars or symbols represent means of six samples ($\pm\text{SE}$). The main factors pressure and position, and their interaction, were not significant (*n.s.*). Dotted line in panel b represents the $\delta^{15}\text{N}$ of NO_3^- in the hydroponic medium (-1.69‰). 32
- Figure 2.3. Diurnal patterns in concentrations of total N (a), nitrate (b) and organic N (c), and $\delta^{15}\text{N}$ of total N (d), nitrate (e) and organic N (f) in xylem sap of *Populus trichocarpa*. Bars or symbols represent means of 10 samples ($\pm\text{SE}$). Effects of the main factor time are indicated: *n.s.*, not significant; *, $P<0.05$; **, $P<0.01$; ***, $P<0.001$. Dotted lines in panels d, e and f represent the $\delta^{15}\text{N}$ of nitrate in the hydroponic medium (63.81‰)..... 35

Figure 2.4. Whole-plant and organ level discrimination ($\Delta^{15}\text{N}$) in five genotypes of *Populus trichocarpa* in Experiment 2. Shown are means \pm SE ($n=5$). Different letters indicate significant difference between genotypes at $P<0.05$ 38

Figure 2.5. Model-derived efflux/influx (E/I , upper panel) and the proportion of nitrogen assimilated in the root (P_{root} , lower panel) of five genotypes of *Populus trichocarpa*. Empty bars are based on tissue $\delta^{15}\text{N}$ values assuming Δ_{enzyme} is 25.1‰ (i.e., P_{root} predicted via Equations (2.7) and (2.10)) and solid bars are based on measurements of xylem sap N content (P_{root} measured from Equation (2.6)). Both estimates of P_{root} also rely on the same tissue N content data, so some autocorrelation is expected. Shown are means \pm SE ($n=5$). Different letters indicate significant differences between genotypes at $P<0.05$ 40

Figure 3.1. Locations of 34 populations of heart-leaf willow (*Salix eriocephala*) sampled from the natural range of the species across eastern and western Canada. Stars indicate the populations from which the 21 genotypes used in the hydroponics experiment were selected. The green shaded area represents the dominant continuous range of heart-leaved willow while the yellow shaded area shows the discontinuous range..... 56

Figure 3.2 The relationship between leaf carbon isotopic composition ($\delta^{13}\text{C}$) and leaf carbon to nitrogen (C/N) ratio of heart-leaf willow (*Salix eriocephala*) based on (a) population means (\pm SE) and (b) individual plants from the common garden experiment. 61

Figure 3.3. Nitrogen isotopic composition ($\delta^{15}\text{N}$) and carbon isotopic composition ($\delta^{13}\text{C}$) of leaves and stems in heart-leaf willow (*Salix eriocephala*) (panels a&c and b&d, respectively) from common garden and hydroponic experiments (a&b and c&d, respectively) plotted against latitude of origin. Each point for the common garden data represents one population with 10 replicates, while each point for the hydroponic data represents one genotype with six replicates. Data are means \pm SE..... 62

Figure 3.4. Whole-plant nitrogen and carbon isotopic compositions ($\delta^{15}\text{N}$ & $\delta^{13}\text{C}$; panels a&b, respectively) plotted against latitude of origin in the hydroponic experiment. Each point represents one genotype with six replicates. Data are means \pm SE. 65

Figure 3.5. Root efflux/influx ratio derived from the Isotope Mass Balance (IMB) model plotted against latitude of origin. Each point represents one genotype with six replicates. Data are means \pm SE. 65

Figure 3.6. 3D scatter plot showing efflux/influx ratio (E/I), whole-plant carbon isotopic composition ($\delta^{13}\text{C}$) and whole-plant C/N ratio of the 21 genotypes used in the hydroponics experiment. Each dot represents the mean of six replicates per genotype. The STL-2 genotype is singled out for its combination of high $\delta^{13}\text{C}$, high C/N, and low E/I 70

Figure 4.1. Locations of 107 populations of black cottonwood (*Populus trichocarpa*) sampled from the natural range of the species in western North America, as shown in blue. The green area represents the dominant continuous range of the species. 81

Figure 4.2 Relationships between leaf isotope discrimination ($\Delta^{15}\text{N}$) and whole-plant (WP) $\Delta^{15}\text{N}$ (a), and root efflux/influx (b) in *Populus trichocarpa* accessions. Each point represents one genotypic mean with three replicates across batches 1-4 and 9 ($n=209$). 89

Figure 4.3 Relationships between root $\Delta^{15}\text{N}$ and whole-plant $\Delta^{15}\text{N}$ (a), and root efflux/influx (b) in *Populus trichocarpa* accessions. Each point represents one genotypic mean with three replicates across batches 1-4 and 9 ($n=209$). 90

Figure 4.4 Relationships between root-to-shoot (R:S) ratio and whole-plant (WP) $\Delta^{15}\text{N}$ (a), and root efflux/influx (b) in *Populus trichocarpa* accessions. Each point represents one genotypic mean with three replicates across batches 1-4 and 9 ($n=209$). 91

Figure 4.5 Relationship between root-to-shoot (R:S) ratio and leaf, root and the leaf-root difference in nitrogen isotope discrimination ($\Delta^{15}\text{N}$) in *Populus trichocarpa* accessions. Each point represents one genotype with at least three replicates across 9 batches ($n=362$). 92

List of Abbreviations

ADI	annual dryness index
AgCan <i>Salix</i>	Agriculture Canada <i>Salix</i>
CATE	compartmental analysis of tracer efflux
CONT	continentality (°C)
C/N ratio	carbon to nitrogen ratio
$\delta^{13}\text{C}$	carbon isotope composition (‰)
$\delta^{15}\text{N}$	nitrogen isotope composition (‰)
$\Delta^{15}\text{N}$	nitrogen isotope discrimination (‰)
EA-IRMS	elemental analysis-isotope ratio mass spectrometer
<i>E/I</i>	efflux over influx
FFP	frost-free period (days)
<i>f_{leaf}</i>	fraction of leaf nitrogen over plant nitrogen
<i>f_{root}</i>	fraction of root nitrogen over plant nitrogen
<i>f_{stem}</i>	fraction of stem nitrogen over plant nitrogen
GC-IRMS	gas chromatograph-isotope ratio mass spectrometer
GS	glutamine synthetase
GS-GOGAT	glutamine synthetase-glutamine oxoglutarate aminotransferase
GWAS	genome-wide association study
HATS	high affinity transport system
H^2	broad-sense heritability
IMB model	Isotope mass balance model
LATS	low affinity transport system

MAP	mean annual precipitation (mm)
MAT	mean annual temperature
MSP	mean summer temperature from May to September (mm)
MST	mean summer precipitation from May to September (°C)
MWMT	mean warmest month temperature (°C)
NiR	nitrite reductase
NR	nitrate reductase
NUE	nitrogen use efficiency
$[Ni]_{\text{xylem}}$	inorganic nitrogen concentration of xylem sap (mM)
$[No]_{\text{xylem}}$	organic nitrogen concentration in xylem sap (mM)
$[Nt]_{\text{xylem}}$	total nitrogen concentration of xylem sap (mM)
P_{root}	proportion of inorganic nitrogen assimilated in the roots
R:S ratio	root-to-shoot ratio
SDI	summer dryness index
SNPs	single nucleotide polymorphisms
Ti/Tt	percentage ratio of inorganic nitrogen relative to total nitrogen translocated to the leaves (%)
WUE	water use efficiency

Acknowledgements

Foremost, I would like to express my deepest appreciation to my PhD supervisor Professor Robert Guy for his extraordinary support during my PhD study and this dissertation. Professor Guy is a mentor to me, not only because he guided me how to do research properly, but also provided me with encouragement and patience throughout the duration my journey. Finishing a PhD was never an easy task, especially for an international student, and I truly appreciate his help.

I also would like to extend my sincere thanks to my supervisory committee members, Professor Barbara Hawkins, Professor Shawn Mansfield and Professor Lee Kalcsits, for their advice and suggestions on my experimental designs and this dissertation. I must also thank Dr. Raju Soolanayakanahally for his contributions to the willow field experiment in Chapter 3 and access to analytical services for isotope analysis in Chapter 4. I also wish to thank Dr. Mina Momayyezi, Dr. Alice Chang, and Dr. Shannon Guichon for their help with stable isotope measurements. I would like to acknowledge assistance from Ms. Melina Biron with building the hydroponic system in the greenhouse. I very much appreciate the help from Mr. Shofiul Azam for growing most of plant materials in Chapter 4, and the help from Dr. Jaroslav Klápště on the further bioinformatics assistance. Thanks also for funding from the Natural Sciences and Engineering Research Council of Canada (NSERC), the China Scholarship Council (CSC), Genome Canada and the Agriculture and Agri-Food Canada (AAFC) Research Affiliate Program.

In the end, I would like to thank my family for their emotional support, especially to my wife Han Li. I feel very blessed to have you on my side over the years and I love you for the rest of my life.

Dedication

To the memory of my grandmother, Shuwen Liu. Although she was my inspiration to pursue my doctoral degree, she was unable to see my graduation. This is for her.

1. Introduction and research objectives

1.1 Nitrogen use and availability

Nitrogen (N) is a critical component of proteins, DNA, and amino acids, and the fourth most abundant element found in organic matter. Nitrogen is the primary limiting nutrient for most plants growing in natural and agricultural ecosystems (Glass *et al.* 2002). To grow and compete under N-limiting conditions, plants have evolved to acquire different forms of N such as nitrate, ammonium, and even amino acids (Xu *et al.* 2012). Nitrogen dynamics vary climatically, and availability of different N forms is different between environments (Giesler *et al.* 1998). In temperate forests, total soil N can range from 0.05 to 1.65 Kg N m⁻² (Callesen *et al.* 2007), while Marty *et al.* (2017) reported 0.42 to 1.26 Kg N m⁻² in Canadian boreal forest soils.

In modern agricultural production, nitrogen is a critical nutrient for plant growth. Total global N fertilizer in use today is more than eight times higher than it was at the start of the green revolution (1950s) (Wu *et al.* 2020). Although N fertilization has contributed to a doubling of the world's crop production, a large portion of applied fertilizer is lost through leaching, volatilization or denitrification (Vitousek *et al.* 1997; Hirel *et al.* 2007), which has had negative impacts on the environment as well as causing economic burden in crop production. Improving plant N use efficiency not only reduces the environmental impacts of modern society, but also reduces overall fertilizer requirements, potentially making production feasible on marginal lands (Fageria and Baligar 2005).

Plant nitrogen use efficiency (NUE) is determined by plant yield (biomass) relative to the amount of N applied. At the crop or whole-plant level, the efficiency of N uptake is one physiological process that may influence the overall NUE (Glass *et al.* 2003).

Nitrate and ammonium are the two most important inorganic N sources for plants. Both nitrate and ammonium have two major transport systems responsible for N uptake: high-affinity (HATS) and low-affinity (LATS) transport systems that are most effective at low or high N concentrations, respectively (Glass *et al.* 2002). It is possible under certain conditions for a substantial portion of the gross nitrate and/or ammonium uptake (influx) to return to the rooting medium (efflux) (Kronzucker *et al.* 1997; Hawkins and Robbins 2010). The ratio of efflux over influx (E/I) describes the bidirectional movement of inorganic N between root and rhizosphere but also relates to the N uptake efficiency; *i.e.*, a low E/I indicates a high uptake efficiency because of less leakage of inorganic N back to the medium. Once retained by the root, nitrate must first be reduced to nitrite and then ammonium before it can be assimilated further. Nitrate is converted into nitrite in the cytoplasm by nitrate reductase (NR), and nitrite is converted to ammonium by nitrite reductase (NiR). Ammonium, whether directly taken up by root cells or produced from nitrate, is assimilated into glutamine by glutamine synthetase (GS).

1.2 Stable isotopes

There are two stable isotopes of nitrogen (^{14}N and ^{15}N), with ^{14}N being the predominant form (99.636% of total natural nitrogen). Variation in $\delta^{15}\text{N}$ between plants or N pools can provide both process and tracer information to understand N uptake and assimilation in plants, as well as N flux through ecosystems (Evans 2001; Robinson 2001). In the atmosphere, the relative ratio of ^{15}N to ^{14}N is virtually constant. However, due to their differences in atomic mass, the stable isotopes of N may show differences in rates of chemical reaction, or in physical processes, such as diffusion. Processes that change the relative abundance of ^{15}N and ^{14}N cause isotope fractionation. For example, during inorganic N assimilation, there is discrimination by the assimilation enzymes against the heavier isotope (^{15}N) over the lighter isotope (^{14}N), which results in

differences in relative abundance between the substrate and the product (fractionation). Small but easily determined differences in N isotope ratios are generally expressed in delta notation ($\delta^{15}\text{N}$, ‰) relative to the arbitrary standard, atmospheric N:

$$\delta^{15}\text{N} = (R_{\text{sample}}/R_{\text{standard}} - 1) \times 1000$$

where, R_{sample} and R_{standard} are the $^{15}\text{N}/^{14}\text{N}$ ratios of the measured sample and arbitrary standard (0.00365, air N_2), respectively. Substances with isotope ratios that are greater or lower than the reference ratio are ^{15}N enriched or depleted, respectively (Peterson and Fry 1987). A similar expression yields $\delta^{13}\text{C}$ values that describe the $^{13}\text{C}/^{12}\text{C}$ ratio of any measured sample relative to a carbonate standard.

The $\delta^{13}\text{C}$ of plant tissue is a widely employed indicator of carbon fixation pathway (e.g., C3 vs. C4 plants) and, within the C3 plants, is a temporally- and spatially-integrated proxy measure of photosynthetic water-use efficiency (Farquhar *et al.* 1982). In principle, variation in $\delta^{15}\text{N}$ could similarly provide temporally- and spatially-integrated information about the nature of N sources, and also the N relations of the plant. Foliar $\delta^{15}\text{N}$ reflects both isotopic composition of the soil N as well as the fractionations that occur during N uptake, assimilation, and reallocation inside the plant (Kalcsits and Guy 2013a). At very large scales, soil $\delta^{15}\text{N}$ tends to increase with increasing temperature and decreasing precipitation across spatial gradients (Amundson *et al.* 2003). However, global relationships between soil $\delta^{15}\text{N}$ and climatic variables are largely indirect and can be affected by other variables, such as soil depth (Hobbie and Ouimette 2009), soil age (Brenner *et al.* 2001), dominant plant species (Templer *et al.* 2007), and clay and carbon concentrations (Craine *et al.* 2015b). Soil pH is also an important factor affecting soil $\delta^{15}\text{N}$, as arid soils tend to be alkaline and therefore susceptible to gaseous losses of ammonia (McCalley and Sparks 2009). Spatial and temporal variations in soil $\delta^{15}\text{N}$ make it difficult to interpret plant $\delta^{15}\text{N}$ in samples collected in field studies. Interpretation is

frequently not feasible even in greenhouse pot studies because, as plants grow, they may modify the isotopic composition of their source nitrogen, which in turn affects the isotopic composition of the plant.

It is well recognized that changes in plant $\delta^{15}\text{N}$ occur during nitrate or ammonium assimilation causing plants to be depleted in ^{15}N by about 2-3‰ compared to the soil N (Evans 2001). This difference implies that there is enzymatic discrimination against the heavier isotope, in either N transport or assimilation. It is now more than thirty years since the first reports of $^{14}\text{N}/^{15}\text{N}$ isotope effects associated with NR and GS measured *in vitro* using preparations from spinach leaves, yielding discrimination factors of ~15‰ for NR (Ledgard *et al.* 1985) and ~17‰ for GS (Yoneyama *et al.* 1993). However, under N-limited conditions, plant $\delta^{15}\text{N}$ was found to be close to the $\delta^{15}\text{N}$ values of soil inorganic N because both isotopes are assimilated to near completion (Mariotta *et al.* 1982; Evans 2001). There is greater fractionation when substrate concentrations are high, but rarely (if ever) does the $\delta^{15}\text{N}$ reflect the full discrimination factor of nitrate reductase or glutamine synthetase (Evans *et al.* 1996; Yoneyama *et al.* 2002; Pritchard and Guy 2005), indicating that assimilation is not the only step affecting fractionation.

The enzyme discrimination factors noted above (15‰ and 17‰) are often assumed to be correct by authors working in the field but are, in fact, poorly constrained. More recent research has suggested greater discrimination for NR, ranging from 17-22‰ (Needoba *et al.* 2004, Liu *et al.* 2014; Cui *et al.* 2020), or even as much as 32‰ (Carlisle *et al.* 2014). Similarly, estimates of discrimination by GS have ranged from 16.5‰ to 29‰, depending on the external ammonium concentration (Yoneyama *et al.* 2001). It is important to note that all of the aforementioned NR and GS discrimination factors were measured *in vitro*, and the ranges obtained suggest that discrimination may not necessarily be the same, or constant, *in vivo*. Therefore, the development of a

direct non-destructive method to estimate discrimination factors for NR and GS in plants would provide essential clarity.

There is also fractionation between plant parts. For example, several studies in both the laboratory and under field conditions have shown differences in $\delta^{15}\text{N}$ between roots and shoots (Dijkstra *et al.* 2003; Kalcsits and Guy 2013a; Kalcsits *et al.* 2015; Pritchard and Guy 2005), with shoots generally being ^{15}N -enriched compared to roots. The differential allocation of nitrogenous compounds of differing isotopic composition causes differences in $\delta^{15}\text{N}$ between plant parts. For instance, during the process of nitrate reduction in roots, nitrate molecules left behind after reduction are ^{15}N -enriched and available for translocation to shoots, which causes the difference in $\delta^{15}\text{N}$ between roots and shoots (Robinson *et al.* 1998; Evans 2001; Comstock 2001). Since ammonium is largely considered to be primarily assimilated in the roots instead of leaves (Raven and Smith 1976), less difference in $\delta^{15}\text{N}$ between roots and shoots is expected when plants are grown with ammonium than with nitrate, as observed in balsam poplar (Kalcsits *et al.* 2014) and trembling aspen (*Populus tremuloides* Michx.) (Kalcsits *et al.* 2015). Sites of assimilation do, however, vary between species (Gessler *et al.* 2000; Johnson and Berry 2013). For example, in conifers both nitrate and ammonium are mostly root-assimilated (Lupi *et al.* 2013). There are organ-level $\delta^{15}\text{N}$ differences between species consistent with this general observation. For example, leaf $\delta^{15}\text{N}$ was generally 2-4‰ heavier than the root $\delta^{15}\text{N}$ in the angiosperm trees European beech (*Fagus sylvatica* L.) (Peuke *et al.* 2006) and trembling aspen, whereas in the conifers lodgepole pine (*Pinus contorta* Douglas) and white spruce (*Picea glauca* (Moench) Voss) leaf and root $\delta^{15}\text{N}$ values were similar regardless of the inorganic N source (Kalcsits *et al.* 2015). Within-plant variation in N isotope composition in plants has also been reported in herbaceous plants such as barley (*Hordeum vulgare* L.) (Kolb and Evans 2003; Robinson *et al.* 2000), wheat (*Triticale aestivum* L.) (Yousfi *et al.* 2013) and rice (*Oryza*

sativa L.) (Yoneyama *et al.* 2001), and also in oil palm (*Elaeis guineensis* Jacq.) (Cui *et al.* 2020). Such root-shoot variation in isotopic composition, whether genetically based or environmentally induced, suggests that $\delta^{15}\text{N}$ values may also have potential to provide information about N transport and allocation. Kalcsits *et al.* (2013a) have used organ- and whole-plant $\delta^{15}\text{N}$ values in an isotopic mass balance (IMB) model to estimate integrated nitrogen-use traits, such as relative rates of root vs. leaf assimilation, fluxes across the root plasma membrane, and translocation of inorganic N to the shoot.

1.3 Poplar and willow as model species

Unlike most crop plants, and the model plant *Arabidopsis*, trees differ fundamentally in being long-lived perennials of considerable height and size. The most obvious manifestation is the development of wood, or secondary xylem, from the vascular cambium (Taylor 2002). This makes trees particularly ideal for studying nutrient transport from roots to shoots, as xylem vessels are made of a series of dead cells (elements) that enable water and mineral conduction with minimal effect on composition occurring during transport over long distances. Also, by a variety of means, xylem sap can be collected from woody plants in decent quantity and with minimal contamination from other tissue types such as phloem (Schurr 1998).

Black cottonwood (*Populus trichocarpa* Torr. & Gray) and heart-leaved willow (*Salix eriocephala* Michx.) are two widespread North American hardwood species in the *Salicaceae* family and of increasing interest in the development of suitable feedstock for bioenergy purposes and other applications. Black cottonwood exists across a broad range of climates, from the Pacific coast inland to the prairies, and from northern Baja California (Mexico) to the Kenai Peninsula (Alaska) (Farrar 1995). The heart-leaved willow has an even larger range across North America between 25°30 and 55°19 N latitude, including grassland and temperate and boreal forests (Brockman 1968). These

two species are good models to study adaptive patterns due to their wide range of habitats. Like many members of the *Salicaceae*, both species are easily propagated, have well-established and extensive genetic resources, and possess relatively small but well-characterized genomes (Djomo *et al.* 2011; McKown *et al.* 2014a, 2014b, 2014c, 2019; Murphy *et al.* 2021). Significant genotypic and population-wide variation in many phenology and ecophysiological traits has been reported from common garden studies (McKown *et al.* 2014b, 2014c; Shunmugam *et al.* 2016). In black cottonwood, phenotypic traits such as bud-set phenology, photosynthesis rates, stomatal densities, etc., were correlated to geoclimatic variables (McKown *et al.* 2014b). Hundreds of genes underlying those phenotypic traits are implicated in local adaptation (McKown *et al.* 2014a, 2019).

1.4 Impacts of N transport, remobilization, relocation and loss on $\delta^{15}\text{N}$

Xylem and phloem transport have been studied for many years because of their dominant roles in long-distance signalling, and water and nutrient/assimilate delivery, from roots to shoots and *vice versa*. Xylem sap primarily contains nutrients obtained from the soil in raw form or assimilated into organic molecules, whereas phloem sap is much more viscous and contains sugars or other products of photosynthesis, as well as amino acids and proteins (Turgeon and Wolf 2009; Peuke 2010). Nitrate is the most common inorganic N form in the xylem sap, whereas ammonium is less common as it is assimilated mostly in the roots and there is little transported from roots to shoots (Tobin and Yamaya 2001). Since leaf N metabolism follows a diurnal pattern and isotope fractionations may be flux-dependent, xylem N profile and isotopic composition may also show diurnal patterns. In fact, Peuke *et al.* (2013) found significant diurnal variation in $\delta^{15}\text{N}$ in xylem sap of potted castor bean (*Ricinus communis* L.). However, physiological

interpretation of those results was limited by spatial, and possibly temporal, soil N heterogeneity.

The remobilization of previously existing N may affect the isotope ratio of both source and sink organs, and this consideration may affect the accuracy and applicability of the IMB model. The origin of pre-existing N, or subsequent isotope effects associated with biochemical processing, can result in fractionation. For example, for scions used to vegetatively propagate poplar plants, ~50% of the N contained within the original scions was remobilized to support the growth of the new plant (Kalcsits and Guy 2013b). Moreover, if the isotopic signatures between media sources and pre-existing N differ significantly ($>2\text{‰}$), the pre-existing N could affect the IMB model output if it is not properly accounted for (Kalcsits and Guy 2013b).

Similarly, in woody perennials, N from senescing leaves is remobilized to stem tissues during autumn to be re-used by developing tissues the following spring (Malaguti *et al.* 2001). During active growth, N can be distributed via the phloem to growing sinks, such as roots, soon after it is assimilated in the leaves, just as N assimilated in the roots may be translocated to the shoots in organic form within the xylem. The IMB model predicts the latter but ignores the former. Since N remobilization through phloem is often related to senescence or abiotic stress, the IMB model assumes that phloem N transport from shoot to root is negligible when young plants are growing rapidly under hydroponic conditions.

Nitrogen loss from the roots or the shoots can affect plant $\delta^{15}\text{N}$ if it is (1) lost in significant quantities and/or (2) the $\delta^{15}\text{N}$ of N lost from the plant strongly deviates from the bulk whole-plant $\delta^{15}\text{N}$ (Kalcsits *et al.* 2014). Root organic N may be lost through exudation, which occurs in many plant species under many conditions and contributes to improved bioavailability of macro and micronutrients (Johnson *et al.* 1996, Dakora

and Phillips 2002). Robinson *et al.* (1998) suggested that exudation of enriched organic N causes roots to have lower $\delta^{15}\text{N}$ than leaves. Root exudates, however, generally represent a small fraction of the total plant nitrogen budget, and given the wide range of nitrogenous compounds and their isotopic differences, the calculated impact on root $\delta^{15}\text{N}$ is small (Kalcsits *et al.* 2014). Similarly, nitrogen loss from leaves through the volatilization of NH_3 gas during the process of photorespiration might increase the $\delta^{15}\text{N}$ of leaves relative to roots. Schjoerring and Mattson (2001) reported 1–4% of shoot nitrogen was volatilized as NH_3 from a variety of crop plants which, in combination with the observation that fractionation associated with NH_3 volatilization from NH_4^+ is as much as 40‰ (Mariotti *et al.* 1982). Importantly, however, most of this loss occurred during senescence, which can be avoided as mentioned above. Johnson and Berry (2013) estimated the isotope fractionation associated with volatilization of NH_3 from leaves of actively growing plants was minimal (i.e. <1‰) when stomatal conductance was high and temperatures were below 25 °C.

1.5 Model testing

Kalcsits and Guy (2013a, 2016a) took two different approaches to assess the validity of the IMB model. The first approach was to examine N isotope discrimination in nitrate reductase 2 (*nia2*), nitrate reductase 1 (*nia1*) and nitrate transporter (*nrt2*) knockout mutant lines of *Arabidopsis thaliana*. A greater difference in $\delta^{15}\text{N}$ between leaf and root was found in the NR knockout lines, indicating changes in the site of nitrate assimilation between leaf and root. Application of the IMB model suggested that the *nia2* line had an increased proportion of assimilation in leaves while the *nia1* line had an increased proportion of assimilation in roots, consistent with known ratios of wild-type *NIA1* and *NIA2* gene expression levels. Higher whole-plant $\delta^{15}\text{N}$ was found in the *nrt2* line suggesting more efflux of unassimilated nitrate back to the rooting medium,

possibly resulting from decreased symplastic intercellular movement of nitrate within the root.

In the second approach, the IMB model was tested by comparing it to compartmental analysis of tracer efflux (CATE) using stable isotope tracing to determine N efflux/influx (E/I) in balsam poplar roots. Both methods suggested E/I was much higher when plants were supplied with 0.5 mM ammonium rather than 0.5 mM nitrate. However, E/I was estimated to be approximately 33-50% lower when using the CATE method. The CATE method indicated that E/I averaged 0.4 and 0.22 for ammonium and nitrate, while the IMB model estimated E/I to be 0.65 and 0.45, respectively. The authors suggested that these discrepancies could have been caused either by temporal differences in N uptake patterns, or by the use of discrimination factors that were too low in the IMB model. When the discrimination factor for the assimilatory enzymes was increased to 22‰, there was much better concurrence between E/I estimated by CATE and by the IMB model, suggesting that discrimination factors for NR and GS may currently be underestimated.

Nitrate that is not lost in efflux is either assimilated in the roots or translocated to shoots through the xylem (Cui *et al.* 2020), in whole or in part (Figure 1.1). Several authors have suggested that measurements of $\delta^{15}\text{N}$ values in xylem sap would be valuable (Raven 1987; Robinson 2001; Kalcsits *et al.* 2014). For example, if xylem nitrate were to have the same isotopic composition as source nitrate provided to the roots, then the clear implication would be that there is either no discrimination *in vivo* or no assimilation in the roots. On the other hand, if xylem sap were to contain unassimilated but enriched nitrate, then there must be discrimination during partial assimilation in the root. The IMB model, at its core, predicts the N isotopic composition of xylem sap under these conditions. Therefore, a key test of the model is to investigate the isotopic composition of inorganic and organic N forms in xylem sap under conditions expected to

influence N assimilation and allocation in particular ways. Because xylem loading of organic and inorganic nitrogen occurs continuously in the roots, xylem sap analysis should constitute a proxy sampling of the instantaneous product and remaining substrate during nitrate assimilation in the roots. If so, the difference in isotopic composition between organic N and nitrate would approximate the discrimination factor associated with NR. Therefore, in the first part of my thesis, I set out to measure the $\delta^{15}\text{N}$ values of organic and inorganic N in the xylem sap as a critical test of the IMB model. If the IMB model prediction is correct, the $\delta^{15}\text{N}$ difference between inorganic and organic N in xylem sap should be greater than or equal to $\sim 15\text{‰}$. As a further test, the IMB model also predicts the proportions of N translocated in organic and inorganic form, which should be equal to the ratio of the organic and inorganic N concentrations measurable within the xylem sap.

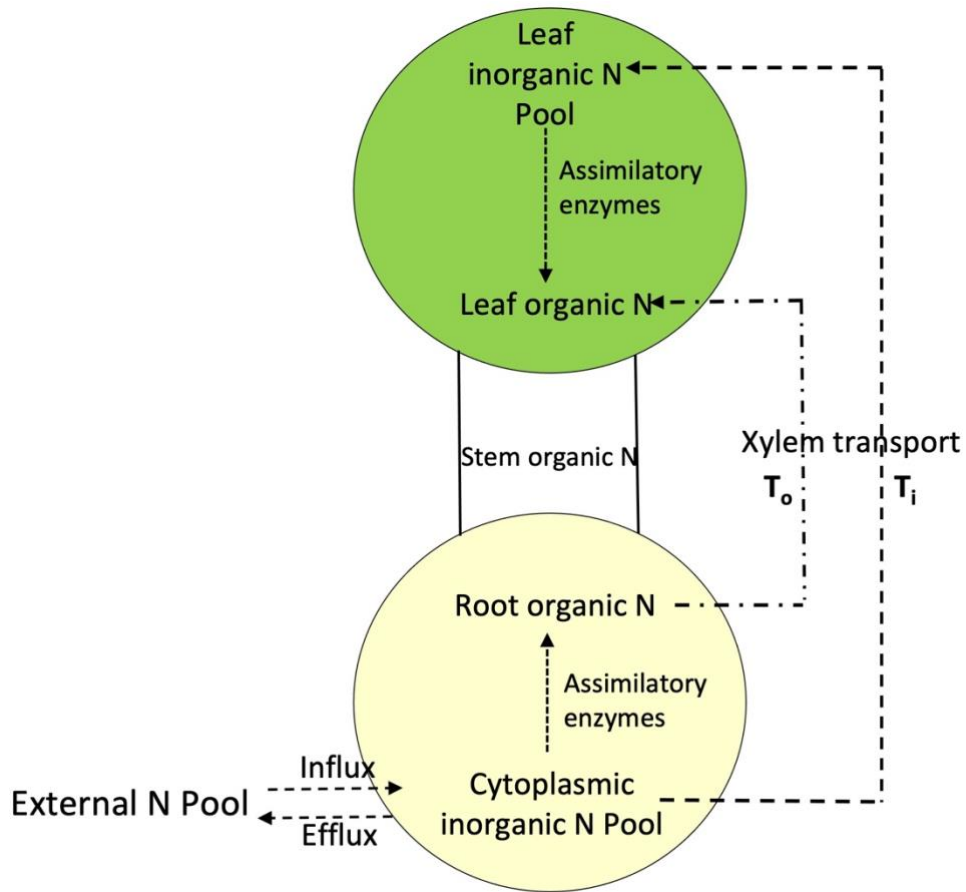


Figure 1.1. Diagram of plant nitrogen fluxes during the uptake of inorganic nitrogen from the substrate pool and assimilation into either root or leaf organic nitrogen as proposed in the isotope mass balance model. Arrows refer to unidirectional fluxes of nitrogen between leaf (green) and root (yellow) pools. T_o represents the organic nitrogen translocated to the leaves and T_i represents the inorganic nitrogen translocated to the leaves. Stem tissue is assumed to arise from a mixture of leaf and root organic pools.

1.6 Model application

Following model validation and refinement, the IMB model can be used on a grander scale. Species with large natural habitats may encounter divergent selection pressures because of wide variation in environmental factors, such as temperature, precipitation, growing season length, photoperiod, and soil nutrient conditions, resulting in environment-correlated intraspecific variation (Eckert and Dyer 2012; McKown *et al.* 2014a). Study of particular traits and how they vary can be used to examine the evolution of these traits and test adaptive hypothesis. For example, nitrogen and water are usually the most limiting resources for plants in temperate and boreal ecosystems; consequently, selective pressure towards maximization their respective use efficiencies is expected (Weih *et al.* 2006).

Though much is known about biogeographic variation in forest trees, there have been fewer studies focusing on N isotope discrimination, and clearly this area needs further research. Kalcsits and Guy (2016b) found significant genetic variation in N isotope discrimination in balsam poplar grown hydroponically, both within and between populations. There was no particular biogeographic pattern with provenance of origin, but only a very limited number of populations were sampled (just five). Genotypic variation within populations exceeded variation between populations. They also found that whole-plant N isotope discrimination of nitrate- and ammonium-grown plants was correlated across genotypes, implying that the genetic variation in $\delta^{15}\text{N}$ was affected by additional factors that are not N-source specific (e.g., such as root-to-shoot [R:S] ratio). There is a gap in knowledge between measurement of N-use under controlled conditions that limits the extension of results to field conditions. For instance, a large common garden assessment of phenotypic trait variation in black cottonwood reported 0.08 broad-sense heritability in leaf $\delta^{15}\text{N}$, suggesting very little inherent variation in $\delta^{15}\text{N}$

(McKown *et al.* 2014). Although this study assessed 461 genotypes from 136 provenances, the level of genetic variation in $\delta^{15}\text{N}$ was much lower than observed by Kalcsits and Guy (2016b), which is likely attributable to spatial variation in soil $\delta^{15}\text{N}$ and, most importantly, the fact that whole-plant discrimination cannot be expressed if the utilization of available soil N approaches completion (*i.e.*, if unused N cannot diffuse away from the roots before being consumed). Therefore, assessment of plant $\delta^{15}\text{N}$ using a decent number of genotypes from multiple provenances under tightly controlled hydroponic conditions is needed.

Both the efficiency of N use (NUE, carbon fixed per unit N assimilated) and the efficiency of water use (WUE, carbon fixed per unit water transpired) are tied to the diffusion gradient for CO_2 into the leaf through stomata. Most water used by plants is in support of photosynthesis by way of transpiration. More than half of total leaf N is related to photosynthesis (Evans 1989), and total leaf N content and photosynthetic capacity are typically correlated (Field and Mooney 1986, Larcher 2003). Reductions in stomatal conductance (g_s) or higher investments in foliar N can result in higher WUE if the CO_2 diffusion gradient steepens, but lower intercellular CO_2 concentrations may reduce NUE by reducing rates of C fixation per unit N. A negative correlation between WUE and NUE is implied, suggesting an evolutionary trade-off. However, changes in mesophyll conductance (g_m) should impact WUE and NUE similarly and without trade-off because, in contrast to g_s , there is no effect of g_m on the diffusion of water vapor (Lauteri *et al.* 1997). Variation in sites of N assimilation and allocation within plants might also uncouple NUE from WUE, but in more indirect ways. For example, in *Populus*, when under N-limiting conditions, both fast- and slow-growing hybrids showed increased root surface area, decreased photosynthetic rate, and reduced NUE (Luo *et al.* 2015). The slow-growing hybrid (*Populus* × *popularis*) had an increased WUE, while the fast-growing hybrid (*Populus alba* × *Populus glandulosa*) had a decreased WUE. Because

similar differences may occur within species, it is unclear if a trade-off between WUE and NUE should be expected among locally adapted populations. Therefore, in this thesis, genotypic and population-level variations in $\delta^{15}\text{N}$, $\delta^{13}\text{C}$ (proxy for WUE), and C/N ratio (proxy for NUE) were explored from both common garden and hydroponics experiments.

Though very fundamental, our understanding of N uptake and assimilation is still incomplete, especially for trees. Uncovering the molecular and physiological basis for these complex traits is critical for breeding programs. In poplars, as well as other species of dual ecological and economic importance, there is great interest in establishing links between relevant phenotypes and genetic variation (Ingvarsson and Street 2010; McKown *et al.* 2018). Genome-wide association studies (GWAS) are widely used for this purpose and, in *Populus*, have implicated numerous genes in the control of various wood characteristics (Porth *et al.* 2013), stomatal patterning and bud-break phenology (McKown *et al.* 2014, 2018, 2019), which may contribute to local adaptation (Savolainen *et al.* 2013). Plant NUE is an inherently complex trait and GWAS in NUE-related traits has been widely used in crop plants, such as rice (*Oryza sativa* L.) (Tang *et al.* 2019), maize (*Zea mays* L.) (Ertiro *et al.* 2020), and barley (*Hordeum vulgare* L.) (Karunaratne *et al.* 2020). Associations with several high affinity nitrate or ammonium transporters were reported in these studies. So far, GWAS on $\delta^{15}\text{N}$ has been limited to black cottonwood (McKown *et al.* 2014) and at least three studies investigating soybean (*Glycine max* (L.) Merr.) (Dhanapal *et al.* 2015; Steketee *et al.* 2019; Bazzar *et al.* 2020). As expected, no significant associations were found for black cottonwood given that the trees were field-grown (as noted earlier). In contrast, numerous SNP associations have been found in soybean, despite also being field-grown (broad sense heritability of tissue $\delta^{15}\text{N}$ in soybean was 0.15 to 0.2). Soybean, however, is a N-fixing legume and, as such, plant $\delta^{15}\text{N}$ provides a measure of the amount of N obtained directly from the atmosphere

relative to what is taken up from the soil. To date, no GWAS has been published on $\delta^{15}\text{N}$ -related traits obtained on plants grown hydroponically. Furthermore, the many GWAS conducted on crop plants have not generally been done in the context of exploring the genetic underpinnings of natural biogeographic variation in N-use traits and the possibility of local adaptation.

1.7 Research objectives

For my thesis, the research objectives were:

1. Determine a time-integrated estimate of inorganic and organic nitrogen concentration and isotope composition in xylem sap
2. Explore intraspecific variation in isotopic composition of heart-leaved willow and black cottonwood
3. Apply GWAS with hydroponically grown black cottonwood to detect nitrogen isotope-related SNPs and genes

2. Isotopic composition and content of total nitrogen and nitrate in xylem sap under near steady-state hydroponics

2.1 Summary

After root uptake, nitrate is effluxed back to the medium, assimilated locally, or translocated to shoots. Rooted black cottonwood scions were supplied with a NO_3^- -based (0.5 mM) nutrient medium of known $\delta^{15}\text{N}$, and xylem sap was collected via a pressure bomb. To establish a sampling protocol, sap was collected from lower and upper stem sections at 0.1-0.2 MPa above the balancing pressure and after increasing the pressure by a further 0.5 MPa. Xylem sap from upper stem sections was partially diluted at higher pressure. Further analysis was restricted to sap obtained from intact shoots at low pressure. Total-, NO_3^- -N and, by difference, organic-N concentrations ranged from 6.1-11.0 mM, 1.2-2.4 mM, and 4.6-9.4 mM, while discrimination relative to the nutrient medium was -6.3 to 0.5‰, -23.3 to -11.5‰, and -1.3 to 4.9‰, respectively. There was diurnal variation in $\delta^{15}\text{N}$ of total- and organic-N, but not NO_3^- . The difference in $\delta^{15}\text{N}$ between xylem NO_3^- and organic-N suggests that discrimination by nitrate reductase is near $25.1 \pm 1.6\%$. When this value was used in an isotope mass balance model, the predicted xylem sap NO_3^- -N to total-N ratio closely matched direct measurement.

2.2 Introduction

Nitrogen is the primary limiting nutrient for most plants in terrestrial ecosystems (Glass *et al.* 2002). The various forms and pools of N in the environment, and in the plant, typically have differences in the relative abundance of ^{15}N ($\delta^{15}\text{N}$). These differences in isotopic composition are widely used in the study of N cycling in ecosystems and individual organisms (Dawson *et al.* 2002). However, interpretation of

variation in $\delta^{15}\text{N}$ at natural abundance levels can be problematic. For example, the $\delta^{15}\text{N}$ of an individual plant or one of its parts is not only determined by the external N source, of which there is often more than one, but also by internal physiological factors such as different N uptake mechanisms, different pathways of assimilation and transport, and the possibility of differential recycling of N within the plant, all of which may discriminate against ^{15}N (Robinson 2001). A better understanding of isotope discrimination that may or may not be associated with these various factors is needed before variation in $\delta^{15}\text{N}$ can be routinely used in ecological and/or physiological research.

Nitrogen sources in soils include nitrate, ammonium, and organic N. These are distributed unevenly in time and space in varying proportions that depend on profile position, local vegetation, climate, and many other edaphic factors (Amundson *et al.* 2003). For example, boreal forest soils generally have less inorganic N than temperate forest soils because of colder temperatures and slower rates of mineralization (Näsholm *et al.* 1998). Furthermore, because they are often acidic, boreal forest soils tend to have higher concentrations of ammonium than nitrate (Nordin *et al.* 2001). In contrast, temperate forest soils are relatively rich in nutrients with higher concentrations of nitrate (Lupi *et al.* 2013). Both nitrate and ammonium are taken up by roots, but nitrate must be converted to ammonium prior to assimilation into organic N. Nitrate enters root cells by diffusion or via a nitrate transporter across the plasma membrane and may then be converted to nitrite and then ammonium in the cytoplasm by NR and NiR, respectively. Therefore, the ammonium derived from nitrate is assimilated by GS. Both of the initial assimilatory enzymes (*i.e.*, NR in the case of nitrate, and GS in the case of ammonium) have considerable potential to affect plant $\delta^{15}\text{N}$ because they discriminate against ^{15}N relative to ^{14}N . Discrimination causes the product organic N to be depleted in ^{15}N relative to the original source, while the remaining unassimilated inorganic N

becomes enriched. Discrimination factors for GS and NR are poorly constrained, but have long been considered to be $\sim 17\text{‰}$ and $\sim 15\text{‰}$, respectively (Yoneyama *et al.* 1993; Ledgard *et al.* 1985). Other research, however, suggests that discrimination by NR is greater than 15‰ , in the range of $19\text{--}22\text{‰}$ (Yoneyama 2003; Needoba *et al.* 2004), or possibly even higher (Olleros-Izard 1983; Karsh *et al.* 2012).

After uptake, neither the assimilation of nitrate nor the assimilation of ammonium is quantitative. Unassimilated inorganic N (enriched in ^{15}N) either effluxes back into the rooting medium or is transported to the shoot together with organic N (Kalcsits and Guy 2013a). Efflux can be substantial, ranging from 19% to 79% of N initially taken up, depending on the substrate concentration, root maturity, and plant N demand (Kalcsits and Guy 2016a). Because effluxed N is enriched in ^{15}N , this process can cause plants to have total tissue, whole-plant $\delta^{15}\text{N}$ values that are negative relative to the source. Differential xylem transport of ^{15}N -depleted organic N and ^{15}N -enriched inorganic N can cause variation in $\delta^{15}\text{N}$ to occur at the organ level (*e.g.*, between roots and shoots). These differences are affected by the form of the source N (Kalcsits *et al.* 2015). Subsequent retranslocation and/or N losses associated with senescence, volatilization, or other processes may also cause variations in tissue $\delta^{15}\text{N}$ (Robinson *et al.* 1998).

Few connections between nitrogen-use physiology and nitrogen isotope discrimination have been established. Kalcsits and Guy (2014 & 2016b) presented an isotope mass balance (IMB) model that combines $\delta^{15}\text{N}$ ratios and tissue N contents. Net discrimination was suggested to be a function of inorganic N efflux back to the growing medium relative to gross uptake at the root (efflux/influx), the proportion of net uptake assimilated in the roots, and the export of remaining N for assimilation in the leaves. This deliberately simple model attempts to explain the relationship between N-use physiology and N isotope discrimination under steady-state hydroponic conditions in

young, rapidly growing plants where there is substantial N assimilation in the roots and there has been little opportunity for N remobilization between organs (e.g., from senescent tissues). Similarly, under these specific conditions, the return of N to the roots in either inorganic or organic form is of little consequence to the plant or organ level N budget and is ignored. However, Cui *et al.* (2020) have recently argued that the return of residual, unassimilated ^{15}N -enriched nitrate back to the roots via phloem transport can be isotopically significant in oil palm and sunflower, two species where N assimilation is primarily in the leaves. Since there is no evidence for significant isotope discrimination associated with membrane transport (Handley and Raven 1992; Evans 2001), the IMB model considers the cytosolic and vacuolar nitrate pools within root cells to be in isotopic equilibrium, and similarly, that there is no discrimination during xylem loading. Furthermore, unless roots are damaged and the endodermis is breached, all nitrate entering the xylem must pass through some portion of the symplast.

Under the above conditions, xylem sap analysis should constitute a proxy sampling of the $\delta^{15}\text{N}$ of instantaneous product and residual substrate remaining during nitrate assimilation by nitrate reductase, and thus the difference in isotopic composition between organic nitrogen and nitrate would approximate the discrimination factor associated with nitrate reductase. I set out to test this hypothesis in rooted black cottonwood scions given access to a very large nitrate supply at a realistic concentration (0.5 mM). Cottonwoods are ideal to our purposes because of their rapid growth, woody stems to yield relatively high volumes of xylem sap free of contamination from phloem, propensity for root-based N assimilation (Dluzniewska *et al.* 2006), and their use of glutamine as the main constituent of organic N in xylem transport (Escher *et al.* 2004; Millard *et al.* 2006). My first objective was to validate my xylem sap collection protocol; *i.e.*, by testing the effects of collection pressure and sampling position on xylem sap composition. The second objective was to quantify the concentration and isotopic

composition of inorganic and organic N in xylem sap and explore possible diurnal variation. Towards validation of the IMB model, my third objective was to compare direct measurement of xylem sap nitrate- and organic-N concentrations with model predictions.

2.3 Material and Methods

2.3.1 Plant material and experiment design

First year scions from black cottonwood genotypes (Table 2.1) originally collected by the British Columbia Ministry of Forests, Lands and Natural Resource Operations were obtained in early February from a stool bed at Totem Field, University of British Columbia (UBC), Vancouver, Canada. My reasoning to include different genotypes of black cottonwood from a large part of its natural range was to ensure that results would be reasonably representative of the species as a whole. Scions were stored in black plastic bags at 4°C for 4 months until used in two experiments. Single-node scions, approximately 3 cm long, were rooted in distilled water and then transferred to a hydroponic system in the UBC Horticulture greenhouse. The first experiment used three genotypes with 20 rooted scions per genotype to test the influence of sampling position (lower and upper shoot sections)¹ and xylem sap collection pressure (0-1 and 1-1.5 MPa) on xylem sap N concentration and $\delta^{15}\text{N}$. Different sampling positions were used to check the stability of the xylem sap composition along the transport pathway. The second experiment, employing five genotypes with 25 rooted scions per genotype, was performed to check for possible diurnal patterns in xylem sap N concentration and $\delta^{15}\text{N}$,

¹ Xylem sap from decapitated root systems was similarly collected but found to be contaminated with hydroponic solution (see Appendix Figure A.1).

and to compare these measured quantities with model predictions from plant tissue analysis.

Table 2.1. Genotypes of black cottonwood (*Populus trichocarpa*) used in this study

Genotype	Latitude (°N)	Longitude (°W)	Elevation (m)
BELA4 ^{a,b}	52.42	126.17	152
CARS2 ^a	45.75	122.83	650
CARS4 ^b	45.75	122.83	650
FNYI4 ^b	49.52	124.85	46
HALS2 ^b	44.42	123.33	300
STHA3 ^b	50.82	124.48	239
NECA4 ^a	54.10	124.43	747

First four letters are the abbreviation for provenances and the last number are the genotype replicates within the provenance; ^{a,b} indicates genotypes included in experiment one (^a) or two (^b).

2.3.2 Hydroponics system

The hydroponic system was comprised of four 150 L bench-mounted acrylic tubs, an 1800 L vertical ground tank (RK400; CANWEST, Surrey, Canada), two water pumps (Little Giant, Fort Wayne, IN, USA) and connecting PVC piping (1 inch diameter; WaterTec, Langley, BC, Canada). Each tub was covered by a floating “raft” made of dense foam bolted between black (lower) and white (upper) sheets of Perspex. Drilled holes (2.5 cm) fitted with partially slit foam plugs provided each raft with the capacity to hold up to 32 plants. One water pump sat in the bottom of the main tank and continuously circulated media to the four tubs. The depth of water in the tubs was set by an overflow outlet draining by gravity into a receiving reservoir at ground level containing the second pump (actuated by a float switch), which returned the media to the main tank. The total volume of the system was maintained at 2000 L. Unused plugs in rafts and other exposed parts of the circulation system were covered with white/black (upper/inner) plastic to prevent algal growth from light infiltration. The hydroponics solution was a modified 1/10th strength Johnson’s solution (Johnson *et al.* 1957) supplemented with 0.25 mM $\text{Ca}(\text{NO}_3)_2$. To ensure aeration of the entire system, an air pump was connected to an air stone in the receiving reservoir. Media NO_3^- concentration was assayed periodically using the perchloric acid (Cawse 1967) method. The intent was to ensure there was no substantial decrease (no more than 10%) in NO_3^- concentration over time that could result in major changes to the $\delta^{15}\text{N}$ of the hydroponics solution. The nutrient medium was completely replaced as necessary. The system was under ambient light conditions supplemented by LED lighting ($600 \mu\text{mol m}^{-2}\text{s}^{-1}$) on an 18/6 h day/night photoperiod. Temperatures in the greenhouse were maintained between 20-24°C to prevent overheating of the hydroponic solution, a 10 m cooling coil of ¼ inch stainless steel pipe was submersed in the main reservoir. Cold tap

water flowed through the coil under the control of a thermostated solenoid valve (Red-Hat, Brantford, ON, Canada).

2.3.3 Sampling and natural abundance isotope analysis

Experiment 1: Plants were grown hydroponically for 45 days before sampling. Sap was collected from 9:00-12:00 and 15:00-19:00 to avoid a period of reduced sap yield when water potential was lower during mid-day. To test the effect of sampling position on the nitrogen concentration and isotopic composition in the xylem sap, shoots were cut 0.5 cm above the root collar and then cut in two in the middle of the remaining section to provide two parts for pressure bombing: upper and lower shoot/stem sections. Stems were stripped of bark (~1 cm) near the cut end and placed into the pressure vessel of a 3005 Series Plant Water Status Console (Soilmoisture Equipment Corp., Goleta, CA, USA). The distal ends of lower stem sections were sealed with Blu Tack putty adhesive (Bostik, Paris, France) to prevent the direct entry of air, and the resulting loss of pressurization and loss of sample caused by sputtering and aspiration (presumably because larger, continuous vessels discharge readily, while most others do not). Xylem sap was collected as described in Dluzniewsk *et al.* (2006), where the pressure was raised to ~0.6-0.7 MPa higher than the initial balancing pressure (~0.8-0.9 MPa), but in two stages. In the first, low pressure stage (LP), the initial drop of water was discarded to avoid contamination and the pressure was increased to 1.0 MPa; *i.e.*, by an increment of just 0.1-0.2 MPa. In the second, higher pressure stage (HP), additional sap was collected as the pressure was raised from 1.0 to 1.5 MPa. There were 60 plants in total, but samples were pooled from 10 individuals to provide enough volume for analysis (*i.e.*, $n = 6$ for each shoot part). Sap samples were stored at -20°C until analysis.

Experiment 2: After 45 days of growth, xylem sap was collected from intact (*i.e.*, unsegmented) shoots at five time “points” over a diurnal cycle (*i.e.*, 1.5 h collection periods centered on 10:00, 15:00, 20:00, 0:00 and 4:00 h). Sap was collected from a total of 125 plants, but pooled from five individuals per genotype at each time point, yielding 25 samples for analysis. After the xylem sap was collected, plants were partitioned into leaves, stems, roots and original scions, and stored on ice until freeze-drying at -50°C for two days. Once dried, these plant parts were weighed and then ground to a fine powder using a Wiley mill followed by pulverization in a stainless-steel ball mill (Fritsch Laborgeratebau, Terochem Scientific, Ottawa, Canada). Sub-samples (3 mg) were packed into tin capsules (Elemental Microanalysis, Devon, UK) and analyzed for nitrogen concentration and $\delta^{15}\text{N}$ using an Elementar (Langensfeld, Germany) Vario EL Cube Elemental Analyzer (EA), in combination with an Isoprime (GV Instruments, Manchester, UK) Isotope Ratio Mass Spectrometer (IRMS) in the Stable Isotope Facility (SIF), Faculty of Forestry, UBC.

Aliquots of xylem sap (1 mL) were dried onto glass microfiber filter disks (Whatman GF/D) and analyzed for total nitrogen concentration and $\delta^{15}\text{N}$ as above. Additional 1 mL aliquots were used to analyze the concentration and $\delta^{15}\text{N}$ of nitrate after conversion to nitrous oxide (N_2O) by the bacterial denitrifying method (Sigman *et al.* 2001). Denitrifying *Pseudomonas aureofaciens* (American Type Culture Collection #13985; Manassas, VA, USA) was incubated for 7 days in a working medium of Tryptic Soy Broth (Difco) amended with KNO_3 , NH_4Cl , and KH_2PO_4 according to the method described by Casciotti *et al.* (2002) and Altieri *et al.* (2014). Before use, *P. aureofaciens* cells were concentrated by centrifugation (7500g, 18°C), and washed and resuspended in NO_3^- -free medium (4 mL). After sparging with N_2 , 2 mL of suspension and 1 mL of xylem sap were injected into a 10 mL crimp-sealed vial. Vials were incubated overnight at room temperature to allow for complete conversion of NO_3^- to N_2O before the

addition of 0.2 mL NaOH to stop the bacterial activity and scavenge CO₂. Incubated vials could be stored at -20°C for up to 5 days. The yield of N₂O was measured by injecting 2 mL of the headspace gas into a trace gas chromatograph (HP5890 Series II, Agilent, Santa Clara, CA, USA) equipped with an electron capture detector (GC/ECD). For δ¹⁵N determination, remaining N₂O in the headspace was cryofocused using a manually built purge-and-trap system (Ribas-Carbo *et al.* 2002) and introduced into a gas chromatograph (HP6890N, Santa Clara, CA, USA) interfaced to the same Isoprime IRMS.

2.3.4 Calculations

Nitrogen isotopic composition (δ¹⁵N) and isotope discrimination (Δ) are expressed as:

$$\delta^{15}\text{N} = \left(\frac{R_{\text{sample}}}{R_{\text{standard}}} - 1 \right) * 1000 \quad (2.1)$$

$$\Delta^{15}\text{N}_{\text{sample}} = \frac{(\delta^{15}\text{N}_{\text{source}} - \delta^{15}\text{N}_{\text{sample}})}{\left(1 + \frac{\delta^{15}\text{N}_{\text{sample}}}{1000}\right)} \quad (2.2)$$

where, R_{sample} and R_{standard} are the ¹⁵N/¹⁴N ratios of the sample and the arbitrary standard (air N₂), respectively. The δ¹⁵N value of the nitrate source used for the growth media was -1.69‰ in the first experiment and 63.81‰ in the second experiment. Tissue δ¹⁵N was corrected for contaminating N from old scions using the method described in Kalcsits and Guy (2013b).

I assume that ammonium synthesized from nitrate in the roots is rapidly assimilated into amino acids via the glutamine synthetase-glutamate synthase (GS-GOGAT) pathway, and any amount of ammonium loading to the xylem can be ignored. Therefore, the organic N concentration of xylem sap ($[No]_{\text{xylem}}$) was calculated by difference from the total N ($[Nt]_{\text{xylem}}$) and nitrate-N ($[Ni]_{\text{xylem}}$) concentrations:

$$[No]_{\text{xylem}} = [Nt]_{\text{xylem}} - [Ni]_{\text{xylem}} \quad (2.3)$$

The $\delta^{15}\text{N}$ of the organic N in xylem sap ($\delta^{15}\text{N}_{\text{organic}}$) was calculated by mass balance from the total $\delta^{15}\text{N}$ value ($\delta^{15}\text{N}_{\text{total}}$) and the nitrate-N $\delta^{15}\text{N}$ value ($\delta^{15}\text{N}_{\text{nitrate}}$):

$$\delta^{15}\text{N}_{\text{organic}} = (\delta^{15}\text{N}_{\text{total}} \times [\text{Nt}]_{\text{xylem}} - \delta^{15}\text{N}_{\text{nitrate}} \times [\text{Ni}]_{\text{xylem}}) / [\text{No}]_{\text{xylem}} \quad (2.4)$$

Plants were divided into three major parts (root, stem, and leaf), and the whole-plant isotope discrimination was calculated as the weighted sum of these parts:

$$\Delta^{15}\text{N}_{\text{whole plant}} = (f_{\text{root}} \times \Delta^{15}\text{N}_{\text{root}}) + (f_{\text{stem}} \times \Delta^{15}\text{N}_{\text{stem}}) + (f_{\text{leaf}} \times \Delta^{15}\text{N}_{\text{leaf}}) \quad (2.5)$$

where, $\Delta^{15}\text{N}_i$ is the discrimination and f_i is equal to the fraction of tissue nitrogen contributing to overall plant nitrogen content.

The proportion of nitrate assimilated in the roots was defined as P_{root} , expressed as a fraction. Assuming all nitrogen translocated from roots to shoots (leaves, stems) remained in the shoots, then the minimum P_{root} based on the measurement in the xylem sap and tissue nitrogen content can be calculated as:

$$P_{\text{root measured}} = 1 - \left((f_{\text{stem}} + f_{\text{leaf}}) \times [\text{Ni}] / [\text{Nt}]_{\text{xylem}} \right) \quad (2.6)$$

The percent ratio of inorganic nitrogen (Ti) relative to total nitrogen (Tt) translocated to the leaves (Ti/Tt), as predicted by the IMB model (Kalcsits *et al.* 2014), was calculated as:

$$\frac{Ti}{Tt} = \frac{(\Delta^{15}\text{N}_{\text{leaf}} - \Delta^{15}\text{N}_{\text{root}})}{\Delta_{\text{enzyme}}} * 100 \quad (2.7)$$

where, Δ_{enzyme} is the discrimination factor for NR. Ti/Tt was compared to the ratio of inorganic nitrogen relative to total nitrogen in the xylem (Ni/Nt), based on the measurement of $[\text{Ni}]_{\text{xylem}}$ and $[\text{Nt}]_{\text{xylem}}$.

Assuming leaves and roots are the major sites of nitrogen assimilation, the amount of stem N (relative to total plant N) that originates from the leaves ($f_{\text{stem-leaf}}$) is approximated by:

$$f_{stem-leaf} = \frac{\Delta^{15}N_{stem} - \Delta^{15}N_{root}}{\Delta^{15}N_{leaf} - \Delta^{15}N_{root}} \times f_{stem} \quad (2.8)$$

and the proportion of total plant nitrogen assigned to the leaf pool is:

$$f_{leaf\ pool} = f_{leaf} + f_{stem-leaf} \quad (2.9)$$

The proportion of total nitrogen assimilated in the leaves is the product of $f_{leaf\ pool}$ and T_i/T_t . The remaining proportion of plant nitrogen is, therefore, the total nitrogen assimilated in the roots ($P_{root\ predicted}$):

$$P_{root\ predicted} = 1 - \left(f_{leaf\ pool} \times \frac{T_i}{T_t} \right) \quad (2.10)$$

Efflux over influx (E/I) is then calculated as:

$$\frac{E}{I} = \frac{\Delta^{15}N_{plant}}{\Delta^{15}N_{enzyme} \times P_{root\ predicted}} \quad (2.11)$$

In essence, and unlike Cui *et al.* (2020) where isotope discrimination associated with efflux is considered fixed, equation (11) rearranged yields whole-plant isotope discrimination as a function of the exchange of cellular nitrate with the external source. This is similar to the accepted model for carbon isotope discrimination during CO₂ fixation in photosynthesis (Farquhar *et al.* 1989).

2.3.4 Statistics

For xylem sap samples, concentration and $\delta^{15}N$ of total nitrogen, nitrate and organic nitrogen were compared using a two-way ANOVA in R (R Core Development Team, 2011) with position and pressure as fixed effects in the first experiment, and with time and genotype as fixed effects in the second experiment. The statistical model was as follows:

$$Y_{ij} = \mu + \alpha_i + \tau_j + \beta_{ij} \quad (2.12)$$

where, μ is the overall mean response, α_i is the effect due to position in Expt. 1 and time in Expt. 2, τ_j is the effect due to pressure in Expt. 1 and genotype in Expt. 2, and β_{ij} is the effect due to any interaction between the position and pressure in Expt. 1 and time and genotype in Expt. 2. Genotype effects on plant biomass, whole-plant and tissue nitrogen concentrations, and whole-plant and tissue $\delta^{15}\text{N}$ were tested by one-way ANOVA:

$$Y_i = \mu + \alpha_i \quad (2.13)$$

where, μ is the overall mean response and α_i is the effect due to genotype. Statistical differences were assessed using Tukey's multiple comparison tests.

2.4 Results

2.4.1 Nitrogen concentration and $\delta^{15}\text{N}$ in xylem sap

Both total N and NO_3^- concentrations of xylem sap were higher than the source hydroponic medium (Figure 2.1a,b). Collection pressure had a significant effect but sampling position did not. The average xylem total N concentration was 6.87 ± 0.57 mM, which was more than 13 times higher than the source medium N concentration (0.5 mM) (Figure 2.1a). The mean xylem NO_3^- concentration was 1.42 ± 0.08 mM (Figure 2.1b). Both total N and NO_3^- in xylem sap were enriched in ^{15}N relative to the source medium (Figure 2.1c,d), by $2.46 \pm 0.57\%$ and $21.42 \pm 0.88\%$, respectively. As was the case with N concentrations, sampling position had no significant effect on isotopic composition. Although collection pressure did not significantly affect the $\delta^{15}\text{N}$ of total N, the $\delta^{15}\text{N}$ of xylem NO_3^- was increased by $3.65 \pm 0.53\%$ at high pressure. In sum, xylem NO_3^- from lower and upper shoot sections was similar in concentration and N isotopic composition at low pressure, but higher pressure resulted in somewhat lower concentration and somewhat higher $\delta^{15}\text{N}$ of NO_3^- in xylem from the upper shoot (Figure 2.1b,d). The average NO_3^- concentration of xylem sap collected at low pressure was

1.64±0.10 mM. The average $\delta^{15}\text{N}$ of total N and NO_3^- in xylem sap collected at low pressure was 0.78±0.16‰ and 19.73±0.88‰, respectively (Figure 2.1c,d).

2.4.2 Estimated organic nitrogen concentration and $\delta^{15}\text{N}$ in xylem sap

The concentration and $\delta^{15}\text{N}$ of organic N in xylem sap, both determined by difference, were unaffected by either position or pressure (Figure 2.2). The average organic N concentration in xylem sap was 5.61±0.55 mM (Figure 2.2a), and the average $\delta^{15}\text{N}$ was -5.14±1.03‰, which was distinctly lower than the $\delta^{15}\text{N}$ of xylem sap total N and NO_3^- , or the source NO_3^- (Figure 2.2b). The average difference in $\delta^{15}\text{N}$ between the NO_3^- and organic N fractions in the xylem was 24.9±1.6‰ (or $\Delta = 25.1\pm 1.6\%$, as defined by Equation 2).

To explore possible genotypic variation, we calculated mean NO_3^- and total N concentrations and $\delta^{15}\text{N}$ values from xylem sap collected at low pressure for each genotype. The mean total N concentration in xylem sap ranged from 6.15 mM to 16.64 mM, with an overall mean across all genotypes of 8.41±0.85 mM. The mean NO_3^- concentration in xylem sap ranged from 1.21 mM to 2.41 mM, with an overall average of 1.64±0.07 mM. Both total N and NO_3^- concentrations were not significant at the genotypic level. Nitrate, on average, accounted for 21±2.77% of total N in the xylem sap. Among the three randomly selected genotypes, only the $\delta^{15}\text{N}$ of NO_3^- showed a significant effect of genotype (Table 2.2).

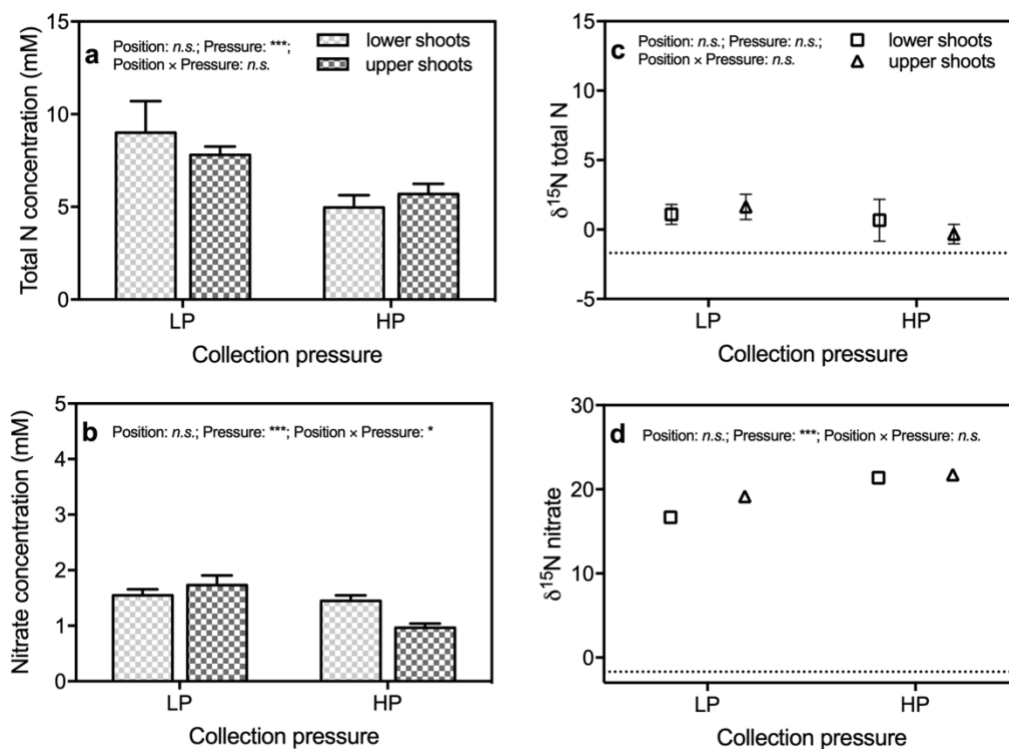


Figure 2.1. Concentrations of total N (a) and nitrate (b), and $\delta^{15}\text{N}$ of total N (c) and nitrate (d) in *Populus trichocarpa* xylem sap collected from lower and upper shoot sections at low pressure and higher pressure. Bars or symbols represent means of six samples ($\pm\text{SE}$; omitted from panel d because they are smaller than the symbol size). Effects of the main factors pressure or position, and their interaction, are indicated: *n.s.*, not significant; *, $P < 0.05$; **, $P < 0.01$; ***, $P < 0.001$. Dotted lines in panels c and d represent the $\delta^{15}\text{N}$ of NO_3^- in the hydroponic medium (-1.69‰).

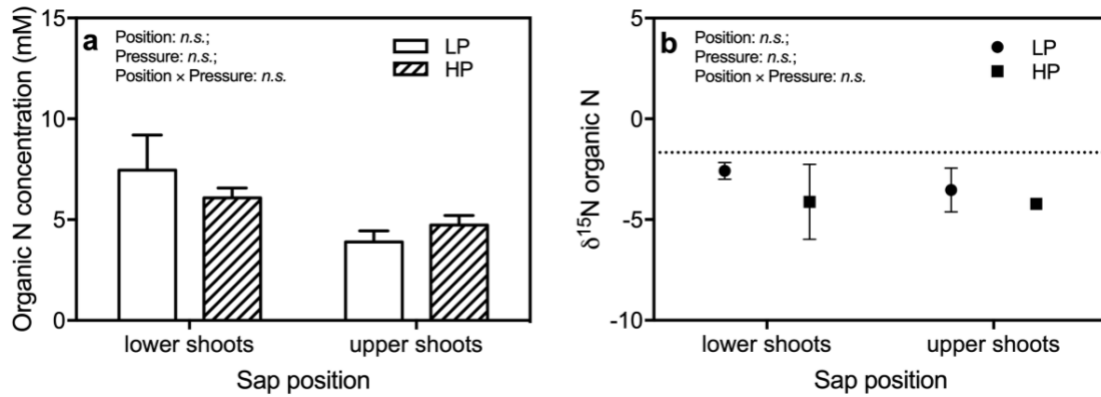


Figure 2.2. Estimated concentration (a) and $\delta^{15}\text{N}$ (b) of organic N in xylem sap collected from lower and upper shoot sections at low pressure and higher pressure. Bars or symbols represent means of six samples ($\pm\text{SE}$). The main factors pressure and position, and their interaction, were not significant (*n.s.*). Dotted line in panel b represents the $\delta^{15}\text{N}$ of NO_3^- in the hydroponic medium (-1.69‰).

Table 2.2. Concentrations and $\delta^{15}\text{N}$ values of total N (Nt) and nitrate (Ni) in xylem sap collected from the shoots of three genotypes of *Populus trichocarpa* hydroponically grown with NO_3^- . Mean values ($\pm\text{SE}$) are for four biological replicates, each representing pooled sap collected from 10 plants over the low pressure range. $[Ni]/[Nt]_{xylem}$ is the percent fraction of NO_3^- in the total N. Different letters indicate significant differences at $P<0.05$.

Genotypes	N concentration (mM)		$\delta^{15}\text{N}$ (‰)		$[Ni]/[Nt]_{xylem}$ (%)
	$[Nt]_{xylem}$	$[Ni]_{xylem}$	Total N	NO_3^-	
BELA4	5.58 \pm 0.53a	1.70 \pm 0.11a	1.96 \pm 1.14a	15.30 \pm 1.73b	22.76 \pm 2.04a
CARS4	8.68 \pm 2.56a	1.85 \pm 0.28a	0.33 \pm 1.84a	20.06 \pm 1.73a	23.27 \pm 3.99a
NECA4	6.69 \pm 1.31a	1.37 \pm 0.09a	0.34 \pm 0.71a	21.73 \pm 1.26a	17.49 \pm 2.11a

2.4.3 Diurnal pattern in nitrogen isotope discrimination in xylem sap

To explore possible diurnal variation in N concentration and $\delta^{15}\text{N}$ during xylem transport, a second experiment was conducted where xylem sap was collected from five black cottonwood genotypes at five different time points over a 24 h cycle. Three time points were during the day (10:00, 15:00 and 20:00 h), and two time points were during the night (4:00 and 24:00 h). Data pooled across genotypes for concentrations and $\delta^{15}\text{N}$ of total N, NO_3^- , and estimated organic N are shown in Figure 2.3. There was no diurnal pattern in total N concentration (Figure 2.3a). The overall average total N concentration was 6.60 ± 0.48 mM. Time of sampling was almost but not quite significant for NO_3^- concentration ($P=0.067$) (Figure 2.3b). However, when daytime and nighttime values were considered separately, lower NO_3^- concentrations were detected during the day ($P=0.015$). The average day vs. night concentration of NO_3^- was 1.41 ± 0.20 mM vs. 2.31 ± 0.32 mM, respectively. The overall average NO_3^- concentration over the full 24 h cycle was 1.78 ± 0.17 mM. There was no significant effect of time on the concentration of estimated organic N (Figure 2.3c). The overall average organic N concentration was 4.88 ± 0.46 mM.

In contrast to concentration, the $\delta^{15}\text{N}$ of total N and the organic N of which it was mostly comprised, showed significant diurnal variation (Figure 2.3d,f). The $\delta^{15}\text{N}$ values of total and organic N were heavier at night than during the day by approximately 2.9 and 2.0‰, respectively. On the other hand, the isotopic composition of xylem NO_3^- was very consistent (Figure 2.3e) and enriched relative to the source media by an overall average of 11.7‰.

Genotypic means for concentration and $\delta^{15}\text{N}$ values of total N, nitrate, and organic N in the xylem sap are presented in Table 2.3. Significant differences between

genotypes were found only in the $\delta^{15}\text{N}$ of NO_3^- . There were no differences in total N, nitrate, and organic N concentrations or in $\delta^{15}\text{N}$ values of total N and organic N.

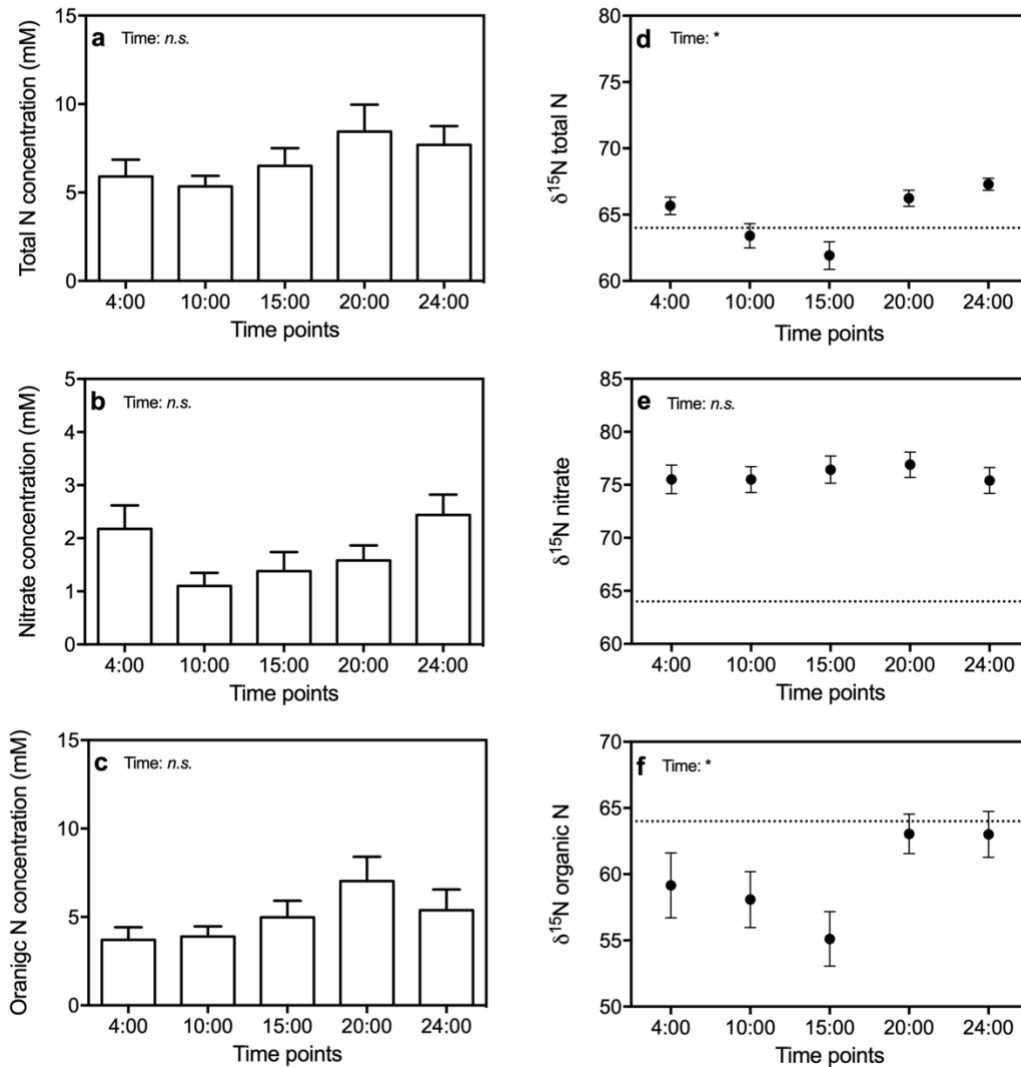


Figure 2.3. Diurnal patterns in concentrations of total N (a), nitrate (b) and organic N (c), and $\delta^{15}\text{N}$ of total N (d), nitrate (e) and organic N (f) in xylem sap of *Populus trichocarpa*. Bars or symbols represent means of 10 samples ($\pm\text{SE}$). Effects of the main factor time are indicated: *n.s.*, not significant; *, $P < 0.05$; **, $P < 0.01$; ***, $P < 0.001$. Dotted lines in panels d, e and f represent the $\delta^{15}\text{N}$ of nitrate in the hydroponic medium (63.81‰).

Table 2.3. Concentrations and $\delta^{15}\text{N}$ values of total N (*Nt*), nitrate (*Ni*) and organic nitrogen (*No*) in xylem sap collected from the shoots of five genotypes of *Populus trichocarpa* hydroponically grown with NO_3^- . Mean values ($\pm\text{SE}$) are for five biological replicates, each representing pooled sap expressed from 10 plants over the 0-1 MPa range. Different letters indicate significant differences at $P<0.05$.

Genotype	N concentration (mM)			$\delta^{15}\text{N}$ (‰)		
	$[\text{Nt}]_{\text{xylem}}$	$[\text{Ni}]_{\text{xylem}}$	$[\text{No}]_{\text{xylem}}$	Total N	NO_3^-	Organic N
BELA 4	5.87 \pm 1.12a	1.84 \pm 0.43a	4.50 \pm 1.11a	64.7 \pm 0.78a	74.6 \pm 1.03ab	60.5 \pm 1.20a
CARS 2	5.63 \pm 0.92a	1.87 \pm 0.47a	3.89 \pm 0.63a	64.8 \pm 1.03a	76.7 \pm 0.98ab	59.9 \pm 1.54a
FNYI 4	7.76 \pm 0.77a	2.13 \pm 0.32a	6.83 \pm 0.97a	64.9 \pm 0.89a	77.9 \pm 1.12ab	60.6 \pm 1.36a
HALS 2	6.25 \pm 0.78a	2.70 \pm 0.92a	2.89 \pm 0.52a	66.6 \pm 0.66a	72.8 \pm 1.05b	60.3 \pm 1.96a
STHA 3	5.01 \pm 0.97a	1.17 \pm 0.30a	3.77 \pm 0.83a	65.2 \pm 0.71a	77.1 \pm 1.52a	55.4 \pm 3.51a

2.4.4 Plant tissue discrimination and IMB model prediction

To compare predicted and actual N isotope compositions during transport in xylem vessels, plant tissue samples were analyzed and $\Delta^{15}\text{N}$ calculated for whole-plants, roots, stems and leaves, was compared across five genotypes (Figure 2.4). Only root $\Delta^{15}\text{N}$ showed a significant difference between genotypes. The STHA3 genotype had the highest root as well as whole-plant $\Delta^{15}\text{N}$ values. Roots in general had the highest $\Delta^{15}\text{N}$ (averaging 7.07‰ across all genotypes), whereas leaves had the lowest $\Delta^{15}\text{N}$ (averaging 0.29‰). Since roots only accounted for ~15% of the total N content, whole-plant $\Delta^{15}\text{N}$ (averaging 1.66‰) more closely reflects the stems and leaves.

The predicted proportion of inorganic N to total N in xylem sap (Ti/Tt), calculated from the leaf and root tissue $\Delta^{15}\text{N}$ values as per Equation 7, was compared to the measured proportion of NO_3^- to total N (Ni/Nt) in the actual xylem sap samples (Table 2.4). The mean Ni/Nt was 26.60%. When the discrimination factor for NR (Δ_{enzyme}) was set at 15.4‰, the average predicted Ti/Tt was $44.08 \pm 2.15\%$, or 1.66 times the measured Ni/Nt . When Δ_{enzyme} was adjusted to 25.1‰, the average predicted Ti/Tt was $27.04 \pm 1.29\%$, which is very similar to the measured Ni/Nt . Subsequently, using Equations 10 and 11, the proportion of total nitrogen assimilated in the root ($P_{root\ predicted}$) and efflux/influx (E/I) were calculated based on a Δ_{enzyme} of 25.1‰ (Figure 2.5). E/I ranged from 0.06 to 0.34 and no significant genotypic effect was found ($P=0.74$). $P_{root\ predicted}$ ranged from 78 to 86% (*i.e.*, only 14-22% of the retained NO_3^- was shoot-assimilated) and $P_{root\ measured}$ ranged from 73 to 85%. The correlation between $P_{root\ predicted}$ and $P_{root\ measured}$ was significant ($P=0.05$). Genotypic variation was found both in $P_{root\ predicted}$ ($P=0.02$) and $P_{root\ measured}$ ($P<0.01$). The HALS2 genotype had the highest $P_{root\ predicted}$ and $P_{root\ measured}$ values.

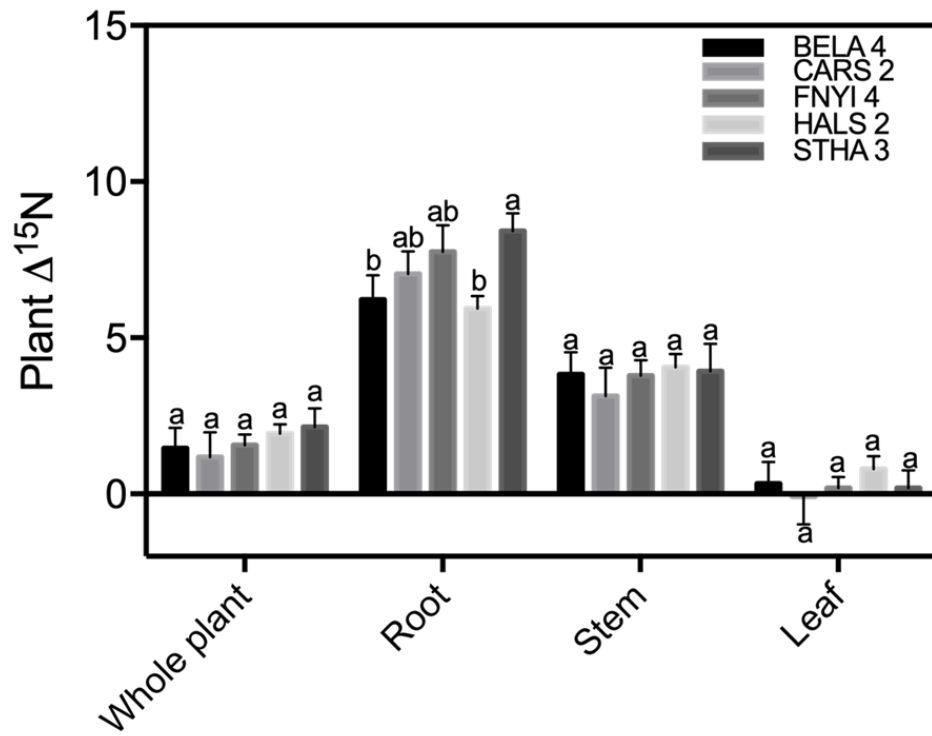


Figure 2.4. Whole-plant and organ level discrimination ($\Delta^{15}\text{N}$) in five genotypes of *Populus trichocarpa* in Experiment 2. Shown are means \pm SE ($n=5$). Different letters indicate significant difference between genotypes at $P < 0.05$.

Table 2.4 Percentages of NO_3^- (Ni) in total nitrogen (Nt) in xylem sap as directly measured after collection ($[Ni]/[Nt]$) or estimated percentage of inorganic nitrogen (Ti) relative to total nitrogen (Tt) translocated to the leaves (Ti/Tt) from the isotope mass balance (IMB) model for *Populus trichocarpa* genotypes grown under 0.5 mM NO_3^- for 45 days. Model predictions of Ti/Tt are given for calculations where discrimination (Δ) by nitrate reductase is taken to be either 15.4‰ or 25.1‰. Data are means \pm SE ($n=5-10$). Different individual ramets were used for sap collection and for model analysis.

Genotypes	Xylem collection	IMB prediction	
	$[Ni]/[Nt]$ (%)	Ti/Tt (%) $\Delta=15.4\text{‰}$	Ti/Tt (%) $\Delta=25.1\text{‰}$
BELA 4	26.35 \pm 1.02a	38.24 \pm 3.32ab	23.46 \pm 1.99ab
CARS 2	30.85 \pm 1.65a	46.22 \pm 5.05ab	28.36 \pm 3.03ab
FNYI 4	24.12 \pm 1.02a	49.13 \pm 3.97a	30.14 \pm 2.38a
HALS 2	21.68 \pm 3.94a	33.35 \pm 3.06b	20.46 \pm 1.83b
STHA 3	26.31 \pm 1.70a	53.44 \pm 2.66a	32.79 \pm 1.59a
Overall Mean	26.60 \pm 2.04	44.08 \pm 2.15	27.04 \pm 1.29

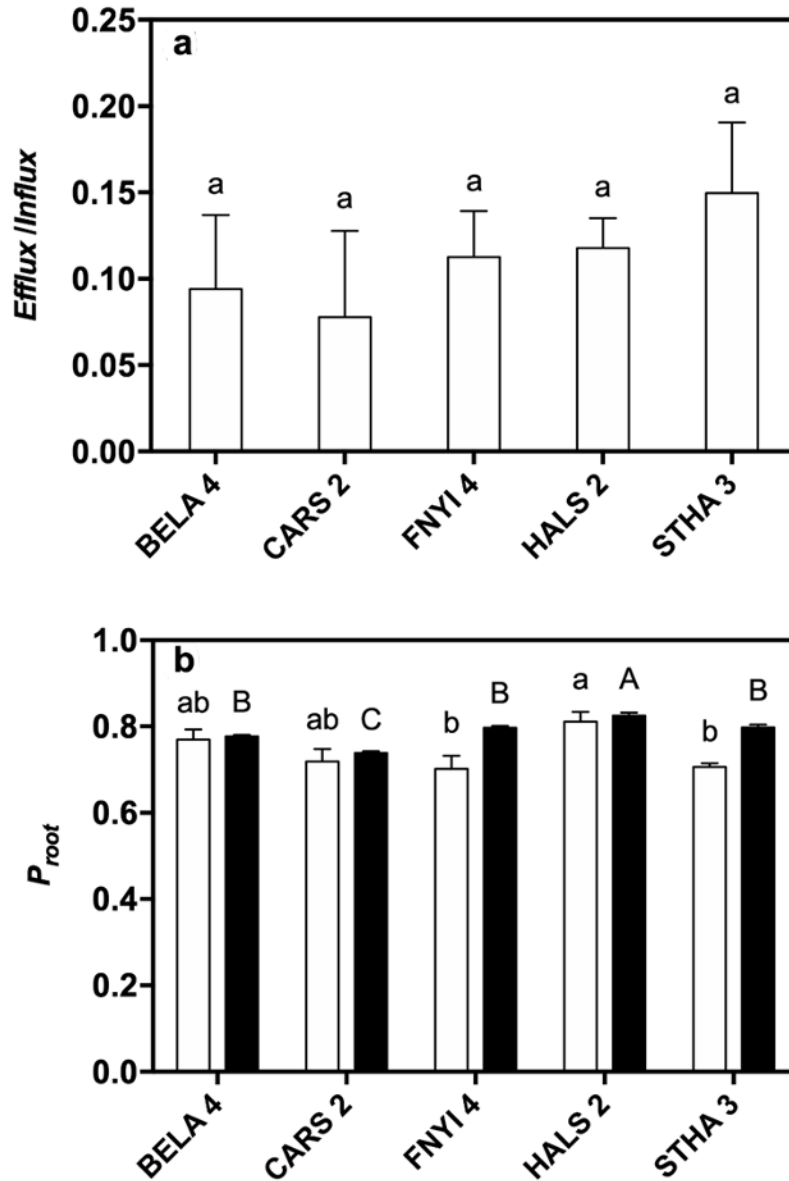


Figure 2.5. Model-derived efflux/influx (E/I , upper panel) and the proportion of nitrogen assimilated in the root (P_{root} , lower panel) of five genotypes of *Populus trichocarpa*.

Empty bars are based on tissue $\delta^{15}\text{N}$ values assuming Δ_{enzyme} is 25.1‰ (i.e., P_{root} predicted via Equations (2.7) and (2.10)) and solid bars are based on measurements of xylem sap N content (P_{root} measured from Equation (2.6)). Both estimates of P_{root} also rely on the same tissue N content data, so some autocorrelation is expected. Shown are means \pm SE ($n=5$).

Different letters indicate significant differences between genotypes at $P < 0.05$.

2.5 Discussion

2.5.1 Whole-plant and organ level variation in $\delta^{15}\text{N}$

There are three major fates for nitrate taken up by roots, including 1) local assimilation in the roots, 2) translocation to the shoot via the xylem, and 3) efflux back to the growing medium. In the present study, the averaged whole-plant $\Delta^{15}\text{N}$ was 1.66‰, indicating that $^{14}\text{NO}_3^-$ was preferentially assimilated in the roots and a greater proportion of the $^{15}\text{NO}_3^-$ was returned to the hydroponic medium. Similar to the results of Kalcsits and Guy (2013b) for the closely related *Populus balsamifera* L. (balsam poplar), and many other species (Cui *et al.* 2020), I found leaves to have higher $\delta^{15}\text{N}$ values (*i.e.*, lower $\Delta^{15}\text{N}$; Figure 2.4) than roots. This is the expected pattern if residual unassimilated NO_3^- (enriched in ^{15}N) is transported from roots to shoots. The average $\Delta^{15}\text{N}$ of leaves was close to 0 (*i.e.*, leaf $\delta^{15}\text{N}$ values were similar to the hydroponic source $\delta^{15}\text{N}$). Stems were in between and, knowing there was no significant direct NO_3^- assimilation from the xylem stream, must have obtained most of their nitrogen in organic form from both roots and leaves. I estimate that, on average, the fraction of stem nitrogen obtained from the leaves (*i.e.*, $f_{\text{stem-leaf}}$) was 46%, with the remaining 54% originating as organic N directly from the roots.

Kalcsits and Guy (2016b) reported organ level genotypic variation in $\Delta^{15}\text{N}$ in balsam poplar. In the present study with black cottonwood and the same media NO_3^- concentration (0.5 mM), I detected modest organ level genotypic variation in $\Delta^{15}\text{N}$, and in $\delta^{15}\text{N}$ of xylem NO_3^- . In contrast to black cottonwood, however, Kalcsits and Guy (2016b) reported that balsam poplar leaves were enriched in ^{15}N by ~4.42‰ relative to the hydroponic source, whereas here the enrichment was only 0.29‰. Indeed, roots, stems, and whole-plant $\Delta^{15}\text{N}$ were all greater in balsam poplar than in black cottonwood. Pending a direct comparison in a common hydroponic experiment, these

differences suggest that root-shoot partitioning of nitrogen assimilation is similar in the two species, but E/I may be considerably higher in balsam poplar.

2.5.2 $\delta^{15}\text{N}$ of total soluble organic N, NO_3^- and organic N of root tissue

Because nitrate reductase discriminates against $^{15}\text{NO}_3^-$ relative to $^{14}\text{NO}_3^-$, the ^{15}N content of glutamine and, in sum, all organic N-containing products derived from it, will be lower than the ^{15}N content of the available substrate at the site of reaction. Accordingly, there are consistent differences in $\delta^{15}\text{N}$ values of bulk tissue, total soluble organic N, NO_3^- and total organic N in roots of black cottonwood (Appendix Table A.2). The difference in $\delta^{15}\text{N}$ between nitrate-N and organic-N suggests that the discrimination factor associated with nitrate assimilation $\sim 18.2\text{‰}$. However, accounting for some contribution from isotopically lighter medium-sourced nitrate clinging to the roots or in the apoplastic space of the cortex would increase this value somewhat. Using leaf tissue, Yoneyama *et al.* (2003) and Cui *et al.* (2020) employed similar approaches to obtain values of 19‰ and 16.8‰, respectively.

Since root inorganic nitrogen in the cytoplasm is the source for inorganic nitrogen loaded into the xylem, NO_3^- loaded into the xylem sap should have a similar isotopic composition. Organic N loaded into the xylem is expected to be depleted in ^{15}N relative to cytoplasmic or xylem sap NO_3^- . Within the xylem, a broad spectrum of transported amino acids and other N-compounds has been reported depending on environment and plant species (Tegeeder and Masclaux-Daubresse 2018). Often aspartate, glutamate, asparagine, and glutamine are the most abundant (Liu *et al.* 2014). The $\delta^{15}\text{N}$ of different free amino acids in plant tissue can vary by almost 10‰, and depends on environmental conditions, metabolic branch points, and relative fluxes (Tcherkez 2011). Glutamine, however, accounts for more than 80% of total proteinogenic amino acids in xylem of *Populus* spp. (Escher *et al.* 2004; Millard *et al.* 2006). Thus, as per a Raleigh distillation,

xylem sap analysis should provide a reasonable proxy sampling of the instantaneous product and the residual substrate remaining, with the difference in isotopic composition between the organic and inorganic N directly reflecting the *in vivo* discrimination factor of NR.

2.5.3 N content and ^{15}N -patterns of shoot xylem sap

The main purpose of my first experiment was to establish a reliable protocol for sampling xylem sap, but also to check for an effect of sampling position and the possibility of further significant assimilation during nitrogen translocation. I collected sap at two sampling positions under two different but sequential ranges of extraction pressure, the first being just 0.1-0.2 MPa and the second being 0.6-0.7 MPa above the balancing pressure. Xylem from these different locations had similar total N and NO_3^- concentrations as well as $\delta^{15}\text{N}$ values when sap was collected at low pressure (Figure 2.1). Though a significant decrease in NO_3^- concentration was found in xylem sap from the upper position at higher pressure, the $\delta^{15}\text{N}$ of NO_3^- and total N, and total N concentration remained similar between lower and upper portions of the shoot. These observations are consistent with Schneider *et al.* (1996) and Geßler *et al.* (1998) who, by monitoring the ATP content of xylem sap, detected negligible contamination originating from parenchyma cells in both roots and shoot at 0.6 MPa above the balancing pressure. However, NO_3^- in more distal sap (as represented by upper shoots at higher pressure) may be reduced in concentration by further assimilation *en route* or, possibly, tissue water re-entering the xylem by reverse osmosis at the highest pressure.

Overall, there was only a small effect of stem position and collection pressure over the full range tested here, and thus samples collected from the lower portions of unsegmented shoots under low pressure should yield reliable results. The data also indicate that the concentration and isotopic composition of major N fractions in stem

xylem sap are relatively stable during transport and, as concluded by Cui *et al.* (2020), not significantly affected by exchange with the phloem. In the first experiment, the average NO_3^- concentration of xylem sap collected at low pressure was 1.64 ± 0.07 mM, which accounted for 21.18% of total N concentration during transport (Table 2.2). The second experiment found an average of 1.78 ± 0.17 mM NO_3^- , or $26.60 \pm 2.04\%$ of total N transport (Figure 2.3a,b). Thus, approximately three-quarters of the N transported in the xylem was already assimilated into organic form. Notably, although most N loaded into the xylem was organic, the NO_3^- concentration was still roughly three times higher than in the source medium (0.5 mM).

From shoot nitrogen content and measured N_i/N_t ratios, I obtained a minimum estimate for the proportion of total plant N that was root assimilated ($P_{root\ measured}$) ranging from 73 to 85% (Figure 2.5). Although this is a high proportion relative to many species (Oh *et al.* 2008; Cui *et al.* 2020), it is not unusual for *Populus*. Dluzniewska *et al.* (2006) obtained a P_{root} of 96% and Siebrecht and Tischner (1999) estimated P_{root} to be 40~60%, both in hybrid aspen (*Populus tremula* × *P. alba*). Min *et al.* (1999) reported a P_{root} of ~70% in *Populus tremuloides*. P_{root} likely varies with age, species, media nitrate concentration, and other growing conditions. For example, in their work, Dluzniewska *et al.* (2006) found that P_{root} decreased to 68% when hybrid aspen was supplied with glutamine in addition to nitrate.

Since analysis of xylem sap is based on point measurements, whereas tissue $\delta^{15}\text{N}$ values and nitrogen concentrations reflect time-integrated assimilation, I investigated the possibility of diurnal variation in the xylem sap. Peuke *et al.* (2013) found that the $\delta^{15}\text{N}$ of total N in xylem sap of *Ricinus communis* is significantly higher during the day than the night. There are several potential causes for diurnal variation in the $\delta^{15}\text{N}$ of xylem sap. There is diurnal variation in gene expression patterns for nitrate and/or ammonium transporters in roots (Ono *et al.* 2000; von Wirén *et al.* 2000; Matt *et al.*

2001) and both roots and leaves show diel rhythms in assimilation and metabolism (Glass *et al.* 2002). In shoots, reductant NADH needed for the assimilation of nitrate is more readily available during the day than at night (Ramarao *et al.* 1981). A direct reliance on reducing power from the light reactions does not apply to roots because they must rely on the delivery of photosynthate in the phloem to provide reductant and carbon skeletons for N assimilation. The driving force for N transport from roots to shoots is the transpiration stream, which obviously does follow a day/night cycle. I detected some diel variation in $\delta^{15}\text{N}$, but it followed a different pattern from Peuke *et al.* (2013); *i.e.*, the NO_3^- concentration, $\delta^{15}\text{N}$ of total N and organic N in the day was significantly lower than at night (Figure 2.3), suggesting more root assimilation of NO_3^- during the day. The $\delta^{15}\text{N}$ of NO_3^- and concentrations of total N and organic N remained steady over the full 24 h cycle (Figure 2.3a,c,e). This stability suggests that the isotopic composition of NO_3^- and the overall N concentration of the xylem sap were relatively flux-independent, possibly aided by the steady hydroponic supply conditions.

Total xylem nitrogen, and particularly xylem NO_3^- , was enriched in ^{15}N relative to the hydroponic medium (Figure 2.1). The $\delta^{15}\text{N}$ of total N in xylem sap averaged $0.78 \pm 0.16\text{‰}$, while the $\delta^{15}\text{N}$ of the NO_3^- averaged $19.73 \pm 0.88\text{‰}$ (Figure 2.1c,d). In contrast, the organic N was depleted in ^{15}N relative to the hydroponic medium and had an average $\delta^{15}\text{N}$ of $-5.14 \pm 1.03\text{‰}$ (Figure 2.2b). The difference in $\delta^{15}\text{N}$ between the NO_3^- and the organic N fractions was $24.9 \pm 1.6\text{‰}$. This difference is of comparable magnitude but, as expected, greater than the difference I found between the total organic N and NO_3^- of root tissue (Appendix Table A.2). Fractionation during NO_3^- reduction by NR *in vitro* has been measured in several studies. Ledgard *et al.* (1985) reported that discrimination by NR purified from spinach was 15.4‰ , and this value is often quoted. However, reported discrimination factors at natural abundance levels range from 12.1‰ for enzyme from the moss *Hypnum plumaeforme* (Liu *et al.* 2012) to 32‰ in

Escherichia coli (Carlisle *et al.* 2014). In addition, Carlisle *et al.* (2014) reported values of 23‰, 23‰, 31‰ and 28‰ in *Arabidopsis thaliana*, *Picea angusta*, *Zea mays*, and *Aspergillus niger*, respectively, whereas Olleros-Izard (1983) obtained discrimination factors of 24-29‰ for enzyme from *Z. mays*. Karsh *et al.* (2012) used enzymes from the fungus *Aspergillus niger* and the diatom *Thalassiosira weissflogii* and reported a mean value of 26.6‰. Species differences are possible and discrimination may also be different *in vivo* (Tcherkez and Farquhar 2006; Liu *et al.* 2014). Needoba *et al.* (2004) estimated NR discrimination to be 22.0‰ in *T. weissflogii*.

If the difference in $\Delta^{15}\text{N}$ between organic and inorganic N in the xylem sap approximates the *in vivo* discrimination factor of NR as I propose, then there should be a constant offset between their respective $\delta^{15}\text{N}$ values; this, however, was not the case (Figure 2.3e,f). These measures may not track each other if loading of the product is delayed relative to the substrate. However, the $\delta^{15}\text{N}$ of NO_3^- was temporally very steady, so irrespective of any delay, I would still expect the $\delta^{15}\text{N}$ of the organic fraction to be steady and not vary over time. Another possible explanation for the lack of a constant offset is the compounding of errors that necessarily occurred when I derived the isotopic composition of the organic N by mass balance. Either way, the overall mean should give a reasonable estimate of isotopic composition integrated over the day, and I would expect the $\delta^{15}\text{N}$ of organic N in the xylem to be close to the $\delta^{15}\text{N}$ of whole roots, as assumed by Kalcsits *et al.* (2014). Indeed, the average $\Delta^{15}\text{N}$ of the roots across five genotypes was -7.66‰ and the average $\delta^{15}\text{N}$ of organic N in the xylem sap was -7.00‰ (Appendix Table A.3). This close agreement suggests that there is little or no further fractionation associated with the identity of the organic N entering the xylem.

2.5.4 Convergence of direct measurement and IMB model prediction

In combination with information about tissue N contents, and knowing the discrimination factor of NR, whole-plant and tissue $\Delta^{15}\text{N}$ can be used to estimate Ti/Tt , P_{root} and ultimately E/I . In the first experiment, I analyzed the $\delta^{15}\text{N}$ values of organic N and NO_3^- in xylem sap and the average difference in $\delta^{15}\text{N}$ was $24.9 \pm 1.6\text{‰}$ (*i.e.*, $\Delta^{15}\text{N} = 25.1 \pm 1.6\text{‰}$). In the second experiment, I analyzed plant tissue data from five genotypes of black cottonwood and compared Ti/Tt from the IMB model with direct measurement of N concentrations in xylem sap. If Ti/Tt is calculated using 15.4‰ for Δ_{enzyme} , the model-predicted Ti/Tt is 66% higher than the direct measurement from xylem sap (Table 2.4). When recalculated using the value of 25.1‰ , the model-predicted Ti/Tt and the directly measured Ti/Tt converge almost exactly. Similarly, the P_{root} obtained by direct measurement was $78.7 \pm 0.6\%$, while the P_{root} predicted by the model was $80.6 \pm 0.9\%$. However, despite this excellent fit, I consider it likely that 25.1‰ is too high, as the average of the various estimates for Δ_{enzyme} reviewed above is closer to 22‰ . In a comparison of the IMB model and compartmental analysis of tracer efflux (CATE) using stable isotope tracing to determine E/I in balsam poplar, Kalcsits and Guy (2016a) found that the two methods yielded highly correlated results that converged when Δ_{enzyme} was fixed at 22‰ .

2.6 Conclusion

Here, I found that pressure bombing of black cottonwood shoots at low pressures (0.1-0.2 MPa above the balancing pressure) yielded xylem sap containing both organic-N and NO_3^- -N fractions differing in isotopic composition by $\sim 24.9\text{‰}$. This difference is consistent with an *in vivo* discrimination factor for NR (25.1‰) that is substantially higher than the first reported direct measurements in the literature, but much closer to recent estimates for Δ_{enzyme} , which average near 22‰ . Utilization of these higher values

for Δ_{enzyme} improves the prediction of T_i/T_t in the IMB model (this study) and also brings estimates of E/I from that model in line with independent tracer efflux measurements (Kalcsits and Guy 2016a). I suggest that the IMB model may be useful for phenotyping traits related to nitrogen uptake and assimilation in hydroponically-grown plants that rely substantially on root assimilation.

3. Genotypic variation in carbon and nitrogen isotope discrimination suggests local adaptation of heart-leaved willow (*Salix eriocephala* Michx.).

3.1 Summary

Plants acquire multiple resources from the environment and may need to adjust and/or balance their respective resource-use efficiencies to maximize growth and survival, in a locally adaptive manner. In this study, tissue and whole-plant $\delta^{13}\text{C}$ and C/N ratios provided long-term measures of WUE and NUE, and a $\delta^{15}\text{N}$ -based mass balance model was used to estimate traits related to N uptake and assimilation in heart-leaved willow. In an initial common garden experiment consisting of 34 populations, I found population level variation in $\delta^{13}\text{C}$, C/N, and $\delta^{15}\text{N}$, indicating different patterns in WUE, NUE, and N uptake and assimilation. Although there was no relationship between foliar $\delta^{13}\text{C}$ and C/N ratios among populations, there was a significant negative correlation between these measures across all individuals, implying a genetic and/or plastic trade-off between WUE and NUE not associated with local adaptation. To eliminate any environmental effect, I grew a subset of 21 genotypes hydroponically with nitrate as the sole N-source, and detected significant variation in $\delta^{13}\text{C}$, $\delta^{15}\text{N}$, and C/N ratios. Variation in $\delta^{15}\text{N}$ was mainly due to genotypic differences in the nitrate efflux/influx ratio (E/I) at the root. Both experiments suggested clinal variation in $\delta^{15}\text{N}$ (and thus N uptake efficiency) with latitude of origin, which may relate to water availability and could contribute to global patterns in ecosystem $\delta^{15}\text{N}$. There was a tendency for genotypes with higher WUE to come from more water replete sites with shorter and cooler growing seasons. I found that $\delta^{13}\text{C}$, C/N, and E/I were not inter-correlated, suggesting that selection for growth, WUE, NUE, and N uptake efficiency can occur without trade-off.

3.2 Introduction

Tree and shrub species within the *Salicaceae* present interesting and convenient models for studying adaptive evolution since many of them have wide geographic distributions, are easily propagated, possess relatively small and well understood genomes, and have well established genetic resources (Djomo *et al.* 2011; Shunmugam *et al.* 2016; Jiahui *et al.* 2019). Populations of species with large natural ranges may encounter divergent selection pressures because of wide variation in environmental factors, such as temperature, precipitation, growing season length, photoperiod, and soil nutrient conditions, resulting in environment-correlated intraspecific variation (Eckert and Dyer 2012; McKown *et al.* 2013). Populations that are more fit to local environments than others are considered to be locally adapted (Kawecki and Ebert 2004; Blanquart *et al.* 2013).

Water and nitrogen are among the most limiting of resources for plants in terrestrial temperate and boreal ecosystems and, consequently, selective pressure towards maximization of water and N use efficiencies is expected (Weih *et al.* 2006). Both the efficiency of water use (carbon fixed per unit water transpired) and the efficiency of N use (carbon fixed per unit N assimilated) are tied, in part, to the diffusion gradient for CO₂ into the leaf through stomata. Most water used by plants is in support of photosynthesis by way of transpiration. More than half of total leaf N is related to photosynthesis (Evans 1989), and total leaf N content and photosynthetic capacity are typically correlated (Field and Mooney 1986; Larcher 2003). Reductions in stomatal conductance (g_s) or higher investments in foliar N can result in higher WUE if the CO₂ diffusion gradient steepens, but lower intercellular CO₂ concentrations may reduce NUE by reducing rates of carbon fixation per unit N. A negative correlation between WUE and NUE is implied, suggesting an evolutionary trade-off. However, changes in

mesophyll conductance (g_m) should impact WUE and NUE similarly and without trade-off because, in contrast to g_s , there is no effect on the diffusion of water vapour (Lauteri *et al.* 1997). Variation in sites of N assimilation and allocation within plants might also uncouple NUE from WUE, but in more indirect ways. For example, in *Populus*, when under N-limiting conditions, both a fast- and slow-growing hybrid showed increased root surface area, decreased photosynthetic rate, and reduced NUE (Luo *et al.* 2015). The slow-growing hybrid (*Populus* × *popularis*) had an increased WUE while the fast-growing hybrid (*Populus alba* × *Populus glandulosa*) had a decreased WUE. Because similar differences may occur within species, it is unclear if a trade-off between WUE and NUE should be expected among locally-adapted populations.

Plant C/N ratio can be used as a proxy measure of NUE over time, while the carbon isotopic composition ($\delta^{13}\text{C}$) of plant tissue can provide information on the long-term WUE of C_3 plants (Sun *et al.* 1996; Seibt *et al.* 2008). Fractionation of carbon isotopes occurs principally during diffusion of CO_2 into the leaf and at fixation by RuBisCO, which both discriminate against the heavier carbon isotope (^{13}C). Net discrimination can be simply modelled as a function of the atmosphere-to-leaf CO_2 diffusion gradient, which also determines the intrinsic WUE of photosynthesis (Farquhar *et al.* 1982). Strong genotypic correlations between $\delta^{13}\text{C}$ and WUE have been demonstrated in many tree species, including members of the *Salicaceae* (Leffler and Evans 1999; Pointeau and Guy 2014).

Although plant nitrogen isotopic composition ($\delta^{15}\text{N}$) does not provide a measure of NUE, variation in $\delta^{15}\text{N}$ can be used to trace N movement and infer N sources and/or N cycle dynamics in vegetation at local, community, and landscape scales. For example, a recent long-term monitoring study of plant $\delta^{15}\text{N}$ in the Tibetan alpine permafrost region suggested that increasing atmospheric CO_2 is causing increased N demand by plants, while climate warming is resulting in more N loss from the soil (Kou *et al.* 2020). Proper

interpretation of such signals, however, depends on a thorough understanding of how plants might differentially use different N forms (nitrate, ammonium, etc.) and the plant physiological processes that can fractionate N isotopes during uptake, assimilation, translocation, and remobilization (Evans 2001).

Pathways for nitrogen acquisition and assimilation in plants, and their genetic and regulatory networks, xylem loading, and patterns of storage/allocation have been extensively studied (Xu *et al.* 2012; Tegeder and Masclaux-Daubresse 2018; Feng *et al.* 2020). The uptake of inorganic N by roots occurs through both high and low affinity transport systems. After uptake, nitrate and/or ammonium may leak out of roots back into the rooting medium (efflux) or be assimilated. Nitrate is reduced into ammonium by nitrate reductase (NR) and nitrite reductase (NiR) working sequentially, and ammonium is assimilated in the glutamine synthetase-glutamine oxoglutarate aminotransferase (GS-GOGAT) cycle (Tischner 2000; Lancien *et al.* 2000). Several studies have shown that assimilated N is generally ^{15}N -depleted, while unassimilated N, both external and internal to the plant, becomes enriched in ^{15}N compared to the initial source (Pritchard and Guy 2005; Tcherkez and Hodges 2008; Cui *et al.* 2020). Discrimination against ^{15}N occurs at the initial assimilatory enzymes, NR and GS. Variability of $\delta^{15}\text{N}$ in plant tissues, therefore, is linked to N metabolism and can reflect changes in N metabolism and fluxes (Dawson *et al.* 2002; Tcherkez 2011). A simple N isotope mass balance (IMB) model proposed by Kalcsits *et al.* (2014), and validated in chapter 2 (Hu and Guy 2020), uses measurements of organ level $\delta^{15}\text{N}$ values under steady-state N supply conditions to identify efficiencies of inorganic N acquisition by roots (*i.e.*, net uptake vs. gross uptake) and variation in the site of assimilation (roots vs. shoots) in plants.

Heart-leaved willow is a deciduous woody plant in the *Salicaceae* family with a wide distribution in North America. In general, willows have high demands for water but

are considered to be efficient utilizers of N (Djomo *et al.* 2011; Fabio and Smart 2018). Here, I explored possible clinal variation in foliar C/N ratio, $\delta^{15}\text{N}$, and $\delta^{13}\text{C}$ of heart-leaved willow using 34 natural populations collected from a large geographic area planted into a common garden field experiment. I tested the hypothesis that population level variation in WUE (as indicated by $\delta^{13}\text{C}$) would show a negative relationship with NUE (as indicated by C/N), or be connected to variation in $\delta^{15}\text{N}$ that might indicate variation in N uptake efficiency and/or sites of N assimilation and allocation. To control for field effects and spatial variation in soil $\delta^{15}\text{N}$, I selected 21 genotypes for isotopic dissection of N acquisition parameters in a controlled environment hydroponic experiment. I uncover largescale geographic trends in $\delta^{15}\text{N}$ in heart-leaved willow associated with variation in N uptake efficiency, but independent from genetic variation in WUE and NUE.

3.3 Methods

This study employed clonal material from the AgCanSalix (Agriculture Canada Salix) collection established from field scions taken over the natural range of heart-leaved willow within Canada in 2012 (Shunmugam *et al.* 2016). This collection includes 34 populations of heart-leaved willow, with 15 genotypes per population (Figure 3.1). Climate variables for each collection site were obtained from ClimateWNA (Wang *et al.* 2012) based on the 1971-2000 Canadian Climate Normal dataset. Variables derived included frost-free period (FFP; days), mean warmest month temperature (MWMT; °C), mean annual precipitation (MAP; mm), mean summer precipitation from May to September (MSP; mm), mean annual temperature (MAT; °C), and continentality (CONT; °C). Annual dryness index (ADI) and summer dryness index (SDI), were obtained according to Guy and Holowachuk (2001):

$$\text{ADI} = (e_{s[\text{MAT}]} \times 1000) / \text{MAP} \quad (3.1)$$

$$\mathbf{SDI} = (e_{s[MTWM]} \times \mathbf{1000})/\mathbf{MSP} \quad (3.2)$$

where, e_s is the saturation vapor pressure in kilopascals at MAT and MTWM, respectively, calculated according to Buck (1981) and Yin (1998).

3.3.1 Common garden experiment

Briefly, the original scions noted above were rooted under greenhouse conditions and transferred after 2 months to a shade house where they were allowed to undergo natural senescence before lifting and storing at -4°C for later use. In spring 2013, this material was used to establish a common garden at Indian Head, Saskatchewan (50.52°N 103.68°W; elevation 605 m; MAT: 1.4°C; MAP: 492 mm; FPP: 103 days). The site preparation involved cultivating to a depth of 20 cm or more and disking. Later, the rows were marked at 3 m intervals in an East-West orientation, with each row running 320 m long. The site was rototilled after amending with micronutrients. The soil texture at the site was sandy clay loam with an average pH of 7.9, and with 13.6, 19.7 and 242.9 ppm of N, P and K, respectively. Rows were mulched using black plastic sheeting (Crawling Valley Plastics, Canada) to avoid intra-row weed competition. Populations were planted on mulched rows as a block with 1.0 m spacing. In each of the three replicates, population blocks were randomized. The site was sprinkler irrigated as necessary during summer months with mechanical weed control between rows. In July 2014, two leaf discs were collected using a hand-held paper punch from 8-10 individuals per population (N=338) for analysis of C and N concentrations and stable isotope ratios. Stem samples for isotopic analysis were collected in the fall at 10 cm above the soil surface. Both sample sets were oven dried at 50°C for 72 hours to constant mass.

3.3.2 Hydroponic experiment

Based on the $\delta^{15}\text{N}$ of leaves and stems from the common garden experiment, a subset of just 21 genotypes was selected to represent the foliar $\delta^{15}\text{N}$ range observed in the common garden experiment, as well as the geographic range from east to west (Figure 3.1). First year whips were collected in early February, 2018 and stored in black plastic bags at 4°C for 4 months before use. Two-node scions, approximately 5 cm long, were rooted in distilled water and then transferred to a hydroponic system in the UBC Horticulture Greenhouse (Vancouver, Canada). There were six replicates per genotype for a total of 126 plants, randomly arranged.

Four 150 L bench-mounted acrylic tubs, an 1800 L vertical ground tank (RK400; Canada), two water pumps (Little Giant, Canwest Tanks, USA), and connecting PVC piping (2.54 cm diameter; WaterTec, Canada) comprised the hydroponic system. Each acrylic tub had a capacity to hold up to 32 plants. One water pump sat in the bottom of the main tank and continuously circulated media to the four tubs. The depth of water in the tubs was set by an overflow outlet draining by gravity into a receiving reservoir at ground level containing the second pump (actuated by a float switch), which returned the media to the main tank. The total volume of the system was maintained at 2000 L. The hydroponics solution was a modified 1/10th strength Johnson's solution (Johnson *et al.* 1957) supplemented with 0.25 mM $\text{Ca}(\text{NO}_3)_2$. To avoid major changes in the $\delta^{15}\text{N}$ of the hydroponics solution over time, media NO_3^- concentration was assayed periodically using the perchloric acid method (Cawse 1967) to ensure no substantial decrease (no more than 10%). The nutrient medium was completely replaced as necessary, usually every 6-10 days. The hydroponics system was under ambient light conditions supplemented by LED lighting ($600 \mu\text{mol m}^{-2}\text{s}^{-1}$) on an 18/6 h day/night photoperiod. Temperatures in the greenhouse were maintained between 20-24°C.

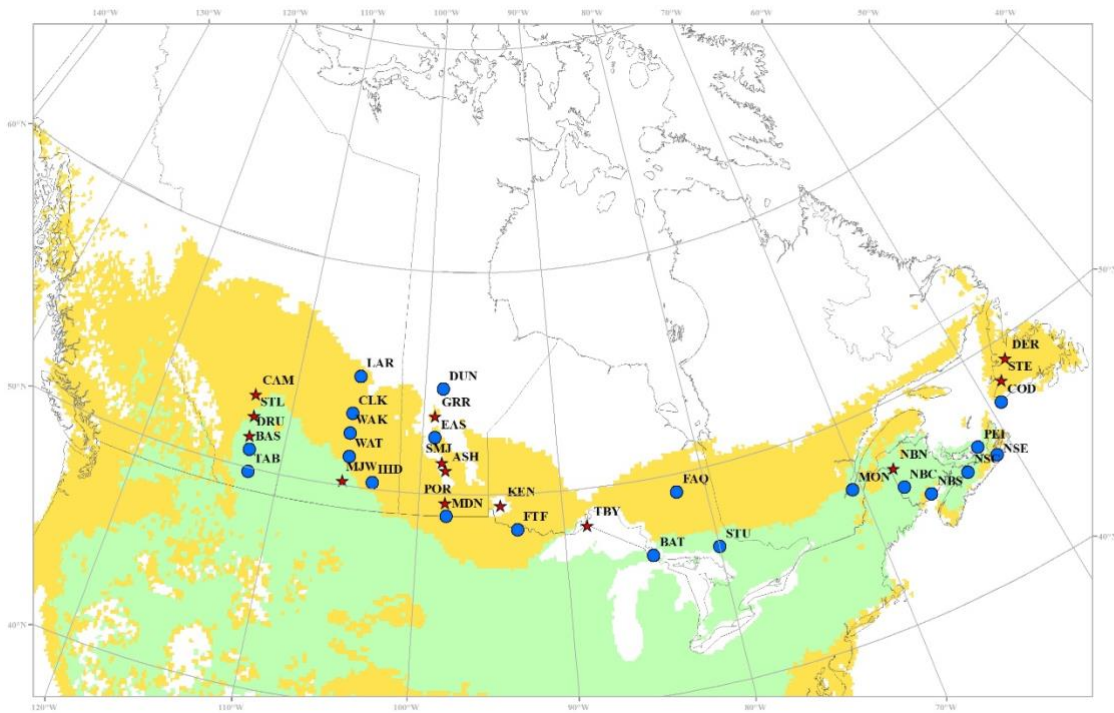


Figure 3.1. Locations of 34 populations of heart-leaf willow (*Salix eriocephala*) sampled from the natural range of the species across eastern and western Canada. Stars indicate the populations from which the 21 genotypes used in the hydroponics experiment were selected. The green shaded area represents the dominant continuous range of heart-leaved willow while the yellow shaded area shows the discontinuous range.

3.3.3 Carbon and Nitrogen Isotope analysis

The leaf and stem samples (1.5 mg for $\delta^{13}\text{C}$; 2.5 mg for $\delta^{15}\text{N}$) collected from the common garden were packed in tin capsules (Elemental Microanalysis, UK) and sent to the UC Davis Stable Isotope Facility (Davis, CA, USA) for analysis of $\delta^{13}\text{C}$, $\delta^{15}\text{N}$, and C and N concentrations. For the hydroponics experiment, plants were harvested after 45 days of growth and divided into leaves, stems, roots, and original cuttings. Once oven-dried, these parts were weighed and then pulverized using a Wiley mill followed by a

Geno/Grinder. Sub-samples (3 mg) were packed into tin capsules and analyzed for C and N concentration, $\delta^{13}\text{C}$ and $\delta^{15}\text{N}$ using a Vario EL Cube Elemental Analyzer interfaced to an Isoprime Isotope Ratio Mass Spectrometer in the Stable Isotope Facility, Faculty of Forestry, UBC.

3.3.4 Calculations

Carbon and nitrogen isotopic compositions were expressed as $\delta^{13}\text{C}$ and $\delta^{15}\text{N}$ values:

$$\delta^{13}\text{C} \text{ or } \delta^{15}\text{N} = \left(\frac{R_{\text{sample}}}{R_{\text{standard}}} - 1 \right) * 1000 \quad (3.3)$$

where, R_{sample} and R_{standard} are the $^{13}\text{C}/^{12}\text{C}$ or $^{15}\text{N}/^{14}\text{N}$ ratios of the sample and the arbitrary standard, respectively. After correcting for carry-over effects of pre-existing N in the original cuttings (Kalcsits and Guy 2013b), the whole-plant isotopic composition of plants from the hydroponics experiment was calculated as the weighted sum of root, stem and leaf:

$$\delta^{15}\text{N}_{\text{whole plant}} = (f_{\text{root}} \times \delta^{15}\text{N}_{\text{root}}) + (f_{\text{stem}} \times \delta^{15}\text{N}_{\text{stem}}) + (f_{\text{leaf}} \times \delta^{15}\text{N}_{\text{leaf}}) \quad (3.4)$$

where, f_i is equal to the fraction of tissue N contributing to overall plant N content. Nitrogen isotope discrimination ($\Delta^{15}\text{N}$) relative to the source hydroponic solution ($\delta^{15}\text{N} = -1.69\text{‰}$) was calculated as:

$$\Delta^{15}\text{N}_{\text{sample}} = \frac{(\delta^{15}\text{N}_{\text{source}} - \delta^{15}\text{N}_{\text{sample}})}{\left(1 + \frac{\delta^{15}\text{N}_{\text{sample}}}{1000}\right)} \quad (3.5)$$

An isotope mass balance (IMB) model as described in detail in Kalcsits *et al.* (2014) was used to estimate N fluxes and rates and locations of N assimilation. From the discrimination factor for nitrate reductase, assumed here to be 22‰ (Hu and Guy 2020), and the $\delta^{15}\text{N}$ and N content of plant tissues, the IMB model yields an estimate of the

proportion of NO_3^- assimilated in the roots (P_{root}), the NO_3^- efflux/influx ratio (E/I) for exchange between the substrate and the roots, and the ratio of inorganic to total N (Ti/Tt) transported to the shoot in the xylem.

3.3.5 Statistics

All statistical analyses used R version 3.5.1 (R Core Development Team, 2011). Linear regression analyses were performed between $\delta^{15}\text{N}$ values (leaves and stems) and site of origin geo-climatic variables. Pearson correlation coefficients (r) were used to examine relationships between all variables determined on the 21 genotypes used in the hydroponic experiment, and canonical correlation analysis was done between physiological and environmental variables using the package “CCA”. Genotype effects on plant biomass, whole-plant and tissue N concentrations, and whole-plant and tissue $\delta^{15}\text{N}$ were tested by one-way ANOVA followed by Tukey’s multiple comparison tests.

3.4 Results

3.4.1 Common garden experiment

There were clear differences between populations in $\delta^{13}\text{C}$, $\delta^{15}\text{N}$, N percentage, and C/N ratios, in both leaves and stems ($P < 0.05$, Table 3.1). In the common garden, leaf $\delta^{13}\text{C}$ ranged from -30.7‰ to -24.7‰ and leaf C/N ratio ranged from 11.45 to 28.98 (Figure 3.2). There was no relationship between $\delta^{13}\text{C}$ and C/N ratio at the population level (Figure 3.2a). However, when data were plotted for the species as a whole, there was a significant negative correlation between leaf $\delta^{13}\text{C}$ and leaf C/N ($P < 0.001$, Figure 3.2b).

The population mean $\delta^{15}\text{N}$ and $\delta^{13}\text{C}$ values of leaves and stems were plotted against latitude of origin (Figure 3.3a,b). The leaf and stem $\delta^{15}\text{N}$ values were quite variable, spanning ranges of 15.5‰ and 11.1‰, respectively. Both leaf and stem $\delta^{15}\text{N}$

values showed a positive correlation with latitude ($P < 0.001$, Figure 3.3a), while the $\delta^{13}\text{C}$ values showed no relationship with latitude ($P > 0.05$, Figure 3.3b). I did, however, find that in both leaves and stems, population mean $\delta^{13}\text{C}$ was negatively correlated with summer dryness index, while $\delta^{15}\text{N}$ was positively correlated (both at $P < 0.001$, Appendix Figure A.3). Consistent relationships with other climate variables were not detected.

Table 3.1. Overall means of measured plant traits, and associated population effects from the common garden experiment. Traits measured or estimated include nitrogen percentage (N, %), carbon isotopic composition ($\delta^{13}\text{C}$, ‰), nitrogen isotopic composition ($\delta^{15}\text{N}$, ‰), the carbon to nitrogen (C/N) ratio of leaves and stems.

	Measurement	Mean \pm SE	Population effect
Nitrogen percentage	Leaf N	2.82 \pm 0.02	***
	Stem N	0.34 \pm 0.01	***
Carbon isotopic composition	Leaf $\delta^{13}\text{C}$	-28.4 \pm 0.1	***
	Stem $\delta^{13}\text{C}$	-27.6 \pm 0.1	***
Nitrogen isotopic composition	Leaf $\delta^{15}\text{N}$	9.9 \pm 0.2	***
	Stem $\delta^{15}\text{N}$	7.1 \pm 0.1	***
Carbon to nitrogen ratio	Leaf C/N	16.19 \pm 0.15	***
	Stem C/N	7.36 \pm 0.18	***

*** indicates significance at $P < 0.001$

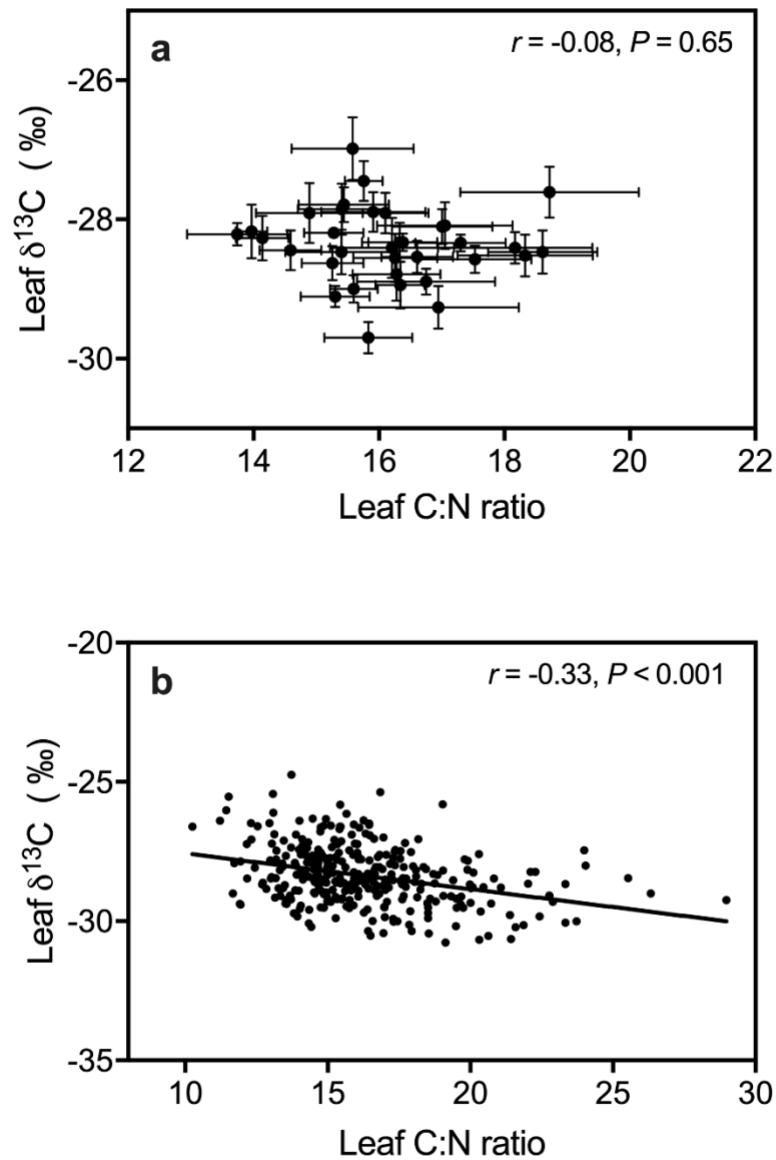


Figure 3.2. The relationship between leaf carbon isotopic composition ($\delta^{13}\text{C}$) and leaf carbon to nitrogen (C/N) ratio of heart-leaf willow (*Salix eriocephala*) based on (a) population means (\pm SE) and (b) individual plants from the common garden experiment.

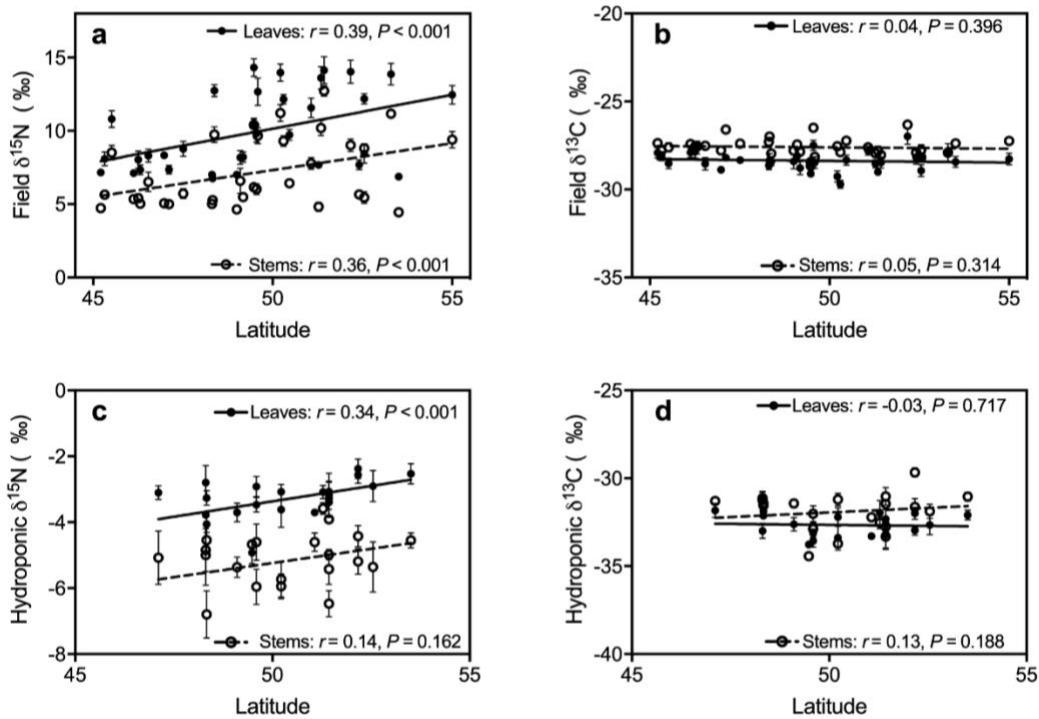


Figure 3.3. Nitrogen isotopic composition ($\delta^{15}\text{N}$) and carbon isotopic composition ($\delta^{13}\text{C}$) of leaves and stems in heart-leaf willow (*Salix eriocephala*) (panels a&c and b&d, respectively) from common garden and hydroponic experiments (a&b and c&d, respectively) plotted against latitude of origin. Each point for the common garden data represents one population with 10 replicates, while each point for the hydroponic data represents one genotype with six replicates. Data are means \pm SE.

3.4.2 Hydroponics experiment

Isotopic analysis of the subset of 21 *S. eriocephala* genotypes grown under controlled environment conditions revealed similar trends with latitude of origin but with much less variation in $\delta^{15}\text{N}$. The leaf $\delta^{15}\text{N}$ significantly increased with latitude ($P < 0.001$, Figure 3.3c) while the $\delta^{13}\text{C}$ of leaves and stems did not (Figure 3.3d). Stem $\delta^{15}\text{N}$ was also not significantly correlated to latitude ($P = 0.162$, Figure 3.3c). The $\delta^{15}\text{N}$ values in this experiment covered a range of 5.4‰ in leaves and 6.2‰ in stems, with leaves being about 1.9‰ heavier than the stems. Foliar $\delta^{13}\text{C}$ spanned a range of 4.5‰ while stems differed by up to 6.3‰.

Whole-plant $\delta^{15}\text{N}$ and $\delta^{13}\text{C}$ showed similar patterns, as did leaves alone (Figure 3.3c,d); *i.e.*, $\delta^{15}\text{N}$ increased significantly with latitude of origin ($P < 0.001$) whereas $\delta^{13}\text{C}$ did not (Figure 3.4a,b). However, the data suggested a parabolic relationship of $\delta^{13}\text{C}$ on latitude, and a second order polynomial regression was significant ($P < 0.001$). In combination with tissue N concentrations, N isotope discrimination relative to the NO_3^- source was used in the IMB model to calculate N fluxes and rates and locations of assimilation. Root efflux/influx (E/I) ratio ranged from 0.04 to 0.19 and was negatively correlated with latitude ($P < 0.001$, Figure 3.5). Other model variables were not significantly different between genotypes, and not correlated to latitude.

Pearson correlation coefficients (r) between geo-climatic parameters and isotopic traits for all 21 genotypes are shown in Table 3.2. In addition to latitude, both leaf and whole-plant $\delta^{15}\text{N}$ increased with longitude (LON) and elevation (ELV). Both measures of $\delta^{15}\text{N}$ were negatively correlated to frost-free period (FFP) and mean annual precipitation (MAP). Although $\delta^{13}\text{C}$ of the hydroponically grown material was not significantly related to the geographic variables (LAT, LON and ELV), it was negatively correlated with mean warmest month temperature (MWMT), annual dryness index (ADI), summer dryness

index (SDI), continentality (CONT), and FFP. A further canonical structure analysis was obtained using those geo-climatic variables and $\delta^{15}\text{N}$ and $\delta^{13}\text{C}$ (Table 3.3). Two significant canonical variables were extracted (CLIM1 and CLIM2). Frost-free period and MWMT loaded highly on CLIM1, while MAP and ADI were most strongly related to CLIM2. The whole-plant root, stem and leaf $\delta^{13}\text{C}$ were negatively loaded on CLIM1, while whole-plant $\delta^{15}\text{N}$ and leaf $\delta^{15}\text{N}$ were negatively loaded on CLIM2.

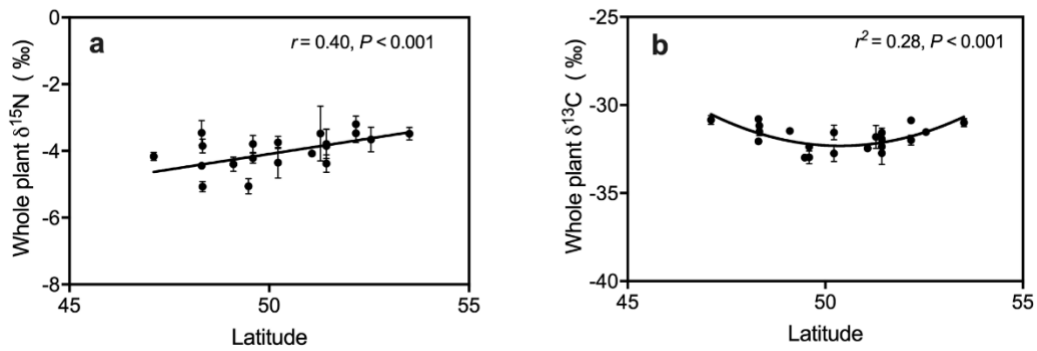


Figure 3.4. Whole-plant nitrogen and carbon isotopic compositions ($\delta^{15}\text{N}$ & $\delta^{13}\text{C}$; panels a&b, respectively) plotted against latitude of origin in the hydroponic experiment. Each point represents one genotype with six replicates. Data are means \pm SE.

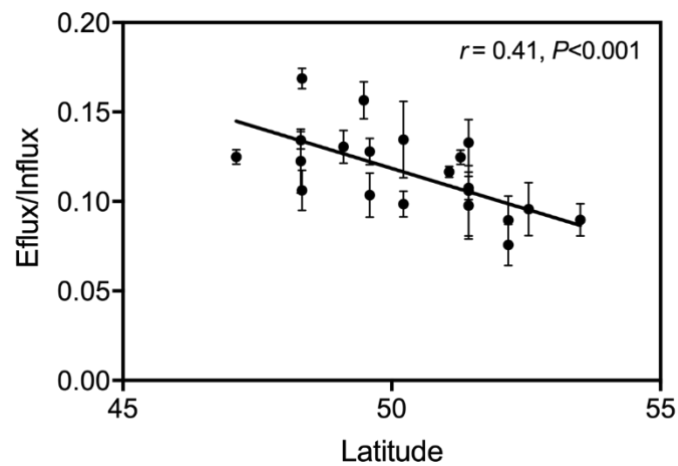


Figure 3.5. Root efflux/influx ratio derived from the Isotope Mass Balance (IMB) model plotted against latitude of origin. Each point represents one genotype with six replicates. Data are means \pm SE

Table 3.2. Pearson correlations (r) between geographic, climatic, and physiological variables for all 21 genotypes in the hydroponic experiment. Bolding indicates significance at $P<0.05$; Bold* indicates significance at $P<0.001$.

	LAT	LON	ELV	FFP	MWMT	MAP	CONT	ADI	SDI
Leaf $\delta^{15}\text{N}$	0.34*	0.27	0.28	-0.29	-0.16	-0.22	0.01	0.22	0.12
Leaf $\delta^{13}\text{C}$	-0.03	-0.18	-0.05	-0.27	-0.38*	0.24	-0.31	-0.19	-0.24
Stem $\delta^{15}\text{N}$	0.14	0.15	0.12	-0.11	0.01	-0.12	0.07	0.05	-0.01
Stem $\delta^{13}\text{C}$	0.13	-0.08	0.04	-0.52*	-0.52*	0.16	-0.32	-0.16	-0.28
Root $\delta^{15}\text{N}$	0.23	0.20	0.14	-0.12	0.06	-0.21	0.18	0.12	0.12
Root $\delta^{13}\text{C}$	0.09	-0.08	0.11	-0.34*	-0.38*	0.16	-0.31	-0.13	-0.24
WP $\delta^{15}\text{N}$	0.40*	0.37*	0.37*	-0.28	-0.10	-0.32	0.07	0.31	0.19
WP $\delta^{13}\text{C}$	0.03	-0.17	-0.04	-0.42*	-0.52*	0.30	-0.39*	-0.27	-0.36*
Biomass	-0.04	0.06	-0.03	0.09	0.16	-0.10	0.16	-0.08	0.12

LAT, latitude ($^{\circ}\text{N}$); LON, longitude ($^{\circ}\text{W}$); ELV, elevation (m); FFP, frost-free period (days); MWMT, mean warmest month temperature ($^{\circ}\text{C}$); MAP, mean annual precipitation (mm); CONT, continentality ($^{\circ}\text{C}$); ADI, annual dryness index; SDI: summer dryness index; $\delta^{15}\text{N}$, nitrogen isotope composition; $\delta^{13}\text{C}$, carbon isotope composition; WP, whole-plant; biomass (g).

Table 3.3. Canonical structure between geoclimatic parameters and plant traits with the first two canonical variables, CLIM1 and CLIM2.

Geoclimatic variables	CLIM 1	CLIM 2	Response variables	CLIM 1	CLIM 2
LAT	-0.25	-0.41	Leaf $\delta^{15}\text{N}$	-0.51	-0.57
LON	0.15	-0.60	Leaf $\delta^{13}\text{C}$	-0.60	-0.07
ELV	-0.05	-0.63	Stem $\delta^{15}\text{N}$	-0.08	-0.30
FFP	0.70	0.20	Stem $\delta^{13}\text{C}$	-0.82	-0.20
MWMT	0.71	-0.09	Root $\delta^{15}\text{N}$	-0.04	-0.07
MAP	-0.25	0.63	Root $\delta^{13}\text{C}$	-0.70	0.04
MAT	0.04	0.14	WP $\delta^{15}\text{N}$	-0.41	-0.71
CONT	0.43	-0.20	WP $\delta^{13}\text{C}$	-0.85	0.10
ADI	0.29	-0.71	Biomass	0.35	0.03
SDI	0.42	-0.53			

LAT, latitude ($^{\circ}\text{N}$); LON, longitude ($^{\circ}\text{W}$); ELV, elevation (m); FFP, frost free-period (days); MWMT, mean warmest month temperature ($^{\circ}\text{C}$); MAP, mean annual precipitation (mm); MAT, mean annual temperature; CONT, continentality ($^{\circ}\text{C}$); ADI, annual dryness index; SDI, summer dryness index; $\delta^{15}\text{N}$, nitrogen isotope composition; $\delta^{13}\text{C}$, carbon isotope composition; WP, whole-plant; biomass (g)

3.4.3 Genotypic differences

Genotypic means and statistical differences are summarized in Table 3.4. Genotypic variation in biomass, root-shoot ratio, tissue and whole-plant level N percentage, $\delta^{13}\text{C}$, and $\Delta^{15}\text{N}$ were found. Genotype effects on most IMB model outputs were not significant except for E/I , indicating that E/I varies significantly across the 21 assessed genotypes. Traits in Table 3.4 were further analyzed for functional correlations as presented in the heat map shown in Appendix Figure B.2. Generally, root growth was significantly related to C/N, $\delta^{13}\text{C}$, and $\delta^{15}\text{N}$ at the whole-plant level. Root biomass was positively correlated to whole-plant C/N and E/I , and negatively correlated to whole-plant $\delta^{13}\text{C}$ and $\delta^{15}\text{N}$. Whole-plant C/N was not correlated to either whole-plant $\delta^{13}\text{C}$ or E/I . Whole-plant $\delta^{13}\text{C}$ was also not correlated with E/I . Therefore, a 3D scatter plot combining whole-plant $\delta^{13}\text{C}$, whole-plant C/N ratio and E/I was plotted to rank all 21 genotypes in the hydroponics experiment (Figure 3.6). The STL-2 genotype outperformed all others in having higher whole-plant $\delta^{13}\text{C}$ and C/N, as well as lower E/I . The biomass of STL-2 was $3.42 \pm 0.25 \text{ g}$, which was nearly 80% higher than the average biomass (Table 3.4).

Table 3.4. Overall means and ranges of measured plant traits, and associated genotype effects, in the hydroponics experiment. Traits measured or estimated include biomass (g), root-shoot ratio, carbon isotopic composition ($\delta^{13}\text{C}$, ‰) at organ and whole-plant (WP) levels, nitrogen isotope discrimination ($\Delta^{15}\text{N}$, ‰) at organ and whole-plant levels, the ratio of inorganic to total nitrogen transported in the xylem (Ti/Tt), the proportion of plant nitrogen assimilated in roots (P_{root}), efflux/influx (E/I), and leaf and root assimilation activity (AC, $\mu\text{mol mg dw}^{-1}$).

	Measured	Mean \pm SE	Genotype minimum	Genotype maximum	Genotype effect
Growth	Biomass	1.94 \pm 0.14	0.46	3.53	***
	R:S ratio	0.36 \pm 0.01	0.17	0.55	***
Carbon isotope composition	Root $\delta^{13}\text{C}$	-30.37 \pm 0.11	-31.67	-28.92	*
	Stem $\delta^{13}\text{C}$	-31.90 \pm 0.13	-34.44	-29.66	**
	Leaf $\delta^{13}\text{C}$	-32.66 \pm 0.10	-33.76	-31.14	***
	WP $\delta^{13}\text{C}$	-31.86 \pm 0.09	-32.98	-30.80	***
Nitrogen isotope discrimination	Root $\Delta^{15}\text{N}$	4.00 \pm 0.10	2.90	5.29	*
	Stem $\Delta^{15}\text{N}$	3.50 \pm 0.12	1.90	5.14	***
	Leaf $\Delta^{15}\text{N}$	1.60 \pm 0.10	0.69	3.25	**
	WP $\Delta^{15}\text{N}$	2.33 \pm 0.08	1.51	3.40	***
Model calculations	Ti/Tt	0.15 \pm 0.01	0.03	0.18	0.28
	P_{root}	0.90 \pm 0.01	0.85	0.94	0.30
	E/I	0.16 \pm 0.01	0.04	0.19	***
	Leaf AC	0.41 \pm 0.03	0.08	0.47	0.19
	Root AC	9.32 \pm 0.96	6.25	15.29	0.64

Significance levels: 0.001 '***' 0.01 '**' 0.05 '*'

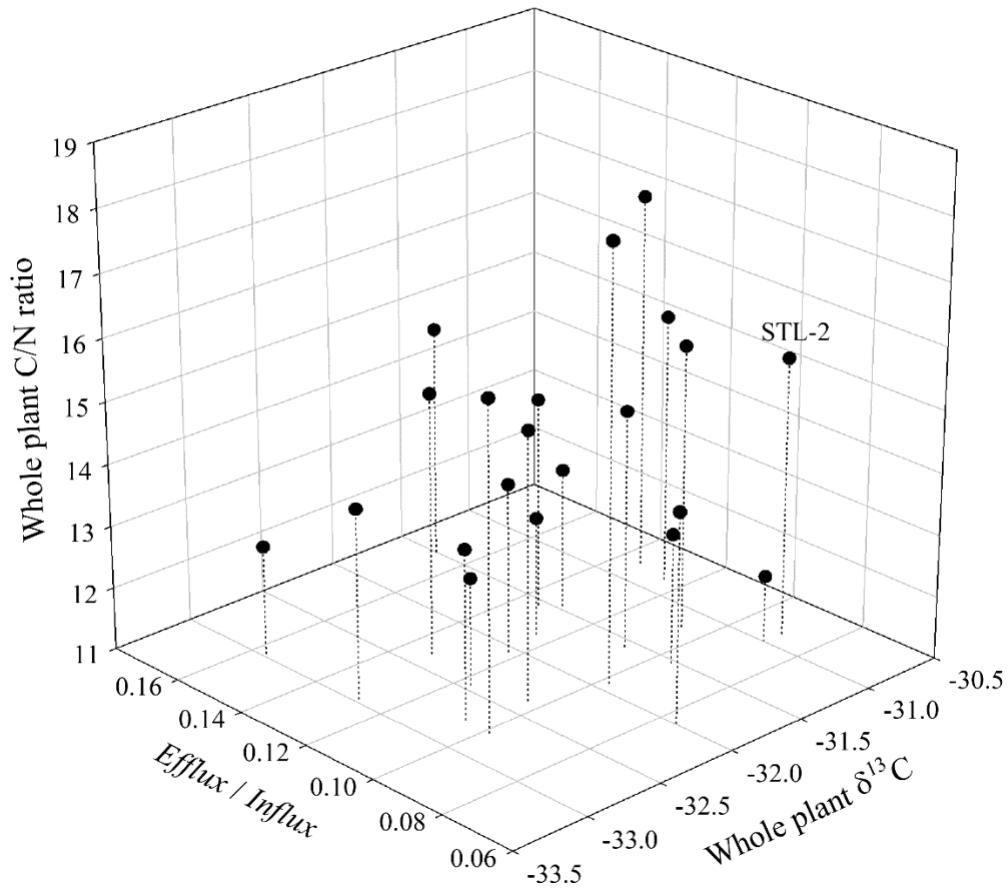


Figure 3.6. 3D scatter plot showing efflux/influx ratio (E/I), whole-plant carbon isotopic composition ($\delta^{13}\text{C}$), and whole-plant C/N ratio of the 21 genotypes used in the hydroponics experiment. Each dot represents the mean of six replicates per genotype. The STL-2 genotype is singled out for its combination of high $\delta^{13}\text{C}$, high C/N, and low E/I .

3.5 Discussion

Patterns in C and N stable isotopes from the outdoor common garden and controlled environment hydroponic experiments were similar in direction, but different in magnitude. In the common garden experiment, I sampled leaves and stems from 34 populations of heart-leaved willow collected across Canada and I found significant population variation in $\delta^{13}\text{C}$ and C/N ratios in leaves and stems, indicating differences in WUE and NUE among populations (Table 3.1). I also found no correlation between $\delta^{13}\text{C}$ and C/N ratios at this level, and thus no trade-off between WUE and NUE (Figure 3.2a). In contrast, across all individuals, there was a significant negative correlation between foliar $\delta^{13}\text{C}$ and C/N (Figure 3.2b), implying a genetic and/or plastic trade-off between WUE and NUE that was unassociated with local adaptation. Plastic variation in WUE, trading off with NUE, is commonly reported in response to changes in water and/or N supply (Patterson *et al.* 1997; Livingston *et al.* 1999; Drenovsky *et al.* 2012), whereas Pointeau and Guy (2014) detected no genotypic trade-off between $\delta^{13}\text{C}$ and C/N in two *Populus* species. I could not distinguish between these two possibilities in my common garden study because the individual genotypes were unreplicated, however, the high within-population variation I observed suggested an environmental effect due to uncontrolled differences between planting spots. I controlled for this possibility by growing clonally replicated plants under hydroponic conditions.

I found many genotypic effects on growth and isotope-based traits in the controlled environment study (Table 3.4), including biomass, root-shoot ratio, whole-plant and organ level $\delta^{13}\text{C}$ and $\Delta^{15}\text{N}$, and *E/I*. There was no significant correlation between $\delta^{13}\text{C}$ and C/N ratios at either the whole-plant or leaf level (Appendix Figure

B.2), confirming the absence of a clear trade-off between WUE and NUE across genotypes.

Genotypic variation in $\delta^{15}\text{N}$ has been reported in Norway spruce (*Picea abies*) and European beech (*Fagus sylvatica*) grown under field conditions (Gebauer and Schulze 1991; Peuke *et al.* 2006), and in white spruce (*Picea glauca*), balsam poplar (*Populus balsamifera*) and black cottonwood (*Populus trichocarpa*) in hydroponics (Prichard and Guy 2005; Kalcsits and Guy 2013b). There is also large-scale geographic variation in site-averaged plant and soil $\delta^{15}\text{N}$ that is significantly correlated to climate variables, such as temperature and precipitation (Handley *et al.* 1999; Amundson *et al.* 2003). However, no population differences or species-level clinal patterns in $\delta^{15}\text{N}$ have previously been reported that might connect genetic variation (between or within species) with climate or geography. Here, $\delta^{15}\text{N}$ values of leaves and plants from both the hydroponics (Figure 3.3c, 3.4a) experiment and from the common garden (Figure 3.3a) were significantly correlated with latitude. The steeper slope obtained from the common garden experiment may reflect unexpected co-variation between latitude of origin and soil conditions at the site, or differential uptake of other N sources, such as ammonium.

The AgCanSalix collection of heart-leaved willow spans 15° in latitude and 52° in longitude (Figure 3.1). Within this collection, latitude, longitude, and elevation for the accessions, and associated climate variables, all tend to inter-correlate because the range of heart-leaved willow in Canada extends further north in the west, towards the continental divide, than it does in the east. Under steady-state hydroponics, whole-plant $\delta^{15}\text{N}$ was positively correlated to geography (latitude, longitude, and elevation) and negatively correlated to length of the frost-free period and mean annual precipitation. In contrast, a parabolic relationship with latitude (Figure 3.4b) suggested a more complicated geoclimatic pattern for $\delta^{13}\text{C}$ (e.g., the provenance closest to the vertex had

the highest summer dryness index). Indeed, whole-plant $\delta^{13}\text{C}$ was positively correlated with mean annual precipitation and negatively correlated with frost-free period, mean warmest month temperature, continentality, and annual and summer dryness indices. The outdoor common garden also showed negative correlations between foliar and stem $\delta^{13}\text{C}$ and summer dryness (Appendix Figure B.1). Both data sets suggest that genotypes or populations with higher WUE originate from more water replete locations.

In a provenance study of lodgepole pine (*Pinus contorta* Dougl.) in British Columbia, Guy and Holowachuk (2001) suggested that high WUE is associated with adaptation to wetter locations not because of lower water use, but because of intrinsically higher photosynthetic capacity, as suggested by higher growth rates in all of three climatically divergent common gardens. If the same is true of heart-leaved willow, however, it is neither positively nor negatively reflected in growth rate. There are similar reports in the literature. For example, Lauteri *et al.* (1997, 2004) also found lower discrimination and higher WUE in *Castanea sativa* genotypes from wet as compared to dry environments in Turkey, but these differences were associated with lower photosynthetic capacities and lower growth rates in the wet-adapted genotypes. Cernusak (2020) suggested that species or ecotypes from areas with less consistent water supplies may be more prone to rapid water use (and lower WUE) when it is available.

The canonical correlation analysis extracted two significant variates that encompass different geo-climatic variables (Table 3.3). CLIM1 appears to be associated with “growing season” because frost-free period and mean warmest month temperature were loaded heavily on it, whereas elevation, mean annual precipitation, and annual dryness index were strongly loaded on CLIM2, which thus appears to reflect “water availability”. Plant $\delta^{13}\text{C}$ was significantly associated with both axes, but more

with “growing season” than with “water availability.” The indication is that accessions with higher WUE are thus also favored by shorter and cooler growing seasons, as reported for several woody plant species (McKown *et al.* 2014; Soolanayakanahally *et al.* 2015; Kaluthota *et al.* 2015; Momayyezi and Guy 2017), including *S. eriocephala* (Shunmugam *et al.* 2016). In contrast to $\delta^{13}\text{C}$, canonical structure analysis suggests that whole-plant and leaf $\delta^{15}\text{N}$ were more tightly (and negatively) related to “water availability” than “growing season”. This pattern suggested plants from wetter locations have low $\delta^{15}\text{N}$ values. Although what I report is a relationship between phenotype and the environment of origin, it is interesting that Handley *et al.* (1999) and Amundson *et al.* (2003) observed that across different sites, foliar $\delta^{15}\text{N}$ was negatively correlated with annual precipitation. To account for this trend, Handley *et al.* (1999) suggested a mechanism whereby there is isotopically important leaching of ^{15}N -enriched dissolved organic nitrogen at wetter sites. In contrast, Amundson *et al.* (2003) suggested that wetter ecosystems have lower losses of ^{15}N -depleted N forms. Either way, my data suggest that local adaptation affecting N isotope discrimination at the whole-plant level may also contribute to this pattern.

The clinal variation in $\delta^{15}\text{N}$ found in both the common garden, as well as the hydroponics experiment (Figure 3.3a,c) suggested possible clinal variation in N uptake and assimilation. The proportion of total plant N assimilated in roots (P_{root}) and the ratio of inorganic to total N transported in the xylem (Ti/Tt) remained relatively stable and did not differ between genotypes (Table 3.4). There was, however, significant genotypic variation in E/I that was correlated with latitude (Figure 3.5), indicating that clinal variation in $\delta^{15}\text{N}$ is caused by differences in efflux relative to influx of NO_3^- at the roots. I am unaware of any other studies examining clinal variation in $\delta^{15}\text{N}$ and nitrate uptake efficiency in plants. Even though root-shoot ratio did not show similar clinal patterns,

reduced uptake efficiency was correlated with higher root-shoot ratios (Appendix Figure B.2), which might result in a lower N demand and a higher N supply at the whole-plant level.

Because E/I was not correlated with either $\delta^{13}\text{C}$ or C/N across genotypes (Appendix Figure B.2), there appears to be no discernible trade-off between N uptake efficiency and WUE or NUE (Figure 3.6). Therefore, through breeding and/or selection, it should be possible to obtain clones or varieties with both high WUE and high NUE, as well as high nitrogen uptake efficiency. Of the 21 genotypes studied here, STL-2 stood out by combining these three traits with high productivity (80% higher than the average overall), suggesting inherently superior growth.

3.6 Conclusion

I conclude that heart-leaved willow shows significant variation in $\delta^{15}\text{N}$, $\delta^{13}\text{C}$, and C/N ratios among genotypes and populations, indicating differences in N uptake and assimilation, WUE, and NUE. There is clinal variation in N isotope discrimination with latitude, which may be related to water availability and could contribute to global patterns in ecosystem $\delta^{15}\text{N}$. The absence of a trade-off between WUE and NUE as well as E/I , suggests that it is possible to capture additive genetic variation in WUE, NUE, and E/I in heart-leaved willow.

Chapter 4 Geographic variation in $\delta^{15}\text{N}$ of black cottonwood (*Populus trichocarpa*) and identification of candidate genes for isotope discrimination by genome-wide association

4.1 Summary

Genotypic variation in nitrogen use traits has not been extensively studied in trees on a range-wide scale, either in the field or in hydroponic experiments. Understanding natural variation in nitrogen-related traits and their relationship to climate is critical for studying local adaptation and also for breeding purposes. In this chapter, I took advantage of a large collection of black cottonwood genotypes covering a major portion of the species range, to study the natural genetic variation in $\Delta^{15}\text{N}$. Nearly 400 genotypes were grown under steady-state hydroponic conditions and analyzed for growth and $\Delta^{15}\text{N}$ -related traits. Strong population level and genotypic variation in biomass, root-to-shoot ratio, carbon-to-nitrogen ratio, and whole-plant and organ level $\Delta^{15}\text{N}$ was found. A significant correlation between root $\Delta^{15}\text{N}$ and precipitation suggests that the efficiency of nitrate uptake plays a role in local adaptation to water availability. There may also have been selection towards lower root-to-shoot ratios in areas where there is reduced risk of drought. To facilitate phenotyping for GWAS analysis, leaf $\Delta^{15}\text{N}$ was shown to be highly representative of whole-plant $\Delta^{15}\text{N}$ and, by extension, reasonably indicative of IMB model-based calculation of efflux/influx (E/I) at the root. GWAS linked a gene for a glutaminyl-tRNA synthetase to root $\Delta^{15}\text{N}$ (and the difference between root and leaf $\Delta^{15}\text{N}$), but did not find any significant associations with genes related to nitrate transport or assimilation. There were, however, several associations for root-to-shoot ratio, which was in turn correlated with whole-plant $\Delta^{15}\text{N}$ and E/I .

4.2 Introduction

Nitrogen-use traits are complex and controlled by genotype, the environment and, likely, their interaction (Tegeteder and Masclaux-Daubresse 2017). Intraspecific variation in nitrogen isotope discrimination and other traits related to nitrogen utilization has been reported under field conditions for many species, such as Norway spruce (*Picea abies*) and European beech (*Fagus sylvatica*) (Gebauer and Schulze 1991; Peuke *et al.* 2006), and under controlled conditions in white spruce (*Picea glauca*), balsam poplar (*Populus balsamifera*) and black cottonwood (*Populus trichocarpa*) (Pritchard and Guy 2005; Kalcsits and Guy 2013b). Although heritability estimates for a particular trait are not fixed and depend on the populations sampled, high estimates, in theory, imply that the trait is subject to spatially variable selection. Conversely, low estimates may indicate that a trait is largely plastic in response to the immediate environment, highlighting the role of phenotypic plasticity as an additional variability reservoir (McKown *et al.* 2014a). Reports of the broad-sense heritability (H^2) for $\delta^{15}\text{N}$ have been limited to just a few species and the value was generally small (less than 0.20), especially in comparison to other N-related traits such as C/N ratio (~ 0.50) and N percentage (~ 0.60) in soybeans (*Glycine max*) and barley (*Hordeum vulgare*) (Dhanapal *et al.* 2015; Karunarathne *et al.* 2020). In poplar, a large common garden assessment of phenotypic trait variation in black cottonwood reported a H^2 of only 0.08 for leaf $\delta^{15}\text{N}$, suggesting very little inherent variation in $\delta^{15}\text{N}$ (McKown *et al.* 2014a). Detectable genotypic variation in $\delta^{15}\text{N}$ under typical field conditions is, however, not expected because of spatial variation in soil $\delta^{15}\text{N}$ and, most importantly, the fact that whole-plant discrimination cannot be expressed if the utilization of available soil N approaches completion (*i.e.*, if unused N cannot diffuse away from the roots before being consumed). Although McKown *et al.* (2014b) assessed 461 genotypes from 136

provenances, the level of genetic variation in $\delta^{15}\text{N}$ was lower than observed in just 25 genotypes from five provenances of balsam poplar when grown hydroponically (Kalcsits and Guy 2016b). Therefore, assessment of plant $\delta^{15}\text{N}$ using a substantial number of genotypes from multiple provenances under tightly controlled hydroponic conditions is necessary. Moreover, Kalcsits and Guy (2016b) observed that individual genotype and/or provenance level variation in growth, root-to-shoot (R:S) ratio, leaf N content, sites of assimilation (*i.e.*, P_{root} , Ti/Tt and proportions of root-assimilated N translocated to shoots), and E/I (provenance level only) were correlated between plants grown on nitrate vs. plants grown on ammonium, suggesting a common underpinning not related to physiological or biochemical processes specific to either N-source. Root-to-shoot ratio, for example, may affect the relationship between N demand by the shoot and N supply by the roots, and thus impact E/I and whole-plant $\delta^{15}\text{N}$ (Pritchard and Guy, 2005).

Though very fundamental, our understanding of N uptake and assimilation is still incomplete, especially for trees. Uncovering the molecular and physiological basis for these complex traits is a growing area in tree biology and requires the integration of extensive genetic and phenotypic data (Eckert *et al.* 2009, 2010; McKown *et al.* 2014c). In poplars, as well as other species of dual ecological and economic importance, there is great interest in establishing links between relevant phenotypes and genetic variation (Ingvarsson and Street 2011). Genome-wide association study (GWAS) using high genome coverage of single nucleotide polymorphisms (SNP) markers is a technique widely used for this purpose. In *Populus*, GWAS studies have implicated numerous genes in the control of various wood characteristics (Porth *et al.* 2013), stomatal patterning and bud-break phenology (McKown *et al.* 2014b, 2019), which may contribute to local adaptation (Savolainen *et al.* 2013). To date, GWAS studies on NUE-related traits have been mainly focused on identifying targets to improve NUE efficiency in crop plants,

such as rice (*Oryza sativa*) (Tang *et al.* 2019), maize (*Zea mays*) (Ertiro *et al.* 2020), and barley (Karunaratne *et al.* 2020). SNPs for ammonium (AMT) and nitrate (NRT1/NRT2) transporter genes were found to be significantly associated with N uptake and transport in those studies. Furthermore, overexpression of *OsNRT1.1* and *OsNRT2.1* increased both NUE and growth in rice (Huang *et al.* 2017; Wang *et al.* 2018). GWAS on $\delta^{15}\text{N}$ has been limited to black cottonwood (McKown *et al.* 2014b) and at least three studies utilizing soybean (Dhanapal *et al.* 2015; Steketee *et al.* 2019, Bazzar *et al.* 2020). As expected, no significant associations were found for black cottonwood given that the trees were field-grown (as noted earlier). In contrast, numerous SNP associations have been found in soybean, despite also being field-grown. Soybean, however, is an N-fixing legume and, as such, plant $\delta^{15}\text{N}$ provides a measure of the amount of N obtained directly from the atmosphere relative to what is taken up from the soil. To date, no GWAS has been published on $\delta^{15}\text{N}$ -related traits obtained on plants grown hydroponically. Furthermore, the many GWAS studies conducted on crop plants have not generally been completed in the context of exploring the genetic underpinnings of natural biogeographic variation in N-use traits and the possibility of local adaptation.

In this chapter, I provide a large-scale assessment of tissue and whole-plant $\delta^{15}\text{N}$ values in black cottonwood clones grown hydroponically, using accessions covering much of the species' range within British Columbia, Oregon, and Washington. All black cottonwood accessions used in this study were previously genotyped for SNPs estimating extensive allelic variation in 3.5K genes distributed across the genome (Geraldes *et al.* 2013). My first hypothesis was that under controlled hydroponic conditions, the nearly 400 poplar genotypes assessed would show significant genetic variation in N isotope discrimination and C/N ratios at both the clone and population level. I further hypothesized that, as in heart-leaved willow (Chapter 3), there would be

relationships between this variation and geoclimatic variables suggestive of local adaptation. The third hypothesis was that genes relating to N-related traits and the balance between N supply and demand (and thus E/I), such as for assimilatory enzymes, transporters or R:S ratio, would be implicated by a GWAS association analysis.

4.3 Methods and materials

4.3.1 Plant materials

This study employed a large collection of native black cottonwood genotypes originating from a large portion of the species range (38.9-59.6°N, 121.2-137.9°W, Figure 4.1), collected by the British Columbia Ministry of Forests, Lands and Natural Resource Operations in the mid-1990s and planted in 2008 into a common garden at Totem Field, UBC, Vancouver, British Columbia, Canada (49.26°N, 123.25°W). Because of space limitations and the large number of genotypes assessed, 362 genotypes were randomly assigned to nine different hydroponic runs blocked in time. The first eight runs were conducted between the spring 2012 and summer 2014. To allow data normalization among runs, one additional run was conducted in summer 2019 which randomly selected at least two genotypes from each of the original eight runs (details in Appendix Figure C.1). Each run was considered as one “block” and each genotype within or between the blocks had a minimum of three replicates. First year scions of *P. trichocarpa* were collected from the common garden in early February each year, and stored in black plastic bags at 4°C. Freshly cut two-node scions, approximately 5 cm long, were rooted in distilled water in the UBC Horticulture greenhouse before transferring to hydroponics.

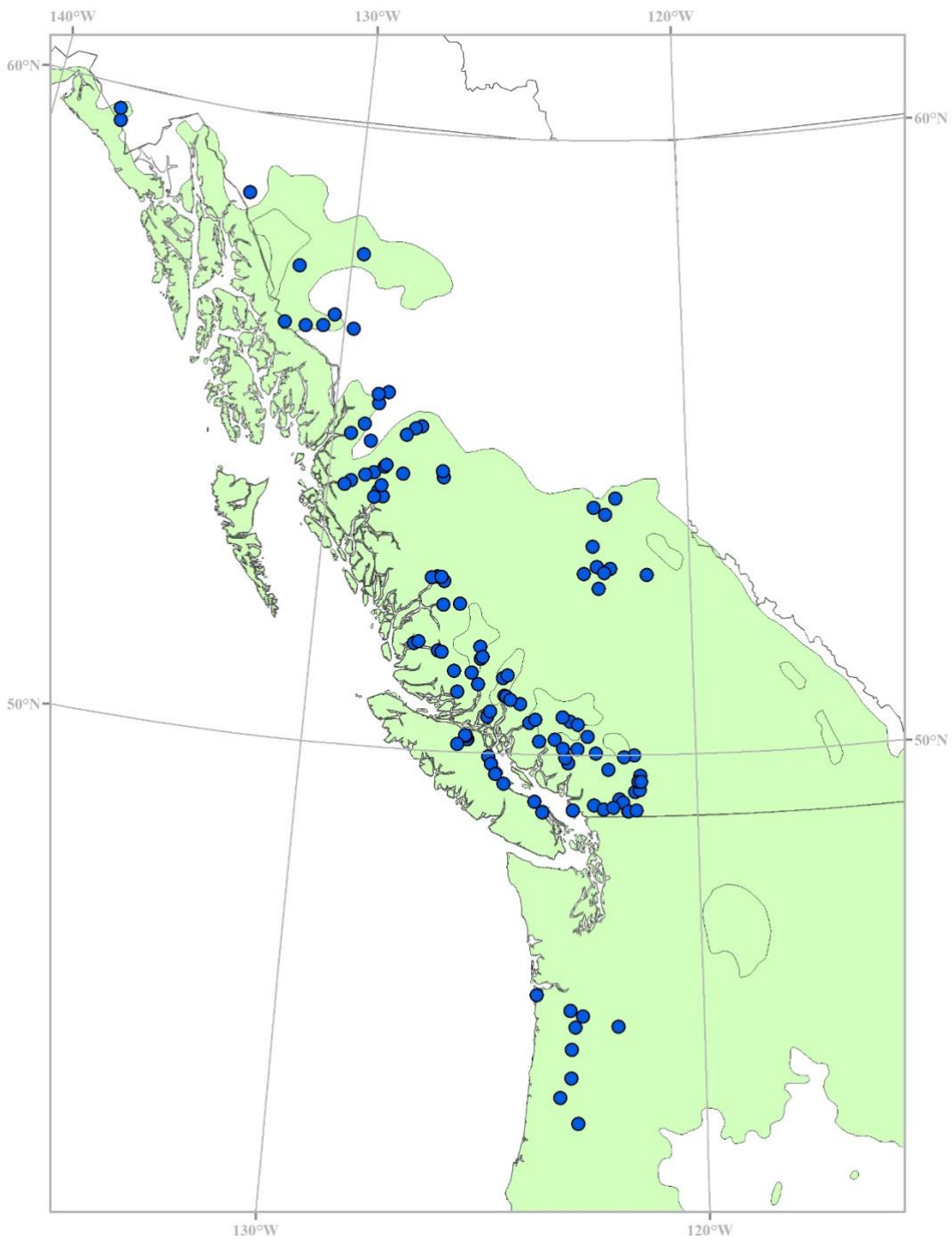


Figure 4.1. Locations of 107 populations of black cottonwood (*Populus trichocarpa*) sampled from the natural range of the species in western North America, as shown in blue. The green area represents the dominant continuous range of the species.

4.3.2 Hydroponic system

The hydroponics system was as described in detail in Kalcsits and Guy (2016ab) and consisted of up to four 1000 L wooden containers lined with rubber pond liner material (Firestone, Nashville, TN, USA), each with a centrifugal pump and an air pump to circulate and oxygenate the media. The containers were fitted with floating Perspex “rafts” that held up to 32 plants per raft. The hydroponics solution was a modified 1/10th Johnson’s solution (Johnson *et al.* 1957) supplemented with 0.25 mM Ca(NO₃)₂. Media NO₃⁻ concentration was monitored using the perchloric acid method (Cawse 1996) to ensure there was no substantial decrease (no more than 10%) in NO₃⁻ concentration over time that could result in major changes to the δ¹⁵N of the hydroponics solution. The nutrients were completely replaced as necessary, usually every one to two weeks. The hydroponic system was under ambient light conditions supplemented by LED lighting (600 μmol m⁻² s⁻¹ PPFD) on an 18/6 hr day/night photoperiod. Temperatures in the greenhouse were maintained between 20 - 24°C.

4.3.3 δ¹⁵N phenotyping

Plants were harvested into leaves, stems, roots, and original cuttings after 45 days of growth. Once freeze-dried, these parts were weighed and then pulverized using a Wiley mill (Fritsch Laborgeratebau, Terochem Scientific, Ottawa, Canada) followed by a Geno/Grinder (SPEX SamplePrep, Metuchen, New Jersey, USA). Sub-samples (3 mg) were packed into tin capsules and analyzed for %C, %N, and δ¹⁵N using a Vario EL Cube Elemental Analyzer (Elementar, Germany) interfaced to an Isoprime Isotope Ratio Mass Spectrometer (GV Instruments, UK) in the Stable Isotope Lab, Agriculture and Agri-Food Canada Lethbridge Research and Development Centre, Lethbridge, Alberta, Canada.

Leaf, stem, root and original cutting samples were all analyzed for blocks 1-4 and 9, but because of budget limitations, only leaf and root samples were analyzed for blocks 5-8 (more than 3000 samples overall).

Nitrogen isotopic composition ($\delta^{15}\text{N}$) and isotope discrimination ($\Delta^{15}\text{N}$) are expressed as:

$$\delta^{15}\text{N} = \left(\frac{R_{\text{sample}}}{R_{\text{standard}}} - 1 \right) \quad (4.1)$$

$$\Delta^{15}\text{N} = \frac{(\delta^{15}\text{N}_{\text{source}} - \delta^{15}\text{N}_{\text{sample}})}{(1 + \delta^{15}\text{N}_{\text{sample}})} \quad (4.2)$$

where, R_{sample} and R_{standard} are the $^{15}\text{N}/^{14}\text{N}$ ratios of the sample and arbitrary standard (air N_2), respectively, and $\delta^{15}\text{N}_{\text{source}}$ is the $\delta^{15}\text{N}$ of the source $\text{Ca}(\text{NO}_3)_2$, which varied slightly between runs (Table 1).

4.3.4 Geo-climatic patterns in $\Delta^{15}\text{N}$

Climatic variables for the provenance of each population were obtained from ClimateNA V.7.0 (Wang *et al.* 2016) based on the 1961-1990 Canadian Climate Normal dataset. Variables in ClimateNA included frost-free period (FFP; days), mean warmest month temperature (MWM; °C), mean annual precipitation (MAP; mm), mean summer precipitation from May to September (MSP, mm), mean annual temperature (MAT; °C), and continentality (CONT; °C). Annual dryness index (ADI) and summer dryness index (SDI), were obtained according to Guy and Holowachuk (2001):

$$ADI = (e_{s[\text{MAT}]} \times 1000) / MAP \quad (4.3)$$

$$SDI = (e_{s[\text{MTWM}]} \times 1000) / MSP \quad (4.4)$$

where, e_s is the saturation vapor pressure in kilopascals at MAT and MTWM, respectively, calculated according to Buck (1981) and Yin (1998).

Population-level relationships between climatic variables as described above and $\Delta^{15}\text{N}$ and C/N mass ratios of leaves, roots and whole-plants were tested using linear mixed effects models with the “LME4” (Bates *et al.* 2015) and “lmerTest” (Kuznetsova *et al.* 2017) packages in R. All climatic variables were included as fixed effects and block was treated as a random effect in the full model. The model with the lowest Akaike Information Criterion (AIC) was selected by stepwise deletion of each fixed effect. I also conducted a linear mixed effects model of $\Delta^{15}\text{N}$ values with genotype and population as fixed effects and block as a random effect to test for genotypic variation across all blocks.

4.3.5 Heritability estimates and GWAS analysis

I estimated broad-sense trait heritability (H^2) using data from individual plants across genotypes for nitrogen-related traits ($n = 627-1196$, depending on the trait). As described in McKown *et al.* (2014a), a linear mixed model was used to estimate variance components as follows:

$$Y = X\beta + Z\mu + e \quad (4.5)$$

where, Y is the vector of measurements; β and μ , vectors of fixed and random effects (population and genotype); and X and Z were matrices assigning fixed and random effects to each measurement in Y . Variance components (σ_g^2 , total genetic variance; σ_e^2 , the residual variance) were then used to calculate H^2 as follows:

$$H^2 = \frac{\sigma_g^2}{\sigma_g^2 + \sigma_e^2} \quad (4.6)$$

GWAS of 29,355 SNPs with R:S ratio, leaf $\Delta^{15}\text{N}$, root $\Delta^{15}\text{N}$, and the difference in $\Delta^{15}\text{N}$ between the root and the leaf ($\Delta^{15}\text{N}_{\text{root-leaf}}$), utilizing mean data for all 392

genotypes was conducted based on the method described in McKown *et al.* (2014b) with the following generalized linear model:

$$\mathbf{Y} = \mu + \mathbf{S}\boldsymbol{\alpha} + \mathbf{X}\boldsymbol{\beta} + e \quad (4.7)$$

where, \mathbf{Y} is the vector of measurements; μ , overall population mean; $\boldsymbol{\alpha}$ and $\boldsymbol{\beta}$, vectors of fixed effects for both SNP genotype and population, respectively; \mathbf{S} and \mathbf{X} , index matrices assigning fixed effects for both SNP genotype and population; and e , residual effect. Significant associations were identified after applying a Bonferroni multiple testing correction whereby α values at 0.05 and 0.1 were adjusted by dividing by the number of tests conducted (29,355) to yield thresholds of $P < 1.7 \times 10^{-6}$ and $P < 3.4 \times 10^{-6}$, respectively. Identities of candidate genes and their annotations were obtained from the online platform Phytozome v13 for *Populus trichocarpa* v3.0. Additional potential functions for identified genes were gleaned from the literature.

4.4 Results

4.4.1 Heritability of biomass and nitrogen related traits

Genotypic means, ranges and broad-sense heritability (H^2) for biomass, root-shoot (R:S) ratio, and organ and whole-plant level discrimination ($\Delta^{15}\text{N}$) are summarized in Table 4.1. Population and genotypic level variation were both highly significant for all traits, but differences between genotypes were stronger than differences between populations. Discrimination relative to the source nitrogen was higher for roots (averaging 5.21‰) than for stems (averaging 2.57‰) and leaves (averaging -0.15‰). The mean for the $\Delta^{15}\text{N}$ difference between root and leaf was 5.35‰, which was similar to the root $\Delta^{15}\text{N}$ (5.21‰). Since roots only accounted for a small proportion of plant N content, whole-plant $\Delta^{15}\text{N}$ (averaging 0.74‰) was closer to the stem and leaf values. The mean H^2 of traits listed in Table 4.1 was 0.22. The highest H^2 among the N-related traits was for the root $\Delta^{15}\text{N}$ (0.40), and the lowest H^2 was for the root C/N (0.10). The H^2 estimates for leaf and whole-plant $\Delta^{15}\text{N}$ were the same (0.19), both being higher than the H^2 of stem $\Delta^{15}\text{N}$ (0.15).

Relationships between growth, discrimination and calculated physiological variables were explored using the data from batches 1-4 and 9, where full data was available for stem and whole-plant $\Delta^{15}\text{N}$ thereby allowing further IMB model calculations for 209 genotypes. Consistent with the observation that most plant N was foliar, mean genotypic leaf $\Delta^{15}\text{N}$ was highly predictive of whole-plant $\Delta^{15}\text{N}$ ($r=0.76$, $P<0.001$, Figure 4.2a) and the IMB model-estimated E/I ($r=0.72$, $P<0.001$, Figure 4.2b). Root $\Delta^{15}\text{N}$ was also predictive of whole-plant $\Delta^{15}\text{N}$ ($r=0.35$, Figure 4.3a) and E/I ($r=0.39$, $P<0.001$, Figure 4.3b), but not so strongly. Whole-plant $\Delta^{15}\text{N}$, and consequently the calculated E/I , were both significantly and positively correlated with the R:S ratio ($r=0.31$ and 0.28 , $P<0.001$, Figure 4.4).

Leaf and root $\Delta^{15}\text{N}$ data were available for all of batches 1-9 (362 genotypes). There was no relationship between R:S ratio and either leaf or root $\Delta^{15}\text{N}$, or the difference between them across this larger dataset (Figure 4.5), or in batches 1-4 and 9 considered alone (not shown).

Table 4.1. Overall genotypic means and ranges of whole-plant (WP) biomass, root-to-shoot (R:S) ratio, organ and whole-plant level nitrogen isotope discrimination ($\Delta^{15}\text{N}$), and carbon to nitrogen ratio (C/N), and related broad-sense heritability estimates (H^2) across *Populus trichocarpa* accessions.

Trait	<i>n</i>	Mean value \pm SD	Data range	H^2	Population effect	Genotype effect
WP Biomass (g)	362	8.41 \pm 2.85	0.05-33.65	0.34	***	***
R:S ratio	362	0.25 \pm 0.05	0.12-0.71	0.16	**	***
Leaf $\Delta^{15}\text{N}$ (‰)	362	-0.15 \pm 0.46	-1.77-1.95	0.19	**	***
Root $\Delta^{15}\text{N}$ (‰)	362	5.21 \pm 0.80	2.33-7.69	0.40	***	***
$\Delta^{15}\text{N}_{\text{root-leaf}}$ (‰)	362	5.35 \pm 0.76	1.46-7.21	0.22	***	***
Stem $\Delta^{15}\text{N}$ (‰)	209	2.57 \pm 0.04	0.62-5.39	0.15	**	***
WP $\Delta^{15}\text{N}$ (‰)	209	0.74 \pm 0.36	-0.19-3.16	0.19	**	***
Leaf C/N	311	10.82 \pm 1.05	6.83-16.33	0.20	*	***
Root C/N	311	12.10 \pm 1.23	3.33-21.34	0.10	***	***

Significance levels: 0.0001 '***' 0.005 '**' 0.001 '*'

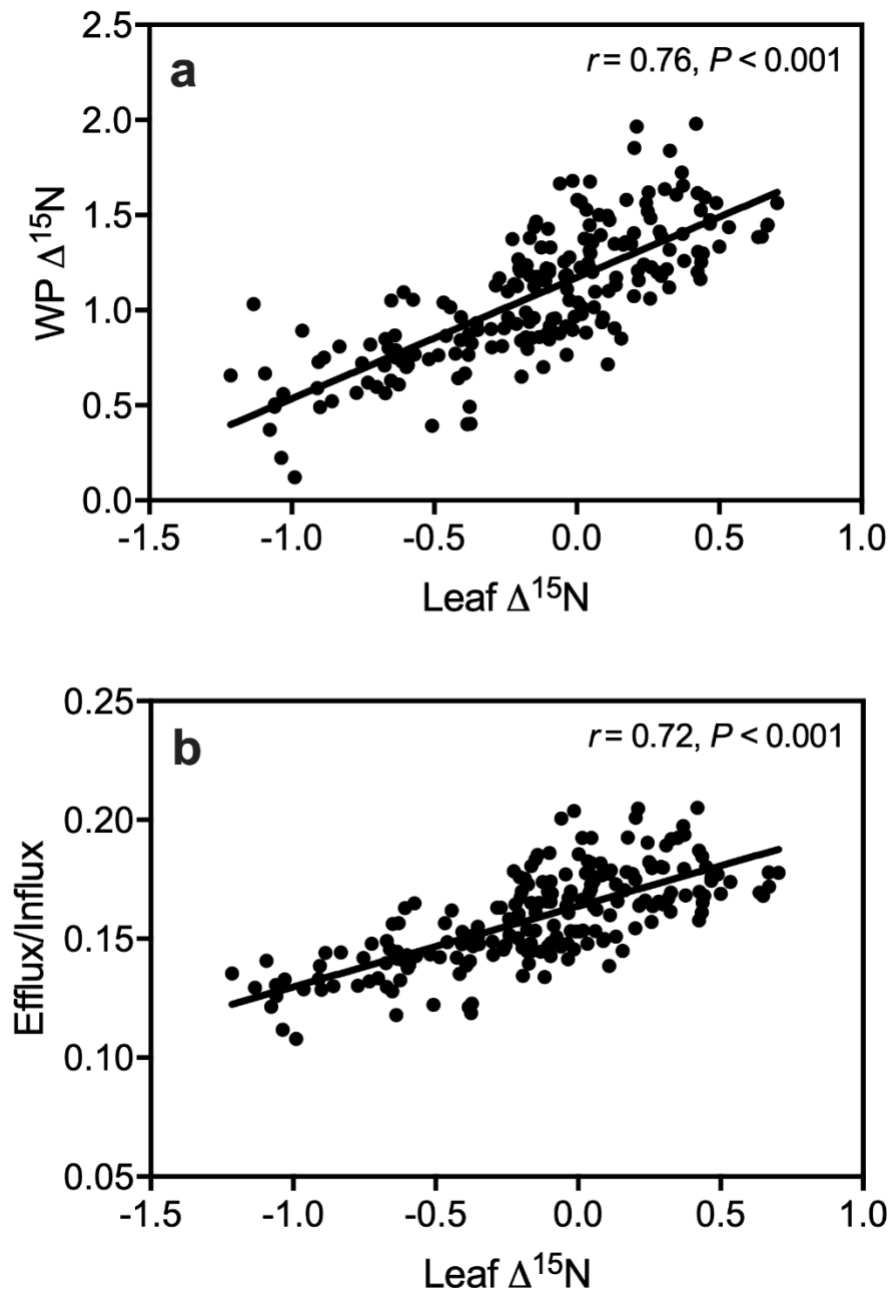


Figure 4.2. Relationships between leaf isotope discrimination ($\Delta^{15}\text{N}$) and whole-plant (WP) $\Delta^{15}\text{N}$ (a), and root efflux/influx (b) in *Populus trichocarpa* accessions. Each point represents one genotypic mean with three replicates across batches 1-4 and 9 ($n=209$).

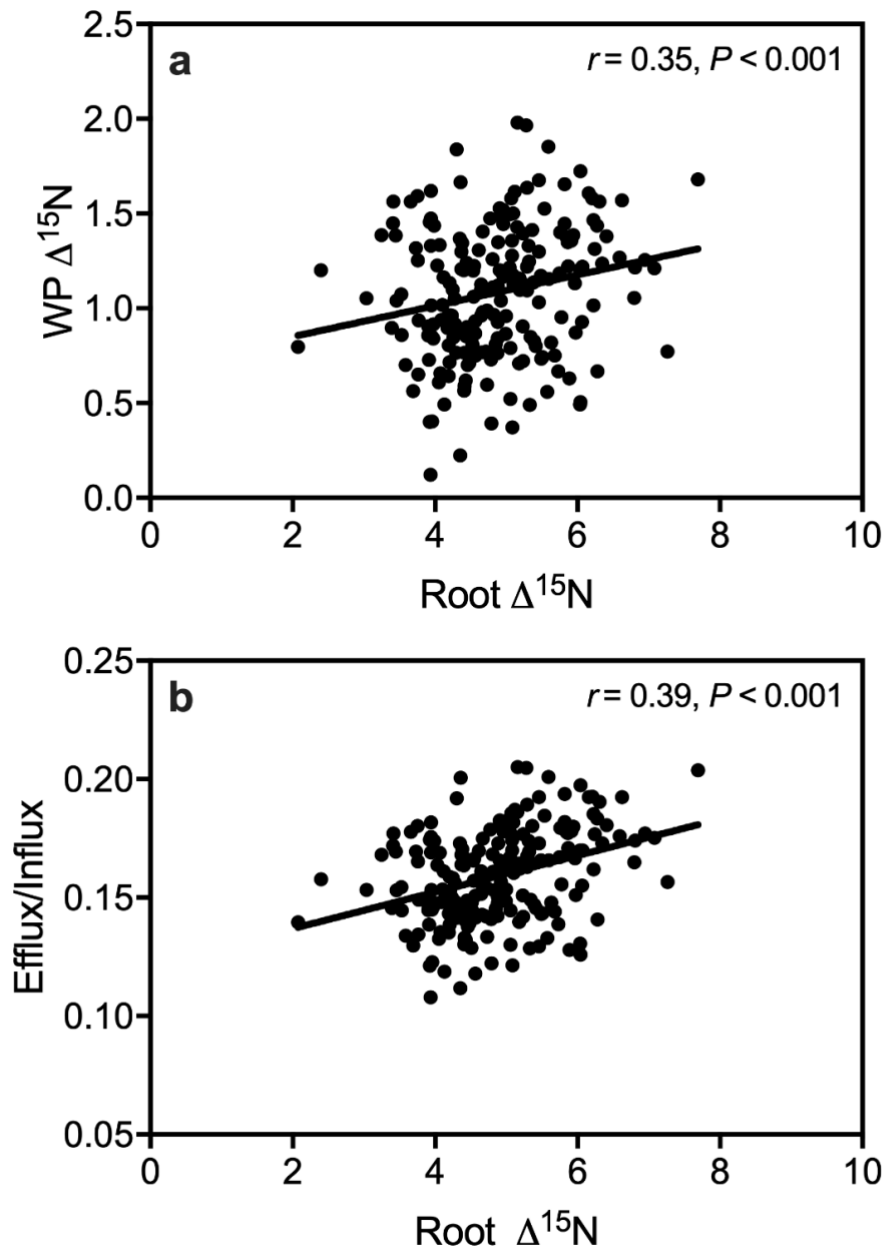


Figure 4.3. Relationships between root $\Delta^{15}\text{N}$ and whole-plant $\Delta^{15}\text{N}$ (a), and root efflux/influx (b) in *Populus trichocarpa* accessions. Each point represents one genotypic mean with three replicates across batches 1-4 and 9 ($n=209$).

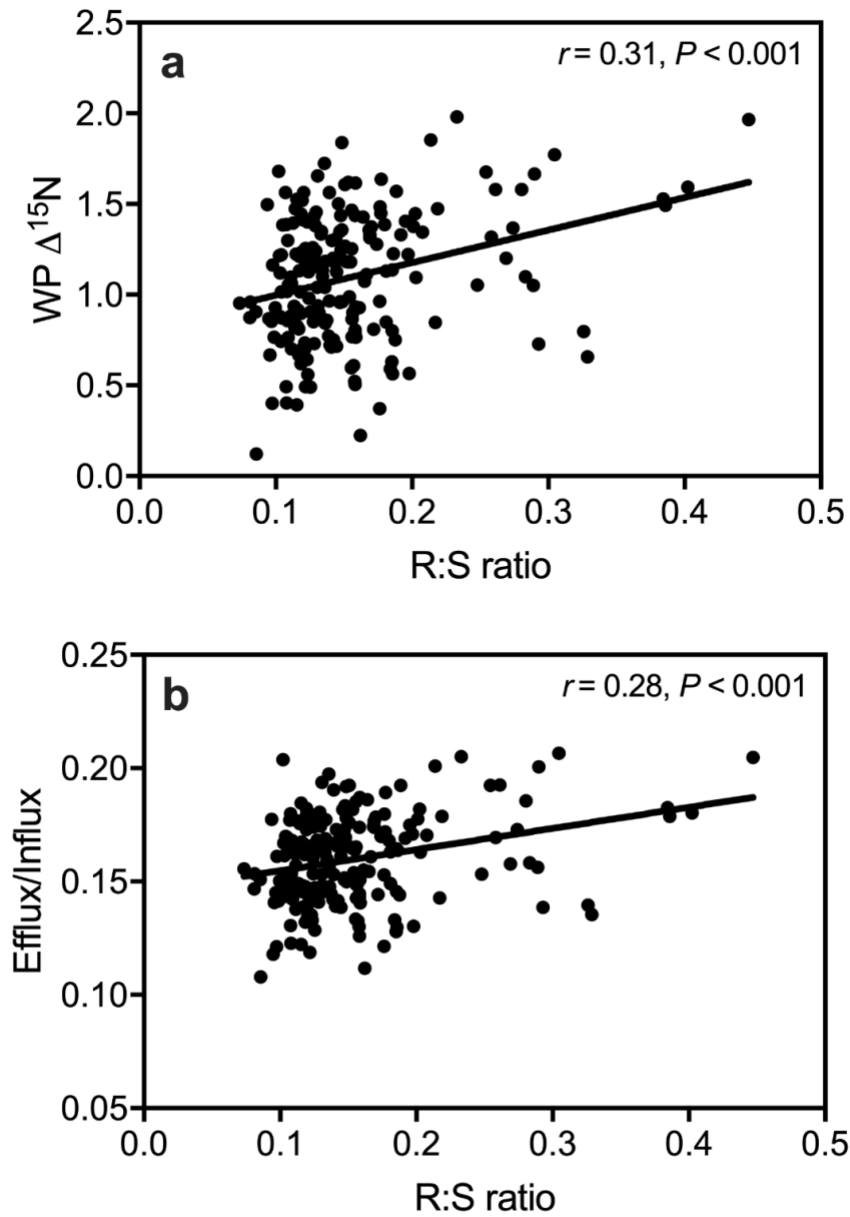


Figure 4.4. Relationships between root-to-shoot (R:S) ratio and whole-plant (WP) $\Delta^{15}\text{N}$ (a), and root efflux/influx (b) in *Populus trichocarpa* accessions. Each point represents one genotypic mean with three replicates across batches 1-4 and 9 ($n=209$).

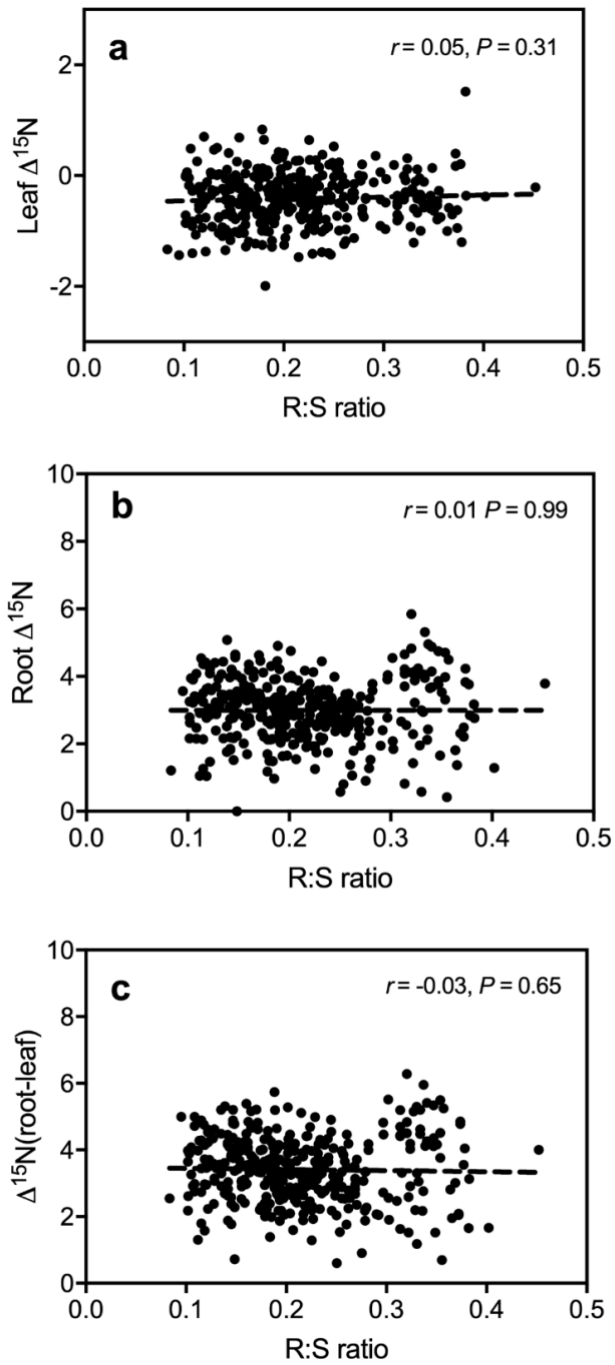


Figure 4.5. Relationship between root-to-shoot (R:S) ratio and leaf, root and the leaf-root difference in nitrogen isotope discrimination ($\Delta^{15}\text{N}$) in *Populus trichocarpa* accessions. Each point represents one genotype with at least three replicates across 9 batches ($n=362$).

4.4.2 Correlation matrix

Collection-wide relationships between geo-climatic parameters and N-related traits for all genotypes are shown in Table 4.2. Unlike the results for heart-leaved willow in Chapter 3, the biomass and N isotopic traits barely show any significant relationship to geo-climatic variables. The most significant correlations observed were for root-related traits. Root C/N was negatively correlated to mean annual precipitation (MAP) and positively correlated to latitude, elevation, continentality (CONT), and annual dryness index (ADI). Root-to-shoot ratio was negatively correlated to frost-free period (FFP) and MAP, and positively correlated to latitude, elevation, CONT, and ADI. Root $\Delta^{15}\text{N}$ was significantly correlated only with ADI.

Further canonical structure analysis (Table 4.3) extracted two significant canonical variables (CLIM1 and CLIM2). In CLIM1, ADI and CONT were negatively loaded, while MAP and FFP were positively loaded. In CLIM2, mean summer precipitation (MSP) and MAP were negatively loaded, while summer dryness index (SDI) and ADI were positively loaded. Root C/N and root mass both were negatively loaded on CLIM1, and root $\Delta^{15}\text{N}$ loaded positively on CLIM2. Root-to-shoot ratio loaded negatively on CLIM1 and positively on CLIM2.

Table 4.2. Relationships between nitrogen-related physiological variables and geoclimatic variables across 107 provenances of *Populus trichocarpa*. There were 2-4 genotypes per provenance and three ramets per genotype. Bolding indicates significance at $P < 0.05$; Bold* indicates significance at $P < 0.01$.

	LAT	LON	ELV	FFP	MWMT	MAP	CONT	ADI	SDI
Leaf $\Delta^{15}\text{N}$	-0.05	-0.01	-0.05	0.04	0.06	0.03	-0.04	-0.04	-0.01
Root $\Delta^{15}\text{N}$	-0.07	-0.05	-0.01	0.03	-0.02	0.11	-0.07	-0.11	-0.04
WP mass	0.05	0.05	0.01	-0.01	-0.04	0.03	0.02	0.01	0.02
Leaf C/N	-0.06	-0.08	-0.02	0.01	0.11	0.01	-0.01	0.03	0.03
Root C/N	0.11	-0.05	0.14*	-0.07	0.02	-0.18*	0.19*	0.21*	0.07
R:S ratio	0.11	0.01	0.10	-0.12	-0.07	-0.12	0.15*	0.14*	0.01

LAT, latitude ($^{\circ}\text{N}$); LON, longitude ($^{\circ}\text{W}$); ELV, elevation (m); FFP, frost free-period (days); MWMT, mean warmest month temperature ($^{\circ}\text{C}$); MAP, mean annual precipitation (mm); CONT, continentality ($^{\circ}\text{C}$); ADI, annual dryness index; SDI, summer dryness index; $\Delta^{15}\text{N}$, nitrogen isotope discrimination; WP mass, whole-plant mass (g); C/N, carbon to nitrogen ratio; R:S ratio, root-to-shoot ratio.

Table 4.3. Canonical structure between geoclimatic parameters and plant traits with the first two canonical variables, CLIM1 and CLIM2.

Geoclimatic variables	CLIM 1	CLIM 2	Response variables	CLIM 1	CLIM 2
LAT	-0.53	-0.11	Leaf $\Delta^{15}\text{N}$	0.05	0.06
LON	-0.04	-0.09	Root $\Delta^{15}\text{N}$	0.04	-0.19
ELV	-0.57	0.07	Leaf C/N	0.05	0.09
FFP	0.42	-0.12	Root C/N	-0.24	0.08
MWMT	0.34	0.29	Leaf mass	-0.06	-0.08
MAP	0.49	-0.36	Root mass	-0.18	-0.03
MSP	0.12	-0.48	WP mass	-0.10	-0.08
CONT	-0.63	0.33	R:S ratio	-0.15	0.16
ADI	-0.64	0.26			
SDI	-0.06	0.48			

LAT, latitude ($^{\circ}\text{N}$); LON, longitude ($^{\circ}\text{W}$); ELV, elevation (m); FFP, frost free-period (days); MWMT, mean warmest month temperature ($^{\circ}\text{C}$); MAP, mean annual precipitation (mm); MSP, mean summer precipitation (mm); CONT, continentality ($^{\circ}\text{C}$); ADI, annual dryness index; SDI, summer dryness index; $\Delta^{15}\text{N}$, nitrogen isotope discrimination; C/N, carbon to nitrogen ratio; biomass traits (g); WP mass, whole-plant mass (g); R:S ratio, root-to-shoot ratio.

4.4.3 Genome-wide association analysis

The GWAS identified 22 SNPs significantly associated with R:S ratio, but only one SNP with significant association to both root $\Delta^{15}\text{N}$ and $\Delta^{15}\text{N}_{\text{root-leaf}}$. No significant SNPs were identified for leaf $\Delta^{15}\text{N}$. Seventeen of the SNPs were located in or close to known genes. The one gene associated with isotope discrimination encodes a glutaminyl-tRNA synthetase (Potri.007G039700). The genes potentially linked to R:S ratio fall into several functional categories and include protein kinases, transcription factors, and stress-related genes (Table 4.4). Of these, one candidate gene (Potri.013G054600) was identified on chromosome 13 encoding a small auxin-up RNA (SAUR). Another candidate gene (Potri.002G168200), on chromosome 2, encodes an auxin-inducible jasmonate-amido synthetase (JAR1). Another candidate gene (Potri.015G119300), on chromosome 15, encodes EXOCYST COMPLEX COMPONENT EXO84C. Another candidate gene (Potri.003G198900), on chromosome 3, encodes a LEUCINE-RICH REPEAT(LRP)-CONTAINING PROTEIN.

Table 4.4. Genes and their *Arabidopsis thaliana* (AT) homologs identified by GWAS with SNP markers associated with root-to-shoot (R:S) ratio, or both root ¹⁵N discrimination ($\Delta^{15}\text{N}$) and the leaf-root difference in discrimination ($\Delta^{15}\text{N}_{\text{root-leaf}}$) in *Populus trichocarpa*. Information under “potential significance” comes from the online platform DICOTS PLAZA V4.5 except where otherwise indicated.

Trait	Gene	AT homolog	Annotated description	Potential significance
R:S ratio	Potri.010G168500	AT1G26810	Beta-1,3-galactosyltransferase (GALT1)	Various types of N-glycan biosynthesis; glycan biosynthesis and metabolism.
R:S ratio	Potri.002G168200	AT2G46370	JASMONIC ACID-AMIDO SYNTHETASE JAR1	Encodes a jasmonate-amido synthetase that is a member of the GH3 family of proteins; auxin-induced gene and localizes to the cytoplasm.
R:S ratio	Potri.013G115400	AT1G71860	PROTEIN TYROSINE PHOSPHATASE 1	Encodes a protein with tyrosine phosphatase activity that is downregulated in response to cold and upregulated in response to salt stress.
R:S ratio	Potri.015G109000	NA	Pentatricopeptide repeat protein	Coexpressed with genes in root specific coexpression subnetwork.
R:S ratio	Potri.005G113000	AT5G66200	ARMADILLO REPEAT ONLY 2 PROTEIN	
R:S ratio	Potri.008G194400	AT2G22430	Homeobox associated leucine zipper (HALZ)	Encodes a homeodomain leucine zipper class (HD-Zip I) protein that regulates hormone response.
R:S ratio	Potri.008G118300	AT1G68640	Transcription factor TGA like domain; Basic-leucine zipper domain	
R:S ratio	Potri.011G123700	AT1G52870	PEROXISOMAL MEMBRANE (MPV17/PMP22) FAMILY PROTEIN	
R:S ratio	Potri.013G054600	NA	Auxin responsive protein	Small auxin-up RNA (SAUR); encodes a short-lived nuclear protein that is related to auxin-mediated cell elongation (Knauss <i>et al.</i> 2003).
R:S ratio	Potri.007G102900	AT3G22560	ALANINE ACETYL TRANSFERASE-LIKE PROTEIN	Differentially downregulated in nitrogen10 in root vs. stem comparison.
R:S ratio	Potri.007G046200	AT4G36920	AP2-like ethylene-responsive transcription factor	Coexpressed with genes in root specific coexpression subnetwork.

R:S ratio	Potri.001G115200	AT4G22810	Similar to DNA-binding protein-related	Highly expressed in root.
R:S ratio	Potri.003G198900	AT3G14470	LEUCINE-RICH REPEAT-CONTAINING PROTEIN	
R:S ratio	Potri.003G126600	AT1G63490	LYSINE-SPECIFIC DEMETHYLASE LID	
R:S ratio	Potri.010G092900	NA	Similar to 4-alpha-D-glucan glucanohydrolase	
R:S ratio	Potri.015G119300	AT1G10180	EXOCYST COMPLEX COMPONENT EXO84C	Integral to root growth; helps establish root meristem size and facilitate rapid cell expansion in the elongation zone (Cole <i>et al.</i> 2014).
Root $\Delta^{15}\text{N}$ & $\Delta^{15}\text{N}_{\text{root-leaf}}$	Potri.007G039700	AT5G66860	Glutaminyl-tRNA synthetase	Enzyme responsible for catalyzing the transfer of glutamine to the A76 2' hydroxyl group of tRNA Gln isoacceptors.

4.5 Discussion

4.5.1 Leaf discrimination is representative of whole-plant discrimination

The first objective of this study was to identify genetic variation in nitrogen isotope discrimination and related traits in poplars at both the clone and population level. Strong genetic variation in $\Delta^{15}\text{N}$ and related traits was observed (Table 4.1). Consistent with most other reports in the literature (Kalcsits and Guy 2013, 2016; Driscoll *et al.* 2021), leaf $\Delta^{15}\text{N}$ was lower than root $\Delta^{15}\text{N}$, while stem $\Delta^{15}\text{N}$ was intermediate. Leaf $\Delta^{15}\text{N}$ was essentially not distinguishable from zero. This was expected based on results reported in chapter 2 (Hu and Guy 2020), where the total $\delta^{15}\text{N}$ of xylem sap was also close to zero (Figure 2.1c) because the ^{15}N -enriched inorganic N (Figure 2.1d) and ^{15}N -depleted organic N (Figure 2.2b) essentially balanced out each other out. Although roots were substantially lighter than leaves, and because leaf nitrogen usually accounted for more than 80 percent of whole-plant N content, the net effect of the differences between organs was for whole-plant $\Delta^{15}\text{N}$ to be only 0.76. This is less than reported for heart-leaved willow (Hu *et al.* 2022).

A strong positive correlation between leaf $\Delta^{15}\text{N}$ and whole-plant $\Delta^{15}\text{N}$ was found for plants grown in batches 1-4 and 9 ($r=0.76$, Figure 4.2a). The predominance of leaf $\Delta^{15}\text{N}$ in determining whole-plant $\Delta^{15}\text{N}$ indicates that it should be a suitable proxy for E/I , the calculation of which is based on whole-plant $\Delta^{15}\text{N}$. Indeed, the IMB model-derived E/I correlated strongly with leaf $\Delta^{15}\text{N}$ ($r=0.72$, $P<0.001$, Figure 4.2b). In addition to leaf $\Delta^{15}\text{N}$, calculated E/I was also significantly but not as strongly correlated with root $\Delta^{15}\text{N}$ ($r=0.39$, Figure 4.3b) and with stem $\Delta^{15}\text{N}$ ($r=0.27$, Appendix Figure C.2). This is not surprising because the calculation of E/I is based on the weighted isotopic compositions of all organs (*i.e.*, whole-plant $\Delta^{15}\text{N}$). In the IMB model, whole-plant $\Delta^{15}\text{N}$ is proposed to be a function of two variables, namely E/I and P_{root} , which are essentially properties of

the root (see Equation 2.11). Although root nitrogen accounts for a relatively small proportion of the overall whole-plant nitrogen, and thus has a limited effect on whole-plant $\delta^{15}\text{N}$, root-based traits have been suggested as contributors of whole-plant nitrogen-use in many studies (Garnett *et al.* 2009; Kalcsits *et al.* 2014). Roots can affect whole-plant $\delta^{15}\text{N}$ by changing the assimilation rates and partitioning between roots and leaves, translocation of inorganic and organic N to shoots, and root efflux relative to influx (Kalcsits and Guy 2013a; Kalcsits *et al.* 2014). Kalcsits and Guy (2013a) showed that whole-plant and organ level $\Delta^{15}\text{N}$ in *Arabidopsis thaliana* was substantially affected in mutant lines with differential expression between roots and shoots of genes involved in nitrogen uptake and assimilation.

Consistent with the expectation that N supply relative to N demand might be reflected at the plant level by carbon allocation to organs acquiring nitrogen (*i.e.*, roots), calculated E/I from batches 1-4 and 9 was positively correlated with the R:S ratio ($r=0.28$, Figure 4.3c). Although both T_i/T_t and P_{root} were strongly correlated with each other ($r=-0.96$, Appendix Figure C.2), as they must be algebraically (Equation 2.10), only P_{root} was significantly correlated with the R:S ratio. Although R:S ratio was correlated with whole-plant $\Delta^{15}\text{N}$ (Figure 4.4a), it was not correlated to leaf $\Delta^{15}\text{N}$, root $\Delta^{15}\text{N}$ or the difference in $\Delta^{15}\text{N}$ between roots and leaves (Figure 4.5). However, the root-leaf difference in $\Delta^{15}\text{N}$ was positively correlated to the size of the foliar nitrogen pool relative to the total plant nitrogen ($f_{\text{leaf pool}}$, Equation 2.9) ($r=0.3$, Appendix Figure C.2). As per equation 2.7, a greater $\Delta^{15}\text{N}_{\text{root-leaf}}$ suggests that a larger proportion of leaf nitrogen is assimilated in the leaves rather than the roots. It appears therefore that genotypes with higher N assimilation in the leaves tend also to invest more N in the leaves.

Leaf and root $\Delta^{15}\text{N}$ were negatively correlated, albeit weakly so (Appendix Figure C.2). This is to be expected if there is variation in the relative amounts of inorganic

versus organic nitrogen being translocated to the shoot. As shown in Chapter 2, organic N translocated in the xylem is depleted in ^{15}N , whereas inorganic N (specifically nitrate) is enriched. Any increase in ^{15}N translocation to the shoot must be balanced by a decrease in ^{15}N in the root, and vice versa. This divergence is the basis for calculating T_i/T_t in the IMB model (Kalcsits and Guy 2013a).

4.5.2 Root-related traits show signals of local adaptation

The POPCAN collection of black cottonwood spans 20° in latitude and 16° in longitude (Figure 4.1) within which there is considerable variation in biogeoclimatic conditions. Correlations between traits measured in this study and climate of origin were relatively weak. Within this collection, latitude, longitude, and to some degree elevation, are inter-correlated with each other and with climate variables because the range of black cottonwood runs roughly in a SSE to NNW direction parallel to the west coast of the Pacific Northwest of North America.

Unlike results for heart-leaved willow (chapter 3), leaf $\Delta^{15}\text{N}$ was not correlated with any geographic or climatic variable and root $\Delta^{15}\text{N}$ was only significantly correlated with mean annual precipitation and the annual dryness index. The whole-plant mass was also not correlated to any geoclimatic variables. In contrast, the root-related traits were correlated to many geoclimatic variables. Root C/N and R:S ratio were both significantly correlated to latitude, elevation, continentality, and annual dryness index, while being negatively correlated to mean annual precipitation. In addition, R:S ratio was also negatively correlated to frost-free period. Hence, root $\Delta^{15}\text{N}$, root C/N, and R:S ratio were all correlated to annual dryness index. Canonical correlation analysis was carried out and two similar variates were extracted (Table 4.3). The high end of CLIM1 appears to be associated with conditions typical of the “south coast” because continentality, annual dryness index, and latitude were all negatively loaded heavily on

it, while frost-free period and mean annual precipitation were positively loaded. CLIM2 appears to reflect “summer drought” since mean summer precipitation and summer dryness index were heavily loaded on it. Root mass and C/N were negatively associated with “south coast”, but not with “summer drought”. Root $\Delta^{15}\text{N}$ was only negatively correlated with “summer drought”. The R:S ratio was negatively associated with “south coast” and positively associated with “summer drought”. Unlike results in willow where leaf $\delta^{15}\text{N}$ was negatively correlated with annual precipitation, root-related traits in poplar were more affected by either annual or summer precipitation. Overall, it appears that there may have been selection towards lower R:S ratios in black cottonwood populations from areas where there is reduced risk of drought.

4.5.3 SNP associations to isotope discrimination and R:S ratio

Nitrogen use efficiency is believed to be largely affected by morphological traits such as rooting depth or relative investments of nitrogen in root vs. shoot growth, etc. (Beatty *et al.* 2010; Safina *et al.* 2010; Ghoneim *et al.* 2018). In this study, I selected R:S ratio along with leaf and root $\Delta^{15}\text{N}$ as promising traits for GWAS in an attempt to identify NUE-related SNPs/genes. I also included the difference in $\Delta^{15}\text{N}$ between root and leaf for GWAS as a proxy indicator for Ti/Tt and, less directly, P_{root} . Unfortunately, the association analyses with leaf $\Delta^{15}\text{N}$, root $\Delta^{15}\text{N}$, and their difference barely showed any significant association and almost all significant SNPs were related to R:S ratio. Previous GWAS studies for NUE with crop plants reported key genes related to ammonium and nitrate transporters (Huang *et al.* 2017; Wang *et al.* 2018; Tang *et al.* 2019), assimilation enzymes (Gao *et al.* 2019; Karunarathne *et al.* 2020; Yu *et al.* 2021) and root morphology (Karunarathne *et al.* 2020). The only candidate gene associated with root discrimination and the difference in $\Delta^{15}\text{N}$ between leaves and roots codes for a glutaminyl-tRNA synthetase (Potri.007G039700). Although presumably not involved in

nitrogen assimilation or transport, glutaminyl-tRNA synthetase is at least involved in nitrogen metabolism, specifically protein synthesis. How this might then impact variation in *Ti/Tt* remains obscure, but could somehow relate to the availability of glutamine for xylem transport. Glutamine is overwhelmingly the predominant form of organic N translocated in the xylem of *Populus* (Dluzniewska *et al.* 2006).

In a quantitative trait locus (QTL) study using maize recombinant inbred lines, Li *et al.* (2005) reported that nearly 70% of the QTLs for NUE overlapped with QTLs for root system architecture. In the present study, two candidate genes associated with R:S ratio were identified that are known to be auxin-related. There are three large families of auxin-response genes, namely AUX/indole-3-acetic acid genes, GRETCHEN HAGEN3 (GH3) genes, and small auxin-up RNA (SAUR) genes (Guilfoyle *et al.* 1998; Hagen and Guilfoyle 2002). SAURs are related to auxin-mediated cell elongation (Knauss *et al.* 2003). One of the identified auxin-related genes (Potri.013G054600) codes for PtSAUR85 and is expressed mainly in roots and xylem tissues. PtSAUR85 is just one of 108 SAUR genes in *Populus trichocarpa* (Hu *et al.* 2018). The other candidate gene (Potri.002G168200) is a GH3 family member and encodes an auxin-inducible jasmonate-amido synthetase (JAR1) involved in pathogen-defense signalling (Suza and Staswick 2008). Since auxin plays a central role regulating the root system (Roychoudhry and Kepinski 2021), these two auxin-related candidate genes may be involved in the control of R:S ratio in black cottonwood.

Another promising candidate gene (Potri.015G119300) associated with R:S ratio codes for EXOCYST COMPLEX COMPONENT EXO84C. Functional studies have demonstrated that the exocyst complex (including SEC3, SEC5, SEC6, SEC8, SEC10, SEC15, EXO70, and EXO84) facilitates rapid cell expansion in the root elongation zone (Cole *et al.* 2014). Another candidate gene (Potri.003G198900) encodes a LEUCINE-RICH

REPEAT(LRP)-CONTAINING PROTEIN. Although the functions of this gene remain unknown in poplar, this LRP-protein was identified in another GWAS associated with low nitrogen treatment in barley (Karunaratne *et al.* 2020). LRP-like proteins include kinases reported to be involved in signal perception and growth in *Arabidopsis* (Osakabe *et al.* 2005).

4.6 Conclusion

I conclude that black cottonwood, like heart-leaved willow, shows significant heritable variation in $\Delta^{15}\text{N}$ and C/N ratios among genotypes and populations, indicating differences in N uptake, assimilation and NUE. Strong correlation between leaf $\Delta^{15}\text{N}$ and whole-plant $\Delta^{15}\text{N}$ suggests leaf $\Delta^{15}\text{N}$ can be a proxy for whole-plant $\Delta^{15}\text{N}$, and thus E/I , in situations where the isotopic composition of the source nitrogen is held constant. Although leaf $\Delta^{15}\text{N}$ did not show signs of adaptation to climate, the positive correlation between root $\Delta^{15}\text{N}$ and precipitation suggests that nitrate uptake efficiency plays a role in local adaptation to water availability. Genotypes with intrinsically low R:S ratios also showed some tendency to come from less droughty locations. GWAS did not find any associations with genes for assimilatory enzymes and/or nitrogen transporters, and directly implicated only one gene that might be responsible for variation in isotope discrimination. There were, however, several SNP associations for R:S ratio, which was in turn significantly correlated with whole-plant $\Delta^{15}\text{N}$ and E/I , providing partial support for my third hypothesis regarding traits affecting the balance between N supply and demand.

5. Conclusion

The development of the Haber-Bosch reaction in the early 20th century, to convert atmospheric nitrogen gas (N₂) into ammonia (NH₃), gave rise to a massive global nitrogen fertilizer industry. Although crop production has doubled over the last 80 years, synthetic nitrogen fertilizer in use today is more than eight times higher than it was at the start of the green revolution (1950s) (Wu *et al.* 2020). A substantial portion of applied fertilizer is lost through leaching and run-off, volatilization, or denitrification (Vitousek *et al.* 1997; Hirel *et al.* 2007), which contributes the single largest source of nitrous oxide (N₂O) emissions (Udvari *et al.* 2021). Excessive use of nitrogen fertilizer not only has negative impacts on the environment, but also results in unnecessary economic burden in crop production. Improving nitrogen-use efficiency will be critical for reducing emissions and environmental impacts from agricultural activities. Over the last three decades, progress in improving nitrogen-use efficiency has been limited because of the complexity of nitrogen relations at the whole-plant level, despite large advances in understanding nitrogen uptake and assimilation mechanisms at molecular and physiological levels. Traditional breeding programs have mainly focused on yield-based selection to achieve genetic gains, and comparisons among crop varieties representing historic and modern materials often show associated increases in mass yield, but not nitrogen use efficiency (Duvick 2005). With more emphasis on reducing greenhouse gas emissions and environmental protection, the development of integrated measures of nitrogen-use in plants is of paramount importance.

Nitrogen isotope discrimination ($\Delta^{15}\text{N}$) is a good candidate trait to provide integrated information about nitrogen fluxes, assimilation, and allocation in plants. The isotope mass balance (IMB) model proposed by Kalcsits *et al.* (2014) simplified the models proposed by Comstock (2001) and Evans (2001) and combined measured traits

such as growth, nitrogen concentration, and isotopic composition ($\delta^{15}\text{N}$) to explain the relationship between nitrogen-use physiology and $\Delta^{15}\text{N}$ under steady-state conditions. Previously, the IMB model was partially validated by comparing estimates of E/I using the IMB model to estimates using compartmental analysis tracer efflux (Kalcsits and Guy 2016a). The model was employed to explore intraspecific variation in time-integrated nitrogen-use traits under either nitrate or ammonium-based nutrition (Kalcsits and Guy 2016b). A high degree of genotypic variation was found among growth, nitrogen uptake, and assimilation traits using the IMB model.

5.1 The N isotopic composition of xylem sap

For Chapter 2, I set out to further validate and/or improve the IMB model by quantifying the concentration and isotopic composition of nitrogen, and their relative distributions in bulk, organic, and inorganic (nitrate) fractions in xylem sap extracted from black cottonwood. I also assessed diurnal and genotypic variation in these quantities. Assuming xylem loading effectively samples the instantaneous product of nitrate assimilation, as well as the residual substrate, I hypothesized that the difference in isotopic composition between organic and inorganic nitrogen should directly reflect the *in vivo* isotope discrimination associated with N assimilation by nitrate reductase. The discrimination I observed ($\sim 25.1\text{‰}$) is indeed consistent with recent published *in vitro* determinations of the discrimination factor. When this value was used in the IMB model, the predicted ratio of inorganic to bulk N in xylem sap (27.0%) very closely matched direct measurement (26.6%), constituting a test for the model. My results suggest the $\Delta^{15}\text{N}_{\text{enzyme}}$ used in the IMB model should be higher (at least 22‰ when other literature is considered), and the model prediction can be useful for phenotyping traits related to nitrogen uptake and assimilation in hydroponically-grown plants that rely substantially on root assimilation.

As alluded to above, there are some studies reporting discrimination factors for the assimilatory enzymes, mostly for NR and a few for GS. Those experiments all measured the $\Delta^{15}\text{N}_{\text{enzyme}}$ *in vitro*, which means the enzymes were extracted and purified. There is still a need to better constrain the *in vivo* discrimination factors for these enzymes, especially GS. Although data in Chapter 2 were noisy, the approach taken to compare the $\delta^{15}\text{N}$ values between inorganic (leftover instantaneous substrate) and organic (product) nitrogen in the xylem is promising. I did grow black cottonwood with 5 μM ammonium as the sole N-source (not reported in this thesis) and attempted to analyze the $\delta^{15}\text{N}$ values of xylem sap. I applied two different methods (Holmes *et al.* 1998; Liu *et al.* 2014), but both failed because the amount of ammonium in the xylem sap was too low. The most commonly used method (Holmes *et al.* 1998) relies on ammonia diffusion and has a minimum requirement of 1-10 μmol , however, I was unable to consistently detect ammonium using 1 mL of xylem sap. The denitrifying method cannot be used for measuring $\delta^{15}\text{N}$ of ammonium directly and needs the ammonium to be converted to nitrate in advance through chemical oxidation (Liu *et al.* 2014). In my case, this method also did not work because the oxidization reaction seemed to be affected by the presence of organic nitrogen in the xylem sap. Therefore, for future *in vivo* estimation of the $\Delta^{15}\text{N}_{\text{enzyme}}$ for GS, it may be worth trying the more recent ammonium tetraphenylborate method described by Stock *et al.* (2019). I also suggest increasing the source ammonium concentration as much as possible (*i.e.*, without causing ammonium toxicity), which might then exceed the capacity of root assimilation and increase the ammonium transport from roots to shoots.

In Chapter 2, one of the main purposes of the first experiment was to establish a reliable protocol for sampling xylem sap. Part of this was to establish whether there were any changes in isotopic composition with position in the transpiration stream or

extraction pressure. Although data presented in Chapter 2 are restricted to the shoots, I did in fact attempt to extract xylem sap from root systems by expressing it from the cut stumps. Hence, sap was collected at three different positions (roots, lower shoots and upper shoots) under two different but sequential ranges of extraction pressure, the first being just 0.1-0.2 MPa and the second being 0.6-0.7 MPa above the balancing pressure. By monitoring the ATP content of xylem sap, Schneider *et al.* (1996) and Geßler *et al.* (1998) detected negligible contamination originating from parenchyma cells in both roots and shoots at 0.6 MPa above the balancing pressure. However, I found significant differences between root and shoot xylem sap both in N concentration and $\delta^{15}\text{N}$ (Figure A.1). These differences were more pronounced when xylem sap was collected at higher pressure. Total N and NO_3^- concentrations of root xylem sap were much lower than shoot xylem sap, and their $\delta^{15}\text{N}$ values were closer to the source. These observations immediately suggested that root xylem sap was contaminated with hydroponic media clinging to the roots, presumably entering at breaks caused by the disturbance of being placed into the pressure bomb. Comparison of the organic N concentration of sap extracted from roots and shoots indicated that root xylem sap was considerably diluted by this external reservoir, accounting for over 70% of the fluid collected. Therefore, I suggest that considerable precaution is needed in experiments that rely on pressurization of root systems to obtain xylem sap, for whatever purpose.

5.2 Intraspecific variation in carbon and nitrogen isotopic composition of heart-leaved willow

After testing and adjusting the IMB model as indicated above, I investigated intraspecific variation in time-integrated nitrogen-use traits in heart-leaved willow grown under field conditions and in the greenhouse under near steady-state hydroponics. Patterns in foliar $\delta^{13}\text{C}$ and $\delta^{15}\text{N}$ between field and hydroponic conditions

(which used only nitrate) were similar. I further applied the IMB model to study the individual and population level variation in $\delta^{13}\text{C}$ and $\delta^{15}\text{N}$ of heart-leaved willow. I tested the hypothesis that variation in water-use efficiency (as indicated by $\delta^{13}\text{C}$) would show a negative relationship with nitrogen-use efficiency (as indicated by tissue C/N ratio) or, through application of the IMB model, be shown to be connected to variation in N uptake efficiency and/or sites of N assimilation and allocation. I uncovered largescale geographic trends in N isotope discrimination in heart-leaved willow associated with genotypic variation in N uptake efficiency, but independent from variation in $\delta^{13}\text{C}$ and C/N ratio. To the best of my knowledge, this is the first demonstration of clinal variation in N isotope discrimination to be reported for any plant species. Since $\delta^{13}\text{C}$, C/N, and $\delta^{15}\text{N}$ were not inter-correlated, I concluded that natural and/or artificial selection on growth, WUE, NUE and N uptake efficiency can occur without trade-off in heart-leaved willow. My results imply that it is possible to use these indicators for breeding and selection purposes to capture additive genetic gains for nitrogen-uptake, water-use, and nitrogen-use efficiencies without compromising growth and other economic traits (Brendel and Epron 2022). An approach that combines the IMB model with stable isotopes is efficient and straightforward because all of $\delta^{13}\text{C}$, C/N, and $\delta^{15}\text{N}$ can be measured together on a single sample, and in large numbers, by EA-IMRS.

I found similar biogeographic patterns in foliar $\delta^{15}\text{N}$ and $\delta^{13}\text{C}$ between field and hydroponic experiments (Figure 3.3). However, unlike $\delta^{13}\text{C}$, the genotypic means for $\delta^{15}\text{N}$ values of leaves and stems did not correlate between experiments and there appeared to be a much steeper latitudinal cline in the field experiment than was found in the greenhouse. As discussed in Chapter 3, data from the common garden experiment may have reflected unexpected co-variation between latitude of origin and soil conditions at the planting site, or differential uptake of other N sources, such as

ammonium. With regard to the former, a significant greenhouse vs. field correlation in $\delta^{15}\text{N}$ might have been found if the *AgCanSalix* accessions were not blocked by provenance.

5.3 Geographic variation in $\Delta^{15}\text{N}$ of black cottonwood and identification of candidate genes by genome-wide association

To optimize carbon sequestration efficiencies, fertilizer inputs must be minimized while, at the same time, achieving rapid growth. Genotypic variation in $\Delta^{15}\text{N}$ has not been extensively studied in trees at relatively large scale, either in the field or in hydroponic experiments. I took advantage of a substantial collection of black cottonwood genotypes covering a large portion of the species range, to study the natural genetic variation in $\Delta^{15}\text{N}$. Similar to heart-leaved willow, black cottonwood showed significant heritable variation in $\Delta^{15}\text{N}$ and C/N ratios among genotypes and populations, indicating differences in N uptake, assimilation and NUE. Although leaf $\Delta^{15}\text{N}$ did not show signs of adaptation to climate, there was a correlation between root $\Delta^{15}\text{N}$ and precipitation suggesting that nitrate uptake efficiency plays some kind of role in local adaptation to water availability. GWAS did not find any associations with genes for assimilatory enzymes and/or nitrogen transporters, and directly implicated only one gene that might be responsible for variation in isotope discrimination. There were, however, several SNP associations for R:S ratio, which was in turn significantly correlated with whole-plant $\Delta^{15}\text{N}$ and *E/I*, suggesting that the balance between N supply and demand is in part mediated by genes controlling the relative investment in root growth.

The genetic association study conducted in Chapter 4 utilized data resulting from the application of a 34 K SNP chip for *Populus trichocarpa* (Geraldes *et al.* 2013). Based on whole genome sequencing however, there is a 2.2 million SNP dataset available for

the same accessions, as reported in McKown *et al.* (2019). Since significant genotypic variation in R:S ratio, leaf $\Delta^{15}\text{N}$, root $\Delta^{15}\text{N}$, and $\Delta^{15}\text{N}(\text{leaf-root})$ was found (Table 4.1), it makes sense to run another whole-genome wide association using the 2.2 M SNPs to detect more candidate genes, especially for the isotope-based traits. A more recent Bayesian approach would be worth attempting that selects SNP regions piece-by-piece over the whole genome instead of using a single-marker approach (Fernando *et al.* 2017), thus preserving the statistical power of the analysis. This method is also more efficient when dealing with high-density SNPs (Lima *et al.* 2022).

In both heart-leaf willow (Appendix Figure B.2) and black cottonwood (Figure 4.4), I uncovered a relationship between R:S ratio and E/I . Thus, one approach to improving nitrogen uptake efficiency in plants might be to select genotypes with greater relative root development. Other root morphology traits such as length/depth, thickness, surface area to volume ratio, cortex thickness, and cell size may also influence nitrogen fluxes and the partitioning of assimilation. If any correlation between such traits turned out to be significantly associated with IMB model outputs, further GWAS analyses might be of utility to explore their genetic underpinnings.

5.4 Limitations and future application of the IMB model

Most of the work conducted for this thesis involved growing and phenotyping plants in hydroponics under greenhouse conditions. Controlled environment conditions allow for genotypic comparisons that minimize environmental effects, but the results obtained may or may not be relevant to field conditions where, after all, selection takes place. The primary limitation to broad application of the IMB model is the need for hydroponic conditions in order to provide a steady sole nitrogen source with constant nitrogen concentration and $\delta^{15}\text{N}$; conditions that are not found in nature. The provision of nitrogen from multiple sources, which is likely in the field, would make the

interpretation of nitrogen uptake, assimilation, and allocation nearly impossible from an isotope mass-balance perspective. On the other hand, physiological interactions between nitrogen sources are well known, as evidenced by the superior growth often observed when both nitrate and ammonium are made simultaneously available (e.g., Pritchard and Guy 2004). Moreover, mycorrhizal fungi, which can play a major role in nitrogen uptake under natural conditions, are usually not present in hydroponics (Veresoglou *et al.* 2012).

Another major limitation in using the IMB model for purposes of phenotyping is that the approach is not high-throughput. There is also considerable labour and expense associated with the preparation and analysis of all plant parts necessary for the model outputs. In Chapters 2 & 3, where the sample sizes were fairly small, the sampling was relatively straightforward and feasible. However, when the sample size turned into thousands in Chapter 4, we were affected by funding and were able to fully analyze only half of plants (leaves, stems, roots, and original cuttings of ~600 individuals) with the rest being limited to just leaves and roots. Larger plants also require larger hydroponic media volumes to ensure close control of substrate concentration and to stabilize its isotopic composition. This necessitated the use of several 1000 L tanks to grow only 32 plants/tank and required multiple solution replacements over the course of each batch, blocked in time. As noted earlier, resulting batch effects may have contributed error to Chapter 4, potentially interfering with strength of association in the GWAS study.

Costs associated with isotope mass spectrometry aside, access to larger facilities (or smaller plants) may allow application of the IMB model to large-scale phenotyping of crop plants. One major advantage of the IMB model as a phenotyping tool for screening in breeding programs would be its ability to estimate the nitrogen uptake efficiency, which is hard to measure directly. This could be of interest to breeders, ideally in

combination with $\delta^{13}\text{C}$, since they can be used together to explore variation in nitrogen-use and water-use traits among dozens, even hundreds of lines within a few weeks. If plants are grown from seed there would be fewer “parts” to prepare, as there would be no need to analyze cuttings to account for the remobilization of pre-existing nitrogen and its contribution to the nitrogen content and isotopic composition of the plant. Additionally, there would be less error and uncertainty, since all pre-existing nitrogen in the seed would be incorporated into the new plant without discrimination and likely in much smaller quantity (depending on the crop and the size of its seeds).

References

Altieri KE, Hastings MG, Peters AJ, Oleynik S & Sigman DM (2014) Isotopic evidence for a marine ammonium source in rainwater at Bermuda. *Global Biogeochemical Cycles* 28:1066-1080.

Amundson R, Austin AT, Schuur EA, Yoo K, Matzek V, Kendall C, Uebersax A, Brenner D & Baisden WT (2003) Global patterns of the isotopic composition of soil and plant nitrogen. *Global Biogeochemical Cycles* 17:1-11.

Blanquart F, Kaltz O, Nuismer SL & Gandon S (2013) A practical guide to measuring local adaptation. *Ecology Letters* 16:1195-1205.

Bazzer SK, Ray JD, Smith JR, Fritschi FB & Purcell LC (2020) Mapping quantitative trait loci (QTL) for plant nitrogen isotope ratio ($\delta^{15}\text{N}$) in soybean. *Euphytica* 216:191.

Buck AL (1981) New equations for computing vapor pressure and enhancement factor. *Journal of Applied Meteorology Climatology* 20:1527-1532.

Brendel L & Epron D (2022) Are differences among forest tree populations in carbon isotope composition an indication of adaptation to drought? *Tree Physiology* 42:26-31

Carlisle E, Yarnes C, Toney MD & Bloom AJ (2014) Nitrate reductase ^{15}N discrimination in *Arabidopsis thaliana*, *Zea mays*, *Aspergillus niger*, *Picea angusta*, and *Escherichia coli*. *Frontiers in Plant Science* 5:317.

Casciotti KL, Sigman DM, Hastings MG, Böhlke JK & Hilkert A (2002) Measurement of the oxygen isotopic composition of nitrate in seawater and freshwater using the denitrifier method. *Analytical Chemistry* 74: 4905–4912.

Cawse P (1967) The determination of nitrate in soil solutions by ultraviolet spectrophotometry. *Analyst* 92:311-315.

- Cernusak LA (2020)** Gas exchange and water-use efficiency in plant canopies. *Plant Biology* 22:52-67.
- Chen JH, Huang Y, Brachi B, Yun QZ, Zhang W, Lu W, Li HN, Li WQ, Sun XD, Wang GY & He J (2019)** Genome-wide analysis of cushion willow provides insights into alpine plant divergence in a biodiversity hotspot. *Nature Communications* 19:1-2.
- Cui J, Lamade E, Fourel F & Tcherkez G (2020)** $\delta^{15}\text{N}$ values in plants are determined by both nitrate assimilation and circulation. *New Phytologist* 226:1696-1707
- Comstock J (2001)** Steady-state isotopic fractionation in branched pathways using plant uptake of NO_3^- as an example. *Planta*, 214:220-234.
- Dawson TE, Mambelli S, Plamboeck AH, Templer PH & Tu KP (2002)** Stable isotopes in plant ecology. *Annual Review of Ecology and Systematics* 33:507–559.
- Dhanapal AP, Ray JD, Singh SK., Hoyos-Villegas V, Smith JR, Purcell LC & Fritschi FB (2015)** Genome-wide association study (GWAS) of carbon isotope ratio ($\delta^{13}\text{C}$) in diverse soybean [*Glycine max* (L.) Merr.] genotypes. *Theoretical and Applied Genetics* 128:73-91.
- Dijkstra P, Williamson C, Menyailo O, Doucett R, Koch G & Hungate BA (2003)** Nitrogen stable isotope composition of leaves and roots of plants growing in a forest and a meadow. *Isotopes in Environmental and Health Studies* 39:29-39.
- Djomo SN, Kasmioui OE & Ceulemans R (2011)** Energy and greenhouse gas balance of bioenergy production from poplar and willow: a review. *Global Change Biology Bioenergy* 3:181-197.
- Dluzniewska P, Gessler A, Kopriva S, Strnad M, Novák O, Dietrich H & Rennenberg H (2006)** Exogenous supply of glutamine and active cytokinin to the roots reduces NO_3^- uptake rates in poplar. *Plant, Cell & Environment* 29:1284-1297.

- Duvick DN (2005).** The contribution of breeding to yield advances in maize (*Zea mays* L.). *Advances in agronomy* 86:83-145.
- Drenovsky RE, Khasanova A & James JJ (2012)** Trait convergence and plasticity among native and invasive species in resource-poor environments. *American Journal of Botany* 99:629-639.
- Eckert AJ, Bower AD, Wegrzyn JL, Pande B, Jermstad KD, Krutovsky KV, Clair JBS & Neale DB (2009)** Association genetics of coastal Douglas fir (*Pseudotsuga menziesii* var. *menziesii*, Pinaceae). I. Cold-hardiness related traits. *Genetics* 182: 1289-1302.
- Eckert AJ, Bower AD, GONZÁLEZ-MARTÍNEZ SC, Wegrzyn JL, Coop G & Neale DB (2010)** Back to nature: ecological genomics of loblolly pine (*Pinus taeda* Pinaceae). *Molecular Ecology* 19:3789-3805.
- Eckert AJ & Dyer RJ (2012)** Defining the landscape of adaptive genetic diversity. *Molecular Ecology* 21:2836-2838.
- Ertiro BT, Labuschagne M, Olsen M, Das B, Prasanna BM, & Gowda M (2020)** Genetic dissection of nitrogen use efficiency in tropical maize through genome-wide association and genomic prediction. *Frontiers in Plant Science* 11:474.
- Escher P, Eiblmeier M, Hetzger I & Rennenberg H (2004)** Spatial and seasonal variation in amino compounds in the xylem sap of a mistletoe (*Viscum album*) and its hosts (*Populus* spp. and *Abies alba*). *Tree Physiology* 24:639-650.
- Evans JR (1989)** Photosynthesis and nitrogen relationships in leaves of C3 plants. *Oecologia* 78:9-19.
- Evans RD (2001)** Physiological mechanisms influencing plant nitrogen isotope composition. *Trends in Plant Science* 6:121-126.

Fabio ES & Smart LB (2018) Effects of nitrogen fertilization in shrub willow short rotation coppice production – a quantitative review. *Global Change Biology Bioenergy* 10:548-564.

Farquhar GD, Ehleringer JR & Hubick KT (1989) Carbon isotope discrimination and photosynthesis. *Annual Review of Plant Biology* 40:503-537.

Farquhar GD, O'Leary MH & Berry JA (1982) On the relationship between carbon isotope discrimination and the intercellular carbon dioxide concentration in leaves. *Functional Plant Biology* 9:121-137.

Feng H, Fan X, Miller AJ & Xu G (2020) Plant nitrogen uptake and assimilation: regulation of cellular pH homeostasis. *Journal of Experimental Botany* 71:4380-4392.

Fernando R, Toosi A, Wolc A, Garrick D & Dekkers J (2017) Application of Whole-Genome Prediction Methods for Genome-Wide Association Studies: A Bayesian Approach. *Journal of Agricultural, Biological and Environmental Statistics* 22:172-193.

Field CH & Mooney HA (1986) Photosynthesis--nitrogen relationship in wild plants. In: Givnish TJ (ed) *On the economy of plant form and function: Proceedings of the sixth Maria Moors Cabot symposium*. Vol. 6. Cambridge University Press, Cambridge, UK, pp 25-55.

Gebauer G & Schulze ED (1991) Carbon and nitrogen isotope ratios in different compartments of a healthy and a declining *Picea abies* forest in the Fichtelgebirge, NE Bavaria. *Oecologia* 87:198-207.

Geraldes A, Difazio SP, Slavov GT, Ranjan P, Muchero W, Hannemann J, Gunter LE, Wymore AM, Grassa CJ, Farzaneh N, Porth I, McKown AD, Skyba O, Li E, Fujita M, Klápště J, Martin J, Schackwitz W, Pennacchio C, Rokhsar D, Friedmann MC, Wasteneys GO, Guy RD, El-Kassaby YA, Mansfield SD, Cronk QCB, Ehling J, Douglas CJ

& Tuskan GA (2013) A 34K SNP genotyping array for *Populus trichocarpa*: design, application to the study of natural populations and transferability to other *Populus* species. *Molecular Ecology Resources* 13:306-323.

Geraldes A, Farzaneh N, Grassa CJ, McKown AD, Guy RD, Mansfield SD, Douglas CJ & Cronk QCB (2014) Landscape genomics of *Populus trichocarpa*: the role of hybridization, limited gene flow, and natural selection in shaping patterns of population structure. *Evolution* 68:3260-3280.

Geßler A, Schneider S, Weber P, Hanemann U & Rennenberg H (1998) Soluble N compounds in trees exposed to high loads of N: a comparison between the roots of Norway spruce (*Picea abies*) and beech (*Fagus sylvatica*) trees grown under field conditions. *New Phytologist* 138:385-399.

Glass ADM, Britto DT, Kaiser BN, Kinghorn JR, Kronzucker HJ, Kumar A, Okamoto M, Rawat S, Siddiqi MY, Unkles SE & Vidmar JJ (2002) The regulation of nitrate and ammonium transport systems in plants. *Journal of Experimental Botany* 53:855-864.

Guy RD & Holowachuk DL (2001) Population differences in stable carbon isotope ratio of *Pinus contorta* Dougl. ex Loud.: relationship to environment, climate of origin, and growth potential. *Canadian Journal of Botany* 79:274-283.

Hamilton JA, Lexer C & Aitken SN (2013) Differential introgression reveals candidate genes for selection across a spruce (*Picea sitchensis* × *P. glauca*) hybrid zone. *New Phytologist* 197:927-938.

Handley LL & Raven JA (1992) The use of natural abundance of nitrogen isotopes in plant physiology and ecology. *Plant, Cell & Environment* 15:965-985.

Handley LL, Austin AT, Stewart GR, Robinson D, Scrimgeour CM, Raven JA & Schmidt S (1999) The ^{15}N natural abundance ($\delta^{15}\text{N}$) of ecosystem samples reflects measures of water availability. *Functional Plant Biology* 26:185-199.

Hirel B, Le Gouis, J, Ney B & Gallais A (2007) The challenge of improving nitrogen use efficiency in crop plants: towards a more central role for genetic variability and quantitative genetics within integrated approaches. *Journal of Experimental Botany* 58: 2369-2387.

Holmes RM, McClelland JW, Sigman DM, Fry B & Peterson BJ (1998) Measuring ^{15}N - NH_4^+ in marine, estuarine and fresh waters: an adaptation of the ammonia diffusion method for samples with low ammonium concentrations. *Marine Chemistry* 60:235-243.

Huang S, Zhao C, Zhang Y & Wang C (2017) Nitrogen use efficiency in rice, in Nitrogen in Agriculture-Updates. Eds. Amanulla K & Fahad S. (London, United Kingdom: IntechOpen), pp187-208.

Hu Y & Guy RD (2020) Isotopic composition and concentration of total nitrogen and nitrate in xylem sap under near steady-state hydroponics. *Plant, Cell & Environment* 43:2112-2123.

Hu Y, Guy RD & Soolanayakanahally RY (2022) Genotypic variation in C and N isotope discrimination suggests local adaptation of heart-leaved willow. *Tree Physiology* 42:32-43.

Ingvarsson PK & Street NR (2011) Association genetics of complex traits in plants. *New Phytologist* 189:909-922.

Johnson CM, Stout PR, Broyer TC & Carlton AB (1957) Comparative chlorine requirements of different plant species. *Plant and Soil* 8:337-353.

Johnson JF, Allan DL, Vance CP & Weiblen G (1996) Root carbon dioxide fixation by phosphorus-deficient *Lupinus albus* (contribution to organic acid exudation by proteoid roots). *Plant Physiology* 112: 19–30.

Johnson JE & Berry JA (2013) The influence of leaf–atmosphere $\text{NH}_{3(g)}$ exchange on the isotopic composition of nitrogen in plants and the atmosphere. *Plant, Cell & Environment* 36: 1783–1801.

Kalcsits LA & Guy RD (2013a) Whole-plant and organ-level nitrogen isotope discrimination indicates modification of partitioning of assimilation, fluxes and allocation of nitrogen in knockout lines of *Arabidopsis thaliana*. *Physiologia Plantarum* 149:249-259.

Kalcsits LA & Guy RD (2013b) Quantifying remobilization of pre-existing nitrogen from cuttings to new growth of woody plants using ^{15}N at natural abundance. *Plant Methods* 9:27.

Kalcsits LA, Buschhaus HA & Guy RD (2014) Nitrogen isotope discrimination as an integrated measure of nitrogen fluxes, assimilation and allocation in plants. *Physiologia Plantarum* 151:293-304.

Kalcsits LA, Min X & Guy RD (2015) Interspecific variation in leaf–root differences in $\delta^{15}\text{N}$ among three tree species grown with either nitrate or ammonium. *Trees – Structure and Function* 29:1069-1078.

Kalcsits LA & Guy RD (2016a) Variation in fluxes estimated from nitrogen isotope discrimination corresponds with independent measures of nitrogen flux in *Populus balsamifera* L. *Plant, Cell & Environment* 39:310-319.

Kalcsits LA & Guy RD (2016b) Genotypic variation in nitrogen isotope discrimination in *Populus balsamifera* L. clones grown with either nitrate or ammonium. *Journal of Plant Physiology* 201:54-61.

Kaluthota S, Pearce DW, Evans LM, Letts MG, Whitham TG & Rood SB (2015) Higher photosynthetic capacity from higher latitude: foliar characteristics and gas exchange of southern, central and northern populations of *Populus angustifolia*. *Tree Physiology* 35:936-948.

Karunaratne SD, Han Y, Zhang XQ, Zhou G, Hill CB, Chen K, Angessa T & Li C (2020). Genome-wide association study and identification of candidate genes for nitrogen use efficiency in barley (*Hordeum vulgare* L.). *Frontiers in Plant Science* 11:571912.

Karsh KL, Granger J, Kritee K & Sigman DM (2012) Eukaryotic assimilatory nitrate reductase fractionates N and O isotopes with a ratio near unity. *Environmental Science and Technology* 46:5727-5735.

Kawecki TJ & Ebert D (2004) Conceptual issues in local adaptation. *Ecology Letters* 7:1225-1241.

Knapp AN, Hastings MG, Sigman DM, Lipschultz F & Galloway J (2010) The flux and isotopic composition of reduced and total nitrogen in Bermuda rain. *Marine Chemistry* 120:83-89.

Koba K, Inagaki K, Sasaki Y & Takebayashi Y (2010) Nitrogen isotopic analysis of dissolved inorganic and organic nitrogen in soil extracts. In Ohkouchi N, Ichiro Tayasu I & Koba K (Eds). *Earth, Life and Isotopes*, Kyoto University Press, Kyoto, Japan, pp17-37.

Kolb KJ & Evans RD (2003) Influence of nitrogen source and concentration on nitrogen isotopic discrimination in two barley genotypes (*Hordeum vulgare* L.). *Plant, Cell & Environment* 26:1431-1440.

Kou D, Yang G, Li F, Feng X, Zhang D, Mao C, Zhang Q, Peng Y, Ji C, Zhu Q & Fang Y (2020) Progressive nitrogen limitation across the Tibetan alpine permafrost region. *Nature Communications* 11:3331.

Lancien M, Gadal P & Hodges M (2000) Enzyme redundancy and the importance of 2-oxoglutarate in higher plant ammonium assimilation. *Plant Physiology* 123:817-824.

Larcher W (2003) *Physiological Plant Ecology: Ecophysiology and Stress Physiology of functional groups*. 4th Edition, Springer, New York.

Lauteri M, Pliura A, Monteverdi MC, Brugnoli E, Villani F & Eriksson G (2004) Genetic variation in carbon isotope discrimination in six European populations of *Castanea sativa* Mill. originating from contrasting localities. *Journal of Evolutionary Biology* 17:1286-1296.

Lauteri M, Scartazza A, Guido MC & Brugnoli E (1997) Genetic variation in photosynthetic capacity, carbon isotope discrimination and mesophyll conductance in provenances of *Castanea sativa* adapted to different environments. *Functional Ecology* 11:675-683.

Ledgard SF, Woo KC & Bergersen FJ (1985) Isotopic fractionation during reduction of nitrate and nitrite by extracts of spinach leaves. *Functional Plant Biology* 12:631-640.

Leffler AJ & Evans AS (1999) Variation in carbon isotope composition among years in the riparian tree *Populus fremontii*. *Oecologia* 119:311-319.

Levens ND, Tiffin P & Olson MS (2012) Pleistocene speciation in the genus *Populus* (Salicaceae). *Systematic Biology* 61:401-412.

Lima LP, Azevedo CF, Resende MDVD & Nascimento M (2022) Evaluation of Bayesian methods of genomic association via chromosomic regions using simulated data. *Scientia Agricola* 79:e20200202.

Liu D, Fang Y, Tu Y & Pan YP (2014) Chemical method for nitrogen isotopic analysis of ammonium at natural abundance. *Analytical Chemistry* 86:3787-3792.

Liu XY, Koba K, Makabe A & Liu CQ (2014) Nitrate dynamics in natural plants: insights based on the concentration and natural isotope abundances of tissue nitrate. *Frontiers in Plant Science* 5:355.

Livingston NJ, Guy RD, Sun ZJ & Ethier GJ (1999) The effects of nitrogen stress on the stable carbon isotope composition, productivity and water use efficiency of white spruce (*Picea glauca* (Moench) Voss) seedlings. *Plant, Cell & Environment* 22:281-289.

Luo J, Zhou J, Li H, Shi W, Polle A, Lu M, Sun X & Luo ZB (2015) Global poplar root and leaf transcriptomes reveal links between growth and stress responses under nitrogen starvation and excess. *Tree Physiology* 35:1283-1302.

Lupi C, Morin H, Deslauriers A, Rossi S & Houle D (2013) Role of soil nitrogen for the conifers of the boreal forest: a critical review. *International Journal of Plant & Soil Science* 2:155-189.

Malaguti D, Millard P, Wendler R, Hepburn A & Tagliavini (2001) Translocation of amino acids in the xylem of apple (*Malus domestica* Borkh.) trees in spring as a consequence of both N remobilization and root uptake. *Journal of Experimental Botany* 52:1665-1671.

Mariotti A, Mariotti F, Champigny ML, Amarger N & Moyse A (1982) Nitrogen isotope fractionation associated with nitrate reductase activity and uptake of NO_3^- by pearl millet. *Plant Physiology* 69: 880–884.

Matt P, Geiger M, Walch-Liu P, Engels C, Krapp A & Stitt M (2001) The immediate cause of the diurnal changes of nitrogen metabolism in leaves of nitrate-replete tobacco: a major imbalance between the rate of nitrate reduction and the rates of nitrate uptake

and ammonium metabolism during the first part of the light period. *Plant, Cell & Environment* 24:177-190.

McKown AD, Guy RD, Klápště J, Gerald A, Friedmann M, Cronk QC, El-Kassaby YA, Mansfield SD & Douglas CJ (2014a) Geographical and environmental gradients shape phenotypic trait variation and genetic structure in *Populus trichocarpa*. *New Phytologist* 201:1263-1276.

McKown AD, Guy RD, Quamme L, Klápště J, La Mantia J, Constabel CP, El-Kassaby YA, Hamelin RC, Zifkin M & Azam MS (2014b) Association genetics, geography and ecophysiology link stomatal patterning in *Populus trichocarpa* with carbon gain and disease resistance trade-offs. *Molecular Ecology* 23:5771-5790.

McKown AD, Klápště J, Guy RD, Gerald A, Porth I, Hannemann J, Friedmann M, Muchero W, Tuskan AG, Ehling JM, Cronk QC, El-Kassaby YA, Mansfield SD & Douglas CJ (2014c) Genome-wide association implicates numerous genes underlying ecological trait variation in natural populations of *Populus trichocarpa*. *New Phytologist* 203:535-553.

McKown AD, Klápště J, Guy RD, Corea OR, Fritsche S, Ehling JM, El-Kassaby YA & Mansfield SD (2019) A role for SPEECHLESS in the integration of leaf stomatal patterning with the growth vs disease trade-off in poplar. *New Phytologist* 223: 1888-1903.

Millard P, Wendler R, Grassi G, Grelet GA & Tagliavini M (2006) Translocation of nitrogen in the xylem of field-grown cherry and poplar trees during remobilization. *Tree Physiology* 26:527-536.

Min X, Siddiqi MY, Guy RD, Glass ADM & Kronzucker HJ (2002) A comparative study of fluxes and compartmentation of nitrate and ammonium in early-successional tree species. *Plant, Cell & Environment* 22:821-830.

- Momayyezi M & Guy RD (2017)** Substantial role for carbonic anhydrase in latitudinal variation in mesophyll conductance of *Populus trichocarpa* Torr. & Gray. *Plant, Cell & Environment* 40:138-149.
- Murphy EK, Mottiar Y, Soolanayakanahally RY & Mansfield SD (2021)** Variations in cell wall traits impact saccharification potential of *Salix famelica* and *Salix eriocephala*. *Biomass and Bioenergy* 148:106051.
- Näsholm T, Ekblad A, Nordin A, Giesler R, Högberg M & Högberg P (1998)** Boreal forest plants take up organic nitrogen. *Nature* 392:914-916.
- Needoba JA, Sigman DM & Harrison PJ (2004)** The mechanism of isotope fractionation during algal nitrate assimilation as illuminated by the $^{15}\text{N}/^{14}\text{N}$ of intracellular nitrate. *Journal of Phycology* 40:517-522.
- Nordin A, Högberg P & Näsholm T (2001)** Soil nitrogen form and plant nitrogen uptake along a boreal forest productivity gradient. *Oecologia* 129:125-132.
- Oh K, Kato T & Xu HL (2008)** Transport of nitrogen assimilation in xylem vessels of green tea plants fed with $\text{NH}_4\text{-N}$ and $\text{NO}_3\text{-N}$. *Pedosphere* 18:222-226.
- Olleros-Izard T (1983)** Kinetische isotopeneffekte der arginase und nitratreduktase reaktion: ein betrag zur aufklärung derentsprechenden reaktionmechanismen. PhD thesis, Technischen, Universität München, Freising-Weihenstephan.
- Ono F, Frommer WB & von Wirén N (2000)** Coordinated diurnal regulation of low- and high-affinity nitrate transporters in tomato. *Plant Biology* 2:17-23.
- Patterson TB, Guy RD & Dang QL (1997)** Whole-plant nitrogen-and water-relations traits, and their associated trade-offs, in adjacent muskeg and upland boreal spruce species. *Oecologia* 110:160-168.

- Perchlik M & Tegerder M (2017)** Improving plant nitrogen use efficiency through alteration of amino acids transport processes. *Plant Physiology* 175:235-247.
- Peuke AD, Gessler A & Rennenberg H (2006)** The effect of drought on C and N stable isotopes in different fractions of leaves, stems and roots of sensitive and tolerant beech ecotypes. *Plant, Cell & Environment* 29:823-835.
- Peuke AD, Gessler A & Tcherkez G (2013)** Experimental evidence for diel $\delta^{15}\text{N}$ -patterns in different tissues, xylem and phloem saps of castor bean (*Ricinus communis* L.). *Plant, Cell & Environment* 36:2219-2228.
- Pointeau VM & Guy RD (2014)** Comparative resource-use efficiencies and growth of *Populus trichocarpa* and *Populus balsamifera* under glasshouse conditions. *Botany* 92:443-451.
- Porth I, Klapšte J, Skyba O, Hannemann J, McKown AD, Guy RD, DiFazio SP, Muchero W, Ranjan P, Tuskan GA, Friedmann MC, Cronk QC, El-Kassaby YA, Douglas CJ & Mansfield SD (2013)**. Genome-wide association mapping for wood characteristics in *Populus* identifies an array of candidate single nucleotide polymorphisms. *New Phytologist* 200:710-726.
- Pritchard ES & Guy RD (2004)** Nitrogen isotope discrimination in white spruce fed with low concentrations of ammonium and nitrate. *Trees – Structure and Function* 19:89-98.
- Ramarao CS, Srinivasan & Naik MS (1981)** Origin of reductant for reduction of nitrate and nitrite in rice and wheat leaves *in vivo*. *New Phytologist* 87:517-525.
- Ribas-Carbo M, Still C & Berry J (2002)** Automated system for simultaneous analysis of $\delta^{13}\text{C}$, $\delta^{18}\text{O}$ and CO_2 concentrations in small air samples. *Rapid Communications in Mass Spectrometry* 16:339-345.

Robinson D (2001) $\delta^{15}\text{N}$ as an integrator of the nitrogen cycle. *Trends in Ecology and Evolution* 16:153-162.

Robinson D, Handley LL, Scrimgeour CM, Gordon DC, Forster BP & Ellis RP (2000) Using stable isotope natural abundances ($\delta^{15}\text{N}$ and $\delta^{13}\text{C}$) to integrate the stress responses of wild barley (*Hordeum spontaneum* C. Koch.) genotypes. *Journal of Experimental Botany* 51:41-50.

Robinson D (2001) $\delta^{15}\text{N}$ as an integrator of the nitrogen cycle. *Trends in Ecology & Evolution* 16:153-162.

Robinson D, Handley LL & Scrimgeour CM (1998) A theory for $^{15}\text{N}/^{14}\text{N}$ fractionation in nitrate-grown vascular plants. *Planta* 205:397-406.

Savolainen O, Lascoux M & Merilä J (2013) Ecological genomics of local adaptation. *Nature Reviews Genetics* 14:807-820.

Schneider S, Geßler A, Weber P, Sengbusch DV, Hanemann U & Rennenberg H (1996) Soluble N compounds in trees exposed to high loads of N: a comparison of spruce (*Picea abies*) and beech (*Fagus sylvatica*) grown under field conditions. *New Phytologist* 134:103-114.

Seibt U, Rajabi A, Griffiths H & Berry JA (2008) Carbon isotopes and water use efficiency: sense and sensitivity. *Oecologia* 155:441-454.

Shunmugan ASK, Soolanayakanahally RY & Guy RD (2016) Geo-climatic gradient shapes functional trait variations in *Salix eriocephala* Michx. *bioRxiv*, 2016.

Siebrecht S & Tischner R (1999) Changes in the xylem exudate composition of poplar (*Populus tremula* x *P. alba*)—dependent on the nitrogen and potassium supply. *Journal of Experimental Botany* 50:1797-1806.

Sigman DM, Casciotti KL, Andreani M, Barford C, Galanter M & Böhlke JK (2001) A bacterial method for the nitrogen isotopic analysis of nitrate in seawater and freshwater. *Analytical Chemistry* 73:4145-4153.

Solórzano L (1969) Determination of ammonia in natural waters by the phenolhypochlorite method. *Limnology Oceanography* 14:799-801.

Soolanayakanahally RY, Guy RD, Street NR, Robinson KM, Silim SN, Albrechtsen BR & Jansson S (2015) Comparative physiology of allopatric *Populus* species: geographic clines in photosynthesis, height growth, and carbon isotope discrimination in common gardens. *Frontier in Plant Science* 14:528.

Steketee CJ, Sinclair TR, Riar MK, Schapaugh WT & Li Z (2019) Unraveling the genetic architecture for carbon and nitrogen related traits and leaf hydraulic conductance in soybean using genome-wide association analyses. *BMC Genomics* 20: 811.

Stock P, Hösch A & Burghardt D (2019) $\delta^{15}\text{N}$ analysis of ammonium in freeze-dried natural groundwater samples by precipitation with sodium tetraphenylborate. *Rapid Communications in Mass Spectrometry* 33:1730-1738.

Suarez-Gonzalez A (2017) Adaptive introgression from *Populus balsamifera* (balsam poplar) in *P. trichocarpa* (black cottonwood). Ph.D. Thesis. University of British Columbia, Vancouver, Canada. pp138.

Suarez-Gonzalez A, Hefer CA, Christe C, Corea O, Lexer C, Cronk QCB & Douglas CJ (2016) Genomic and functional approaches reveal a case of adaptive introgression from *Populus balsamifera* (balsam poplar) in *P. trichocarpa* (black cottonwood). *Molecular Ecology* 25:2427-2442.

Sun ZJ, Livingston NJ, Guy RD & Ethier GJ (1996) Stable carbon isotopes as indicators of increased water use efficiency and productivity in white spruce (*Picea glauca* (Moench) Voss) seedlings. *Plant, Cell & Environment* 19:887-894.

Tang W, Ye J, Yao X, Zhao P, Xuan W, Tian Y, Zhang YY, Xu S, An HZ, Chen GM, Yu J, Wu W, Ge YW, Liu XL, Li J, Zhang HZ, Zhao YQ, Yang B, Jiang ZX, Peng C, Zhou C, Terzaghi W, Wang CM & Wan JM (2019) Genome-wide associated study identifies NAC42-activated nitrate transporter conferring high nitrogen use efficiency in rice. *Nature Communications* 10:1-11.

Taylor G (2002) *Populus*: Arabidopsis for forestry. Do we need a model tree? *Annals of Botany* 90: 681–689.

Tcherkez G (2011) Natural $^{15}\text{N}/^{14}\text{N}$ isotope composition in C_3 leaves: are enzymatic isotope effects informative for predicting the ^{15}N -abundance in key metabolites? *Functional Plant Biology* 38:1-2.

Tcherkez G & Hodges M (2008) How stable isotopes may help to elucidate primary nitrogen metabolism and its interaction with (photo) respiration in C_3 leaves. *Journal of Experimental Botany* 59:1685-1693.

Tcherkez G (2011) Natural $^{15}\text{N}/^{14}\text{N}$ isotope composition in C_3 leaves: are enzymatic isotope effects informative for predicting the ^{15}N -abundance in key metabolites? *Functional Plant Biology* 38:1-12.

Tcherkez G & Farquhar GD (2006) Isotopic fractionation by plant nitrate reductase, twenty years later. *Functional Plant Biology* 33:531-537.

Tegeder M & Masclaux-Daubresse C (2018) Source and sink mechanisms of nitrogen transport and use. *New Phytologist* 217:35-53.

Tischner R (2000) Nitrate uptake and reduction in higher and lower plants. *Plant, Cell & Environment* 23:1005-1024.

Tobin AK & Yamaya T (2001) Cellular compartmentation of ammonium assimilation in rice and barley. *Journal of Experimental Botany* 52:591-604.

Turgeon R & Wolf S (2009) Phloem transport: cellular pathways and molecular trafficking. *Annual Review of Plant Biology* 60:207-221.

Udvardi M, Below FE, Castellano MJ, Eagle AJ, Giller KE, Ladha JK, Liu X, Maaz TM, Nova-Franco B, Raghuram N, Robertson GP, Roy S, Saha M, Schmidt S, Tegeder M, York LM & Peters JW (2021) A research road map for responsible use of agricultural nitrogen. *Frontier in Sustainable Food Systems* 5:660155.

Veresoglou SD, Chen B & Rillig MC (2012) Arbuscular mycorrhiza and soil nitrogen cycling. *Soil Biology and Biochemistry* 46:53-62.

Vitousek PM, Aber JD, Howarth RW, Likens GE, Matson PA, Schindler DW & Tilman DG (1997) Human alteration of the global nitrogen cycle: sources and consequences. *Ecological Applications* 7:737-750.

von Wirén N, Lauter FR, Ninnemann O, Gillissen B, Walch-Liu P, Engels C, Jost W & Frommer WB (2000) Differential regulation of three functional ammonium transporter genes by nitrogen in root hairs and by light in leaves of tomato. *The Plant Journal* 21:167-175.

Wang T, Hamann A, Spittlehouse DL & Murdock TQ (2012) ClimateWNA — High-resolution spatial climate data for western North America. *Journal of Applied Meteorology and Climatology* 51:16-29.

Wang W, Hu B, Yuan DY, Liu YQ, Che R, Hu Y, Ou S, Liu Y, Zhang Z, Wang H, Li H, Jiang Z, Zhang Z, Gao X, Qiu Y, Meng X, Liu Y, Bai Y, Liang Y, Wang Y, Zhang L, Li L, Li L, Jing H,

- Li J & Chu C (2018)** Expression of the nitrate transporter gene OsNRT1.1A/OsNPF6.3 confers high yield and early maturation in rice. *The Plant Cell* 3:638-651.
- Weih M, Rönnerberg-Wästljung AC & Glynn C (2006)** Genetic basis of phenotypic correlations among growth traits in hybrid willow (*Salix dasyclados* × *S. viminalis*) grown under two water regimes. *New Phytologist* 170:467-477.
- Xu G, Fan X & Miller AJ (2012)** Plant nitrogen assimilation and use efficiency. *Annual Review of Plant Biology* 63:153-182.
- Yin X (1998)** The albedo of vegetated land surfaces: systems analysis and mathematical modeling. *Theoretical and Applied Climatology* 60:121-140.
- Yoneyama T, Ito O & Engelaar WM (2003)** Uptake, metabolism and distribution of nitrogen in crop plants traced by enriched and natural ¹⁵N: progress over the last 30 years. *Phytochemistry Reviews* 2:121-132.
- Yoneyama T, Kamachi K, Yamaya T & Mae T (1993)** Fractionation of nitrogen isotopes by glutamine synthetase isolated from spinach leaves. *Plant and Cell Physiology* 34: 489-491.
- Yoneyama T, Matsumaru T, Usui K & Engelaar WMHG (2001)** Discrimination of nitrogen isotopes during absorption of ammonium and nitrate at different nitrogen concentrations by rice (*Oryza sativa* L.) plants. *Plant, Cell & Environment* 24: 133-139.
- Yousfi S, Serret MD & Araus JL (2013)** Comparative response of $\delta^{13}\text{C}$, $\delta^{18}\text{O}$ and $\delta^{15}\text{N}$ in durum wheat exposed to salinity at the vegetative and reproductive stages. *Plant, Cell & Environment* 36:1214-1227.

Appendix – Supplemental measurements

Table A.1. Direct comparison of the denitrifier method to combustion-based method for $\delta^{15}\text{N}$ of three calcium nitrate solutions with the same concentration (5 mM). Shown are means \pm SD ($n=3$).

	$\delta^{15}\text{N}$ from direct combustion (‰)	$\delta^{15}\text{N}$ from denitrifier method (‰)	[N] (mM)	Yield (%)
Calcium nitrate solution #1	-1.69 \pm 0.21	-1.91 \pm 0.38	4.88 \pm 0.11	98
Calcium nitrate solution #2	2.67 \pm 0.23	2.37 \pm 0.55	4.97 \pm 0.21	99
Calcium nitrate solution #3	63.81 \pm 0.45	63.11 \pm 0.32	4.95 \pm 0.16	99

Table A.2. Concentrations, $\delta^{15}\text{N}$ and $\Delta^{15}\text{N}$ values in bulk tissue, soluble N and NO_3^- in roots of *Populus trichocarpa* hydroponically grown with 0.5 mM NO_3^- and a source $\delta^{15}\text{N}$ value of 2.67‰. Soluble N and NO_3^- were extracted from freeze-dried root tissue using methanol:chloroform:water mixture (12:5:3, v/v/v) as describe in Coleman *et al.* (2008). Total soluble organic N was calculated as the difference between bulk tissue and NO_3^- . Shown are means \pm SE ($n=9$).

	[N] (mmol N g dw ⁻¹)	$\delta^{15}\text{N}$ (‰)	$\Delta^{15}\text{N}$ (‰)
Bulk tissue	2.74 \pm 0.05	-2.56 \pm 0.25	5.25 \pm 0.28
Soluble N	0.59 \pm 0.04	7.39 \pm 0.87	-4.68 \pm 0.86
NO_3^-	0.42 \pm 0.02	12.80 \pm 0.50	-10.08 \pm 0.55
Total soluble organic N	2.31 \pm 0.04	-5.38 \pm 0.19	8.11 \pm 0.22

Table A.3. Comparison between root $\delta^{15}\text{N}$ and organic N $\delta^{15}\text{N}$ in the xylem sap at the genotypic level. Mean values ($\pm\text{SE}$) are for five biological replicates. Different letters indicate significant differences at $P<0.05$.

Genotype	Root $\delta^{15}\text{N}$ (‰)	Organic N $\delta^{15}\text{N}$ in xylem sap (‰)
BELA 4	57.23 \pm 0.82ab	57.29 \pm 2.63a
CARS 2	56.37 \pm 0.76ab	48.87 \pm 3.52a
FNYI 4	55.63 \pm 0.89ab	61.04 \pm 1.03a
HALS 2	57.53 \pm 0.42a	54.24 \pm 3.43a
STHA 3	54.94 \pm 0.59b	60.29 \pm 1.54a
Grand Mean	56.34 \pm 0.35	57.00 \pm 1.26

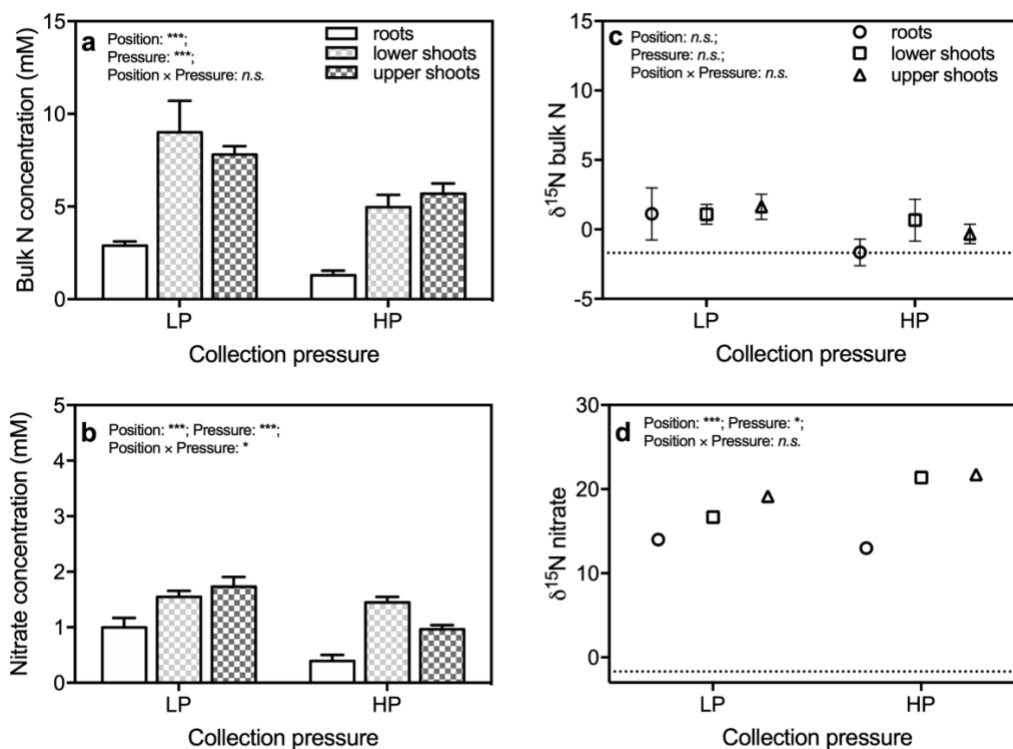


Figure A.1. Concentrations of total N (a) and nitrate (b), and $\delta^{15}\text{N}$ of total N (c) and nitrate (d) in *Populus trichocarpa* xylem sap collected from roots and lower and upper shoot sections at LP and HP. Bars or symbols represent means of six samples (\pm SE; omitted from panel D because they are smaller than the symbol size). Effects of the main factors pressure and position, and their interaction, are indicated: *n.s.*, not significant; *, $P < 0.05$; **, $P < 0.01$; ***, $P < 0.001$. Dotted lines in panels C and D represent the $\delta^{15}\text{N}$ of NO_3^- in the hydroponic medium (-1.69‰).

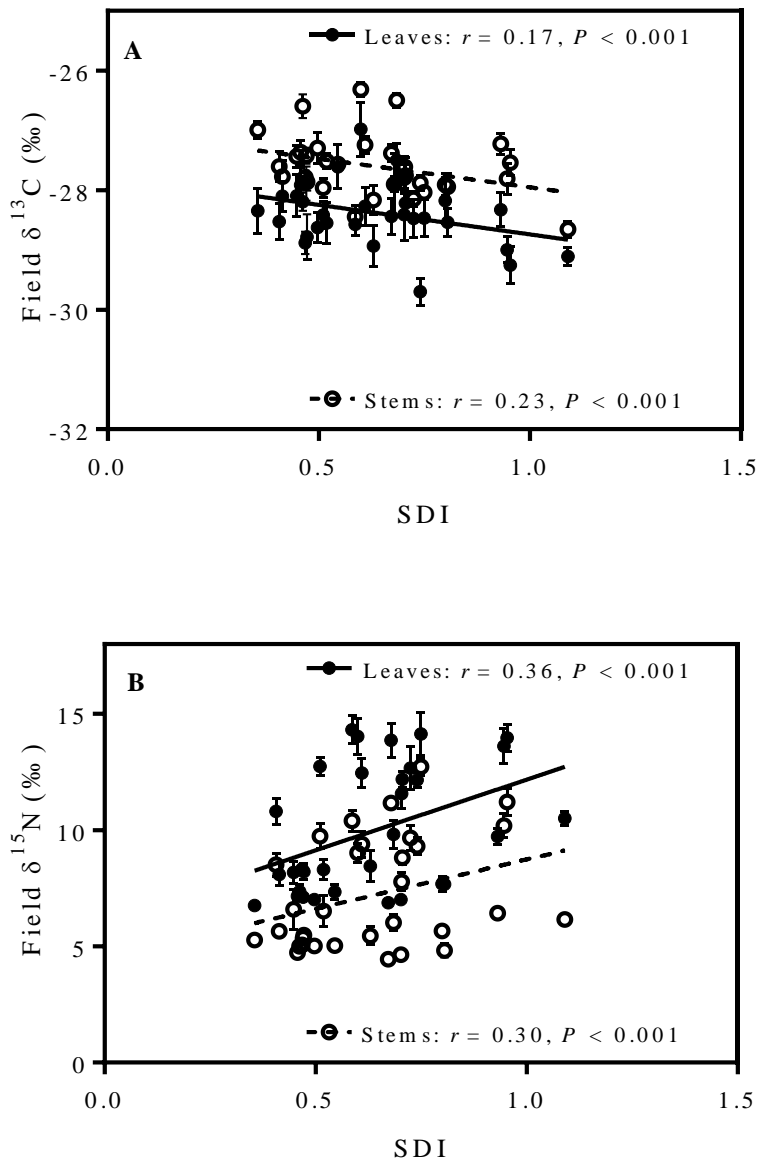


Figure B.1. Carbon and nitrogen isotopes ($\delta^{13}\text{C}$ & $\delta^{15}\text{N}$, ‰) of heart-leaf willow (*Salix eriocephala*) leaves and stems from the common garden experiment plotted against summer dryness index (SDI) for population sites of origin.

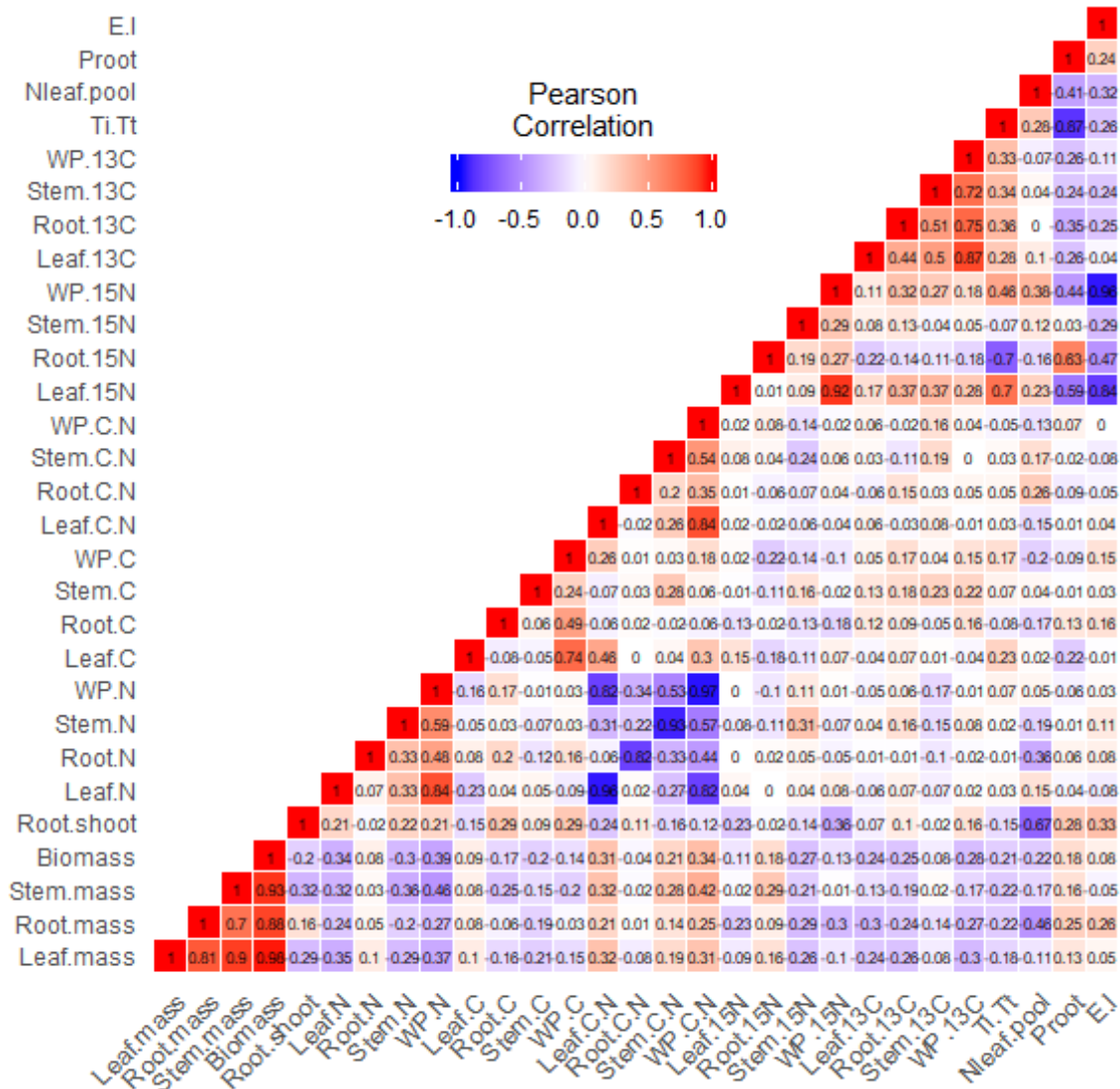


Figure B.2. Heat-map of Pearson's correlations (r) for biomass and physiological traits for all 21 genotypes of heart-leaf willow (*Salix eriocephala*) in the hydroponic experiment. Biomass, g; N, nitrogen percentage; C, carbon percentage; C:N, carbon to nitrogen ratio; $\delta^{15}\text{N}$, nitrogen isotope composition; $\delta^{13}\text{C}$, carbon isotope composition; WP, whole-plant; Ti/Tt , the proportion of inorganic nitrogen transported from roots to leaves; P_{root} , proportion of inorganic nitrogen assimilated in the roots; E/I , root efflux/influx ratio.

30-Jan-12	08-Jun-12	31-Jan-13	26-Jun-13	19-Dec-13	18-Feb-14	06-May-14	14-Jul-14	Summer-2019
#1	#2	#3	#4	#5	#6	#7	#8	#9
ALAA 20-4	BELA 18-4	HARC 26-2	KTMC 12-3	ALSC 1-4	ALAA 20-5	ALAA 20-3	AMER 13-1	CHKD 19-4
ALAA20-1	BELC 18-3	HAZH 10-3	KTMC 12-5	ALSC 1-5	AMER 13-1	BELA 18-1	AMER 13-3	DENB 17-2
BELA 18-3	BELC 18-5	HOMA 21-2	KTWF 10-3	BELC 18-1	BLCG 28-1	BELA 18-5	BULF 11-5	HIXN 16-1
BULH 11-4	BULA 11-4	HOMA 21-4	LAFY 30-1	BELC 18-4	CHWJ 27-1	BLCG 28-3	CEDA 10-2	KIMB 16-2
CARS 29-2	CHKC 19-1	HOMB 21-1	LAFY 30-2	BULG 11-4	DENA 17-2	BOLF 11-3	CHNH 27-4	KIMB 16-5
CARS 29-4	CHKC 19-2	HOMB 21-2	LAFY 30-3	CEDA 10-4	DENA 17-3	BOLG 11-5	CLMD 28-5	KIMB 16-6
CHKC 19-4	CHKC 19-3	HOMB 21-3	LILA 26-1	CMBF 28-1	DENA 17-4	BULF 11-4	CNYH 28-1	KTMA 12-1
CHKD 19-1	CHKD 19-3	HOMB 21-4	LILA 26-5	CMBF 28-2	DEND 17-5	BULG 11-2	DENB 17-1	MCGR 15-7
CHKD 19-2	CHWH 27-1	HOMB 21-5	LILB 26-1	CMBF 28-3	ELAD 25-4	CARS 29-3	DEND 17-1	MCHB 19-4
CHKD 19-4	CHWH 28-4	HOMC 21-1	LILB 26-2	CMBF 28-4	ELAD 25-5	CARS 29-5	HARB 26-3	Q AUS 16-1
CHWH 27-5	CHWK 27-2	HOMC 21-2	LILB 26-3	CMBF 28-5	HAZH 10-1	CHKD 19-5	HOMA 21-1	QBKR 16-3
CHWJ27-2	CHWK 27-4	HOMC 21-4	LILB 26-4	CSYJ 28-2	HIRD 12-2	CHWH 27-2	HOMA 21-5	QBKR 16-4
CHWK 27-3	CNYH 28-3	HOMD 21-2	LILB 26-5	DENB 17-3	HOMC 21-3	CHWH 27-3	HOPF 27-2	QBKR 16-5
DENA 17-1	CNYH 28-5	HOMD 21-3	LILC 26-1	DENC 17-4	HOMD 21-1	CNYH 28-2	JEFF 30-3	QCTN 16-1
DENB 17-2	CSYJ 28-1	HOMD 21-4	LILA 26-2	ELAD 25-2	ISKC 6-3	CNYH 28-4	NHTB 27-1	QFRS 16-3
DENC 17-5	CSYJ 28-3	HOMD 21-5	LILC 26-5	FKRB 6-1	JASP 30-3	DENB 17-4	PHLC 22-4	QFRS 16-4
DEND 17-2	DENC 17-2	HOPF 27-1	LNZK 28-2	FNYY 28-5	JEFF 30-3	DENC 17-3	QBKR 16-2	QFRS 16-5
DEND 17-3	FNYY 28-1	HOPF 27-5	LNZK 28-3	HALS 30-6	KLND 20-2	ELAD 25-1	QFRS 16-3	QLKE 16-1
DEND 17-4	FNYY 28-3	HOPG 27-1	LNZK 28-4	HARB 26-4	KLNE 20-4	GLCB 26-2	QLCA 26-1	QLKE 16-3
ELAD 25-3	FNYY 28-4	HOPG 27-2	LONG 29-1	HARC 26-3	LILD 26-3	HARC 26-5	SHEL 15-2	SHEL 15-1
FNYY 28-2	GLCB 26-1	HOPG 27-3	LONG 29-2	HARC 26-4	PHLA 22-3	HAZH 10-5	SHEL 15-4	SHEL 15-4
GLCB 26-4	GLCB 26-3	HRSO 27-1	LONG 29-5	HAZH 10-2	PITS 29-2	HOPF 27-3	SKWA 24-2	WLOW 15-1
SLMC 28-2	HALS 30-1	HRSO 27-2	MCFA 20-1	HOMC 21-5	PITS 29-4	HOPF 27-4	SLMB 28-4	WLOW 15-3
STHA 21-3	HALS 30-2	HRSO 27-3	MCFA 20-2	HRSO 27-4	PITS 29-5	HOPG 27-5	SLMC 28-3	
STHB 21-4	HALS 30-4	HRSO 27-5	MCFA 20-4	HRSP 27-1	Q AUS 16-3	IRVC 7-1	SLMD 28-1	
TAKA 3-3	HARB 26-1	HRSP 27-3	MCFA 20-5	ISKC 6-5	QBKR 16-3	IRVC 7-5	SLMD 28-3	
	HARB 26-2	HRSP 27-4	MCFA 20-6	JASP 30-1	QBKR 16-4	ISKA 6-4	SQMA 25-1	
	HARB 26-5	HRSP 27-5	MCGR 15-4	PHLA 22-1	QCTN 6-1	ISKC 6-1	SQMA 25-3	
	HARC 26-1	IRVC 7-3	MCGR 15-6	PHLA 22-2	QCTN 6-5	JEFF 30-1	SQMA 25-4	
	HIXN 16-5	IRVC 7-4	MCGR 15-7	PHLA 22-5	QFRS 16-1	KIMB 16-1	SQMA 25-5	
	HIXN 16-1	IRVC 7-6	MCGR 15-8	PHLC 22-4	QFRS 16-2	KIMB 16-4	SQMB 25-3	
	LILD 26-4	IRVD 7-5	MCHA 19-1	PHLC 22-5	QFRS 16-5	KLNC 20-2	SQMB 25-4	
		ISKA 6-1	MCHA 19-2	PITS 29-3	QLKE 16-1	KLND 20-5	SQMC 25-2	
		ISKA 6-2	MCHA 19-3		QLKE 16-2	KLNG 20-3	SQMC 25-4	
		ISKA 6-5	MCHA 19-4		QLKE 16-3	KTMA 12-2	SQMC 25-5	
		ISKC 6-2	MCHA 19-5		SHEL 15-1	KTMC 12-1	STHA 21-2	
		JASP 30-4	MCHA 20-3		SHEL 15-2	KTMC 12-2	STHA 21-4	
		JASP 30-5	MCHB 19-1		SHEL 15-3	KTSJ 10-5	STHA 21-5	
		JEFF 30-2	MCHB 19-2		SHEL 15-5	LAFY 30-5	STHB 21-1	
		JEFF 30-4	MCHB 19-3		SKNB 10-1	LILA 26-2	STHB 21-2	
		KIMB 16-2	MCHB 19-4		SKNB 10-2	LILA 26-4	STHB 21-3	
		KIMB 16-3	MCHB 19-5		SKNC 10-1	LNZK 28-5	STHB 21-5	
		KIMB 16-5	MCMN 27-3		SKNC 10-2	LONG 29-3	STKA 5-5	
		KIMB 16-6	MEBA 28-5		SKNC 10-4	LONG 29-4	STKF 5-1	
		KLNA 20-3	MEMA 28-3		SKND 10-2	MCMN 27-5	STKG 4-4	
		KLNA 20-4	MEMA 28-4		SKNL 10-1	MEMA 28-1	SZMC 28-1	
		KLNA 20-5	MTSM 27-1		SKNL 10-3	MTSM 27-3	TAKA 3-2	
		KLNB 20-2	MTSM 27-2		SKNL 10-4	NASC 8-5	TAKB 3-4	
		KLNB 20-3	MTSM 27-5		SKNM 10-1	NASD 8-2	TAKB 3-5	
		KLND 20-3	NASC 8-2		SKNM 10-6	NECA 14-1	TATB 1-7	
		KLNE 20-1	NASD 8-4		SKNN 10-2	NHTA 27-2	TLKH 11-5	
		KLNE 20-3	NASF 8-2		SKNN 10-5	NHTB 27-2	TOBA 23-2	
		KLNE 20-5	NASH 8-4		SKNO 10-2	NHTB 27-3	TOBA 23-4	
		KLNG 20-1	NBON 29-1		SKNO 10-3	NHTB 27-5	TOBB 23-2	
		KLNG 20-2	NBON 29-2		SKNP 10-2	NPLN 30-5	TOBB 23-3	
		KLNG 20-4	NBON 29-4		SKNP 10-3	PHLA 22-4	TOBB 23-4	
		KLNG 20-5	NECB 14-6		SKNP 10-4	Q AUS 16-7	VNDL 27-5	
		KLNG 20-6	NHTA 27-3		SKNP 10-8	QUAS 16-1	WELC 27-2	
		KLNG 20-7	NHTA 27-5		SKNP 10-9	WHTA 28-1	WELC 27-3	
		KSPA 9-3	NHTB 27-4		SKNQ 10-1	WLOW 15-4	WELC 27-4	
		KTMA 12-1	NPLN 30-3		SKNQ 10-3	WLOW 15-5	WHITE 28-4	
		KTMA 12-3	NPLN 30-4		SKNQ 10-4	WLOW 15-7	WHITE 28-3	
		KTMA 12-4	PHLC 22-2		SKWA 24-2	YALD 27-3	WLOW 15-1	
		KTMB 12-5	PHLC 22-3		SKWA 24-3	YALD 27-4	WLOW 15-3	
							YALD 27-2	
							YALD 27-3	
							YALE 27-1	

Figure C.1. Lists of genotypes within each batch used for the hydroponic experiment in Chapter 4.

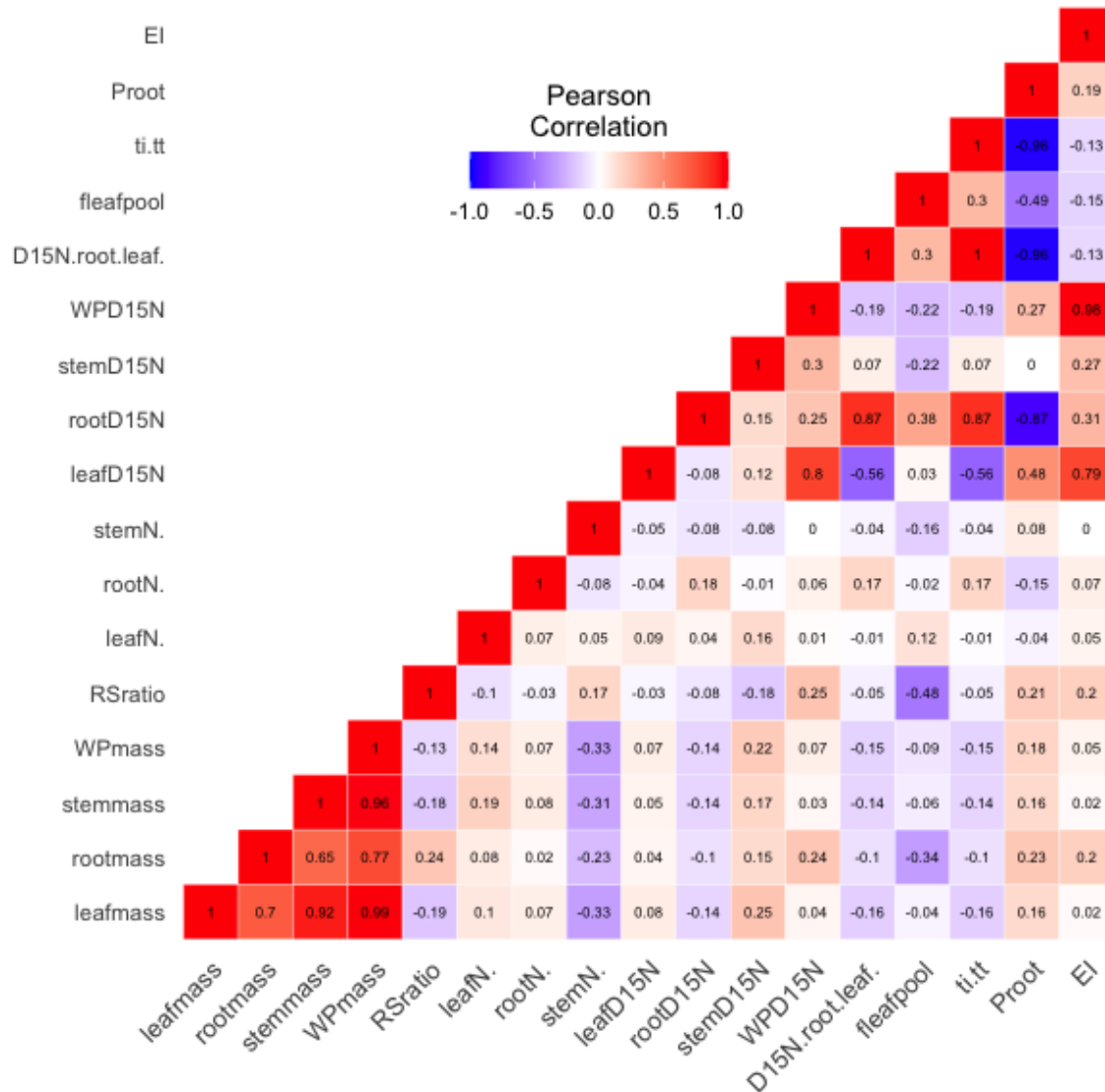


Figure C.2. Heat-map of Pearson's correlations (r) for biomass and nitrogen-related physiological traits for all 362 genotypes of black cottonwood (*Populus trichocarpa*) in the hydroponic experiment. WP, whole-plant; Biomass, g; N, nitrogen percentage; $\Delta^{15}\text{N}$, nitrogen isotope discrimination; f_{leafpool} the proportion of total plant nitrogen assigned to the leaf pool; T_i/T_t , the proportion of inorganic nitrogen transported from roots to leaves; P_{root} , proportion of inorganic nitrogen assimilated in the roots; E/I , root efflux/influx ratio.